TWO EXTREME CASES OF ATMOSPHERIC BLOCKING OVER EUROPE AND NORTH AMERICA

A Thesis presented to
the Faculty of the Graduate School
at the University of Missouri

In Partial Fulfillment
of the Requirements for the Degree

Master of Science

---

by
JUSTIN MICHAEL GLISAN

Dr. Anthony R. Lupo, Thesis Supervisor

December 2007

The undersigned, appointed by the dean of the Graduate School, have examined the thesis entitled

TWO EXTREME CASES OF ATMOPSHERIC BLOCKING OVER EUROPE AND NORTH AMERICA

presented by Justin Glisan,

a candidate for the degree of Master of Science,

and hereby certify that, in their opinion, it is worthy of acceptance.

Associate Professor Anthony Lupo

Professor Bruce Cutter

Associate Professor Patrick Market

Associate Professor Randy Miles

To my Dad, Mom, and brother. Their steadfast dedication and love have made me the person I am.

To my dear friends, too numerous to name, who have been my companions on the road of life.

And, for Mizzou.

ACKNOWLEDGEMENTS

In my six years at the University of Missouri, this gentleman has been my advisor, professor, and mentor. More than this though, he has been my friend. Dr. Anthony Lupo has guided me through the ups and downs of undergraduate and graduate life. I feel very confident in saying that he has been one of the true constants in my college experience, and for this, I am forever indebted to him.

I must thank the members of my thesis committee for their guidance over this entire process. Without their insightful comments and gentle criticism, this thesis would have never taken shape.

Finally, I would be remiss in not acknowledging Dr. Athar Hussain, whose research expertise helped greatly. Athar is a true gentleman and scholar and an asset to our department.

TABLE OF CONTENTS

List of Figures

Figure **Page**

List of Tables

Table **Page**

Public Abstract
First Name: Justin
Middle Name: Michael
Last Name: Glisan
Degree: M.S
Department: Soils, Environmental and Atmospheric Sciences
Adviser's First Name: Anthony
Adviser's Last Name: Lupo
Graduation Term: Fall
Graduation Year: 2007
Title: Two Extreme Cases Of Atmospheric Blocking Over Europe and North America

Atmospheric blocking is simply the inhibition, on the synoptic and planetary scale, of the normal mid-latitude progression of migratory cyclones and anticyclones. While the block itself is readily observable as a 500-hPa positive geopotential height anomaly, the dynamical onset of the blocking flow is still not understood.

It has been shown through various studies that prolonged or episodic atmospheric blocking can impact the climatological character of the region in which they occur for one to two seasons following the event. Seasonal modifications imposed on a given region by blocking anticyclones not only deprive the area of the typical temperature and precipitation regimes, but also produce climatological extremes that can malignantly affect the land and populations residing in specific areas.

In this study, two cases of extreme blocking are analyzed using NCEP-NCAR gridded reanalyses. The first case is the 2003 European heat wave. This event was confined to Western Europe, where the ensuing heat wave produced a death toll on the range of 40,000 over the summer season. The most severe period occurred from 06 – 13 August 2003. The second case is analogous to the 2003 European heat wave in scale and magnitude.

The 2004 Gulf of Alaska event, "Baked Alaska," prompted abnormally high temperatures and less-than-normal precipitation (over the period of June through August) that led to anomalous melting over the summer season. It should be noted that the Gulf of Alaska event was not merely one episode, but two distinct events.

As with events such as those above, the greatest problem affecting the study of blocking flows is the degree to which this phenomenon can be forecasted numerically. In this investigation, a mathematical entity, known as a Lyapunov exponent is utilized in an effort to determine the fluid stability of the atmosphere within a blocking flow. A better understanding of stability may yield an increase in the forecast lead-time as well as a greater understanding of blocking itself. While Lyapunov exponent analysis delves

into the characteristics of flow stability, a more powerful tool emerges in that these exponents can examine the local predictability of the flow itself.

Chapter 1

Introduction

The subject of atmospheric blocking has enjoyed an increasing amount of attention over the past few decades. Perhaps the first major study of blocking flows occurred in 1950, when Rex analyzed and produced one of the first short-term Northern Hemisphere climatologies on blocking anticyclones and their associated flows. In his study, Rex showed that blocking patterns were intimately related to strong surface anticyclones. Rex (1950a&b) also shows that atmospheric blocking may have climatological impacts in that during the events, surface temperatures and amount of sunlight (i.e. less cloud cover) tend to be above normal, while precipitation tends to be lower than normal.

Other research studies concerned with atmospheric blocking have included the study of the temporal duration, strength and regional effects (both upstream and downstream) of the episodes (e.g. Austin 1980; Colucci 1985; Lupo and Smith 1995a&b; Wiedenmann et al. 2002; Galarneau et. al. 2008; Burkhardt and Lupo 2005). It has been shown through various studies that prolonged or episodic blocking over the course of a season can impact the climatological character of the region in which the event occurs for one to two seasons following the event (Rex 1950a&b; Green 1977; Lupo & Bosart 1999).

Seasonal modifications imposed on a given region by blocking anticyclones not only deprive the area of the typical temperature and precipitation regimes, but also produce climatological extremes that can malignantly affect the land and populations residing in specific areas (Galarneau et al. 2008). Of particular interest to this study are two events involving analogous cases of extreme blocking. The first event occurred over Western Europe during the summer of 2003, in which a record setting heat wave caused the deaths of over 40,000 individuals. The second event involved an anomalous warming event in the northwest corner of the North American continent. In both cases, it was found that a large, positive 500-hPa-geopotential height anomaly formed off the western continental coast for each event (Table 1.2).

1.1 The Western European heat wave of 2003

Over the period of June – August 2003, the western extent of the European continent experienced a heat wave that killed tens of thousands of individuals. All major countries in Europe felt the effects of the heat. As summarized in table 1.1, the excess death tolls were extreme. The Excess death percentage is defined in Kovats et al. (2004) as:

$$\%\text{E.D.} = \frac{(\text{observed} - \text{expected})}{\text{expected}} * 100 \qquad (1.1.1)$$

where observed deaths are those that actually happen as opposed to expected deaths, which each country derives from the average expected in a given year. Of the excess deaths, France paid the highest price at around 60% or 14,802 individual (Kovats et al. 2004).

Table 1.1. Provisional deaths attributed to the 2003 Western European heat wave. Time period covers 01 June through 31 July 2004 (Kovats et al. 2004).

Country	Excess Deaths	% of Total Death Rate
England and Wales	2,045	16
France	14,802	60
Italy	3,134	15
Portugal	2009	26
Spain	Count in Progress	-

In France, surface temperatures reached near-record levels in the final weeks of July. As temperatures continued to rise (and then remained constant), the rates of death mirrored this rise. From about 03 August 2003 to 13 August 2003 the maximum surface temperature peaked and then hovered near 37^{o}C. During this same period, daily minimum temperatures hovered around 20^{o}C. For France, this extended period of heat represented the most extreme heat wave (max., min., and avg. temperature as well as duration) in 53 years (Pirard et al. 2005).

1.2 Gulf of Alaska, 2004

The state of Alaska set temperature and precipitation records during the summer season of 2004. Locations from Seward's Peninsula to the

Southeast Panhandle reported positive departures of mean temperatures ranging from -15.9^{o}C to 5.0^{o}C (Alaska NWS 2004). Locations such as Anchorage, Barrow, Fairbanks, Juneau, King Salmon and Valdez experienced the warmest summers on record (Barrow's warmest in 84 years). Juneau experienced seven days of consecutive temperatures above 28.8^{o}C.

In the southern regions of Alaska, the frequency of days with high maximum temperatures was particularly noteworthy. Anchorage reported highs above 21.1^{o}C for 41 days. In a normal summer season, this only occurs around 10 days. Moreover, numerous high and low temperature maxima and high minima were set across the entire state (Alaska NWS 2004).

As for precipitation, most of the southern and eastern interior regions reported drier-than-normal conditions. Fairbanks was one-inch shy of breaking its 1957 record for least amount of rainfall. In fact, Fairbanks only received 38% of the rainfall expected. Juneau reported its third driest summer (since official recorded observations began in 1847), recording only about half of its normal rainfall.

Table 1.2. A list of the atmospheric blocking episodes used in this study.

Location	Year	Block Onset	Block Maturity	Block Decay	Duration (days)	BI
W.Europe	2003	03-06 Aug.	06-13 Aug.	12-14 Aug.	07	1.99
Alaska	2004	21-24 Jun.	24 Jun.-05 Jul.	04-06 Jul.	11	3.11
Alaska	2004	02-05 Aug.	05-28 Aug.	27-29 Aug.	23	2.44

1.3 Purpose & Objectives

1.3.1 Purpose

The purpose of this study is to further the understanding of atmospheric blocking flows occurring as 500-hPa positive height anomalies. Prolonged or episodic atmospheric blocking can impact the climatological character of the region in which the blocking occurs for one to two seasons following the event. Moreover, these events can induce heat waves and deprive regions of regular rainfall, affecting the inhabitants of said regions negatively.

Specifically, this study will address how certain diagnostics may be used to diagnose blocking onset and decay, as well as the dynamics of the period of time in between (which will be referred to as the block itself). Of particular note in this study is the use of a mathematical entity known as a local Lyapunov exponent. This exponent has been shown in past studies (e.g. Lupo et al. 2005 & Hussian et al. 2007) to be a powerful tool in that it is not only helpful in diagnosing atmospheric flow stability characteristics, but also the local predictability of the flow itself. A better understanding of Lyapunov exponent analysis and how it relates to diagnostics already used to study blocking may aid in the development of higher quality forecasts (and in turn, better lead time).

1.3.2 Objectives

Several objectives have been identified to accomplish the aforementioned purpose:

This research will:

- Examine three extreme blocking events and determine how certain diagnostic quantities may aid in resolving the problem of diagnosing block onset.
- Determine if local Lyapunov exponents are high-quality indicators of atmospheric block development and decay.
- Ascertain the role the planetary-scale flow plays on large-scale atmospheric stability around the temporal period of blocking onset and decay.

1.4 Statement of Thesis

Multiple studies on atmospheric blocking have been completed in the past. However, little research has been done using the local Lyapunov exponent as a means of diagnosing abrupt changes in the planetary-scale flow regime. The aims of this thesis are to answer fundamental questions including:

- Does the planetary-scale act as a favorable background and reinforce synoptic-scale processes with respect to blocking?

- Can local Lyapunov exponents (enstrophy) be used as a means of diagnosing blocking onset by determining changes in local flow stability characteristics?
- Does Lyapunov exponent analysis reinforce pressure-on-the-tropopause analysis as a diagnostic quantity?

Chapter 2

Data and Methodology

Multiple datasets were used for this study. The first and most basic dataset was the National Centers for Environmental Predication-National Center for Atmospheric Research (NCEP-NCAR) gridded reanalyses. More detail about this dataset can be found in Kalnay et al. (1996). Archived at NCAR in Boulder, Colorado, these analyses are available from their mass-store facilities. The reanalyses can be located at (http://www.cdc.noaa.gov/cdc/data.ncep.reanalysis.html).

In this study, a wide-range of variables (NCEP-NCAR reanalyzed) were used to study atmospheric blocking characteristics. Such variables include mean sea-level-pressure, 850-hPa mean temperatures, 500-hPa mean geopotential heights, 300-hPa scalar winds, and pressure on the dynamic tropopause.

2.1 The Blocking Index (BI)

For the purposes of basic blocking analysis, the 0000 and 1200 UTC NCEP-NCAR monthly 500-hPa gridded (2.5^{o} lat. x 2.5^{o} long.) mean geopotential height plots were accessed for each event. The Eurasian event covered the months of June through August 2003 while the Gulf of Alaska event covered the same months, except in 2004.

In this study, the blocking criteria used in Lupo and Smith (1995a&b) was employed for analysis. Below, a specific set of conditions must be met to constitute a blocking event:

1. The Rex (1950a) criteria must be satisfied for an anticyclonic flow region at 500-hPa with the exemption that the minimum duration must be five days (Triedl et al. 1981).
2. A negatve or small positive Lejenas and Okland (1983) index must be present on a Hovmöller diagram in the Northern Hemisphere.
3. Conditions one and two must be satisfied together from 24 hours after onset to 24 hours before termination.
4. The anticyclone should be poleward of 35^{o}N and the ridge should have an amplitude greater than 5^{o} latitude.
5. Block onset is described to occur when Condition four and either Condition one or two are met.
6. Termination is designated at the time the event fails Condition five for a 24 hour period or longer.

As specified in Condition two, the Lejenas and Okland (1983) criterion (LO index) is employed. This index is merely a variation of the zonal index plotted on a time-longitude diagram. A blocking event is represented as

either a negative LO value or as a weak “nontranslating” LO value (Lupo and Smith 1995a).

As for the strength of the blocking event, the criterion developed in Weidenmann (2002) as further modified from Lupo and Smith (1995a) and Lupo et al. (1997) gives a “blocking index” or BI value, from one to ten. A value closer to ten yields a stronger block, while values closer to one lend to weaker events. The BI equation, given by;

$$BI = 100.0[(MZ/RC) - 1.0] \tag{2.1.1}$$

where MZ was the maximum 500-hPa height in the closed anticyclone region or on a line associated with the ridge axis, and RC the subjectively chosen representative contour. Thus, Wiedenmann et al. (2002) shows that the resulting BI values are proportional to the gradients of height in the blocking region. Given this proportionality, the BI can be used as a diagnostic quantity for determining the relative strength, within the Northern and Southern Hemisphere blocking regions, of large-scale flow regimes as Lupo et al. (1997) discussed. Table 2.1 outlines the BI criteria with respect to Northern Hemisphere events.

Table 2.1. The strength of a blocking event given by Equation 2.1.1

Block Strength	Value of BI
Weak	BI < 2.0
Moderate	2.0 < BI < 4.3
Strong	BI > 4.3

2.2 Pressure on the Tropopause

The second dataset used in this study is the 0000 and 1200 UTC NCEP-NCAR monthly gridded (2.5^{o} lat. x 2.5^{o} long.) pressure on the tropopause. Just as with the mean geopotential height fields, the dataset's temporal domain is June through August 2003 and 2004.

Further investigation into atmospheric blocking episodes arise from the analysis of distributions of potential vorticity at or near the tropopause. In quasi-balanced flow situations, potential vorticity can offer an efficient description of the dynamic characteristics of synoptic to planetary scale flows (Morgan and Nielsen-Gammon 1998). However, such potential vorticity analysis can be complicated in that this plan of attack relies heavily on the representation of potential vorticity on surfaces of constant pressure or constant potential temperature. Using either isobaric or isentropic surfaces for this type of examination implies that for a valid understanding of the potential vorticity distributions, multiple surfaces and in turn multiple analyses must be performed. (Nielsen-Gammon and Lefevre 1996; Morgan and Nielsen-Gammon 1998; Lupo et al. 2001; Lupo and Burkhardt 2005).

Perhaps the difficulty in this methodology arises simply as an artifact of the standard definition of the tropopause. In the *International Meteorological Vocabulary*, published by the World Meteorological Organization (1992), the tropopause is defined as the layer's lower boundary in which the lapse rate is less than 2^{o}C per kilometer for at least two

kilometers. Due to the lapse rate variation near and in the WMO tropopause, (which act to produce discontinuities near the surface) Danielsen and Hipskind (1980) proposed a new definition for a “dynamic tropopause.” In terms of the dynamic tropopause, the boundary is defined as a specific value of potential vorticity. Thus, where the WMO tropopause lacks in spatial continuity, the dynamic tropopause has a higher degree of continuity over both time and space scales.

When using the dynamic tropopause, a range of potential vorticity values can be utilized as its definition. These values range from as high as 3.5 potential vorticity units (PVU) to 1 PVU, where 1 PVU equals $10^{-6}m^2s^{-1}Kkg^{-1}$ (Hoskins et al. 1985). This range is found below the nearly isothermal stratosphere but still above the weakly stratified upper portion of the troposphere. Nielsen-Gammon (2001) shows a wide range of atmospheric phenomena (from tropopause folding to high amplitude Rossby wave propagation) is very much evident in PV-tropopause studies. Along these same lines, and of particular interest for this study is the development of large anticyclones from anticyclonic plumes of potential vorticity in the mid-latitudes.

In this study, the level of the dynamic tropopause in which analysis is performed is confined to the 2.0 PVU level, as defined in the NCEP-NCAR 40-year reanalysis. Specifically, pressure on the dynamic tropopause is used to

diagnose dynamical characteristics of individual blocking events discussed in this study (Kalnay et al. 1996; Kelsey and Bosart 2006).

2.3 Local Lyapunov Exponents

In an effort to study the stability of the blocking flow itself, a method known as local Lyapunov Exponent analysis will be employed to examine each of the extreme blocking cases. The study of flow stability (via Lyapunov 1966) also contains a powerful tool, in that the use of the exponent also examines the predictability within the flow (e.g. Dymnikov et al. 1992).

Lyapunov exponents mathematically arise from the eigenvalue-solutions to the equations of motion, which describe a system's internal dynamics. In the simplest of terms, the exponent describes the time-averaged rate of change of convergence (or divergence) of nearby trajectories in a system. Since these entities are solutions to eigenvalues, there can exist as many exponents as physical system dimensions. In a system in which the sum of the Lyapunov exponents is negative, the system would exhibit a high degree of predictability. In other words, the trajectories within the phase space would converge (as time approaches infinity) towards or approach an attractor. This attractor is located in the center of the so-called "basin of attraction."

The foundations of Lyapunov exponents are rooted in the mathematical theory of infinite dimensional stability. Following this theory, blocking can naturally be seen as a quasi-stationary atmospheric circulation

(Lupo et al. 2005). With this basic premise, it becomes apparent that the best way to study this phenomenon is through the characteristics of its stability profile.

In a natural progression of thought, Lupo et al. (2005) showed that stability characteristics of a flow can be seen as analogous to the finite dimensional dynamic systems highlighted in Walters (1982). Moreover, Walters (1982) describes how the examination of “local Lyapunov exponents” was devised for the barotropic vorticity equation.

As shown in Lupo et al. (2005), for an initial vorticity field ω_o and time T = nΔt, these Lyapunov exponents are in principle given by;

$$\lambda_i(\omega_o, \mathrm{T}) = \frac{1}{2n}\log v_i \qquad (2.3.1)$$

For v_i the putatative eigenvalues of:

$$\mathrm{M}^*\mathrm{M}, \mathrm{M} = \prod_{k=-n}^{k=n} \mathrm{B}(k\Delta t) \qquad (2.3.2)$$

B(t) the linearization operator of the barotropic equations of ω(t). Through a process known as a Crank-Nicholson scheme, the above is expressed in a numerical way (Dymnikov et al. 1992).

Given a domain D (specific to each blocking event analyzed in this study) data over a three-year period is placed through a planetary-scale (15-day) filter. The sum of the positive Lyapunov exponents shows a strong

correlation to the linearized barotropic flow eigenvalues as well as the domain-integrated enstrophy;

$$\sum \lambda_{+} \approx \int_{D} |\omega|^{2}(x,y)dxdy \tag{2.3.3}$$

The power of enstrophy (at least as a forecasting tool) is truly shown by the fact that the increasing nature of the sum of positive Lyapunov exponents decreases the average time for the ω-trajectories to diverge (Lupo et al. 2005). Physically, enstrophy is to vorticity as kinetic energy is to velocity.

By using Lyapunov exponents as a rigid treatment of atmospheric blocking flows (in other words a dynamic, infinite dimensional system), one must realize that a theory of Lyapunov exponents in infinite dimensions can be developed (Constantin and Foias 1985). When considering a flow in this context, it is apparent that the domain is one of many possible atmospheric flows as opposed to the classical treatment of Lyapunov exponents of a single, steady flow (Cohen and Schultz 2005).

As shown above, there exists a linkage between eigenvalues of the linearization and the positive exponents. In recognition of this premise, Lupo et al. (2005) produced a version simplified for the use on steady flows. Given a full sphere that possesses a steady barotropic flow, with Rayleigh friction and devoid of orography, let;

$$C_1 = \max\left|\nabla\Psi\right|$$
$$C_2 = \max\left|\nabla\Omega_a\right| \qquad (2.3.4)$$

where Ψ represents the streamfunction of a stationary flow and

$$\Omega_a = \nabla^2\Psi + 2\sin\phi \qquad (2.3.5)$$

The eigenvalue problem for the flow linearization can be shown from Skiba (2002) as;

$$\Delta u + Mu = \lambda u \qquad (2.3.6)$$

for $\left|< Mu, u>\right| \le C\left\|u\right\| \left\|\left|u\right|\right\|$, for C = max{$C_1$,$C_2$/2} for two different norms $\|\bullet\|$, $|||\bullet|||$. Prodi then makes the argument in his 1962 paper (pages 385-387) that the discrete spectrum is inside the parabola;

$$\Re(\lambda) = -\frac{1}{4C^2}\left(\Im\lambda\right)^2 + C^2 \qquad (2.3.7)$$

Specifically, (for C = max{C_1,C_2/2}) Equation (2.3.7) shows that the complex plane between the parabola and imaginary axis contains all the stationary flow's unstable modes. Thus, the flow will become increasingly unstable if either the maximum absolute value of $\nabla\Psi$ (a representation of the geostrophic wind) or the maximum absolute value of $\nabla\Omega_a$ (a measure of barotropic instability) increase. The opposite is true for an atmosphere that

becomes increasingly stable; decreasing values of either $\nabla\Psi$ or $\nabla\Omega_a$ tend to stabilize the flow regime (Lupo et al. 2005).

Chapter 3

Synoptic Analysis

3.1 Western Europe: 06 – 13 2003

a. 500-hPa Mean Geopotential Height Analysis

From the NCEP-NCAR 500-hPa mean height reanalysis, a noticeable trough/ridge couplet (Figure 3.1.1) is found over the Northern Atlantic basin and Western Europe (40^{o}W – 20^{o}E latitude; 25^{o}N – 70^{o}N longitude). As seen in Figure 3.1.2, when the zonal mean is subtracted from the height field, two pronounced anomalous regions become evident. Over the North Atlantic basin, an extremely deep (-10 dam) trough is found while over Western Europe, a strong (+6 dam) ridge is present. The location of the ridge is present in the mean 500-hPa height fields.

The ridge axis appeared to be centered around 7^{o}E, which is the eastern part of France. As expected, this 500-hPa height anomaly represented the blocking flow that produced the Western European heat wave. By the end of August, the height anomaly dissipated as a more zonal flow took its place.

According to the Wiedenmann et al. (2002) Blocking Index, the Western European blocking event registered at 1.99, just shy of a moderate strength event and was centered on the Prime Meridian. Officially (Lupo et

al. 2005), the event lasted for seven consecutive days, beginning on 06 August 2003 and ending 13 August 2003.

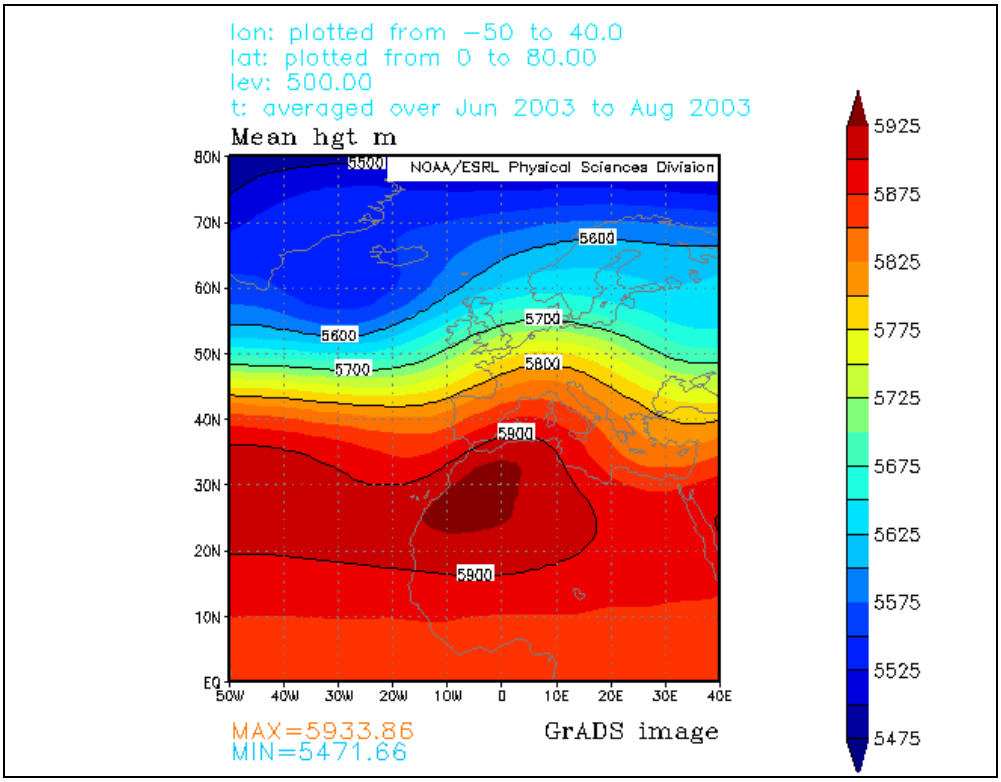

Figure 3.1.1 NCEP-NCAR monthly 500-hPa gridded (2.5^{o} lat. x 2.5^{o} long.) mean geopotential height valid June – August 2003. Solid black lines represent geopotential height contours (m).

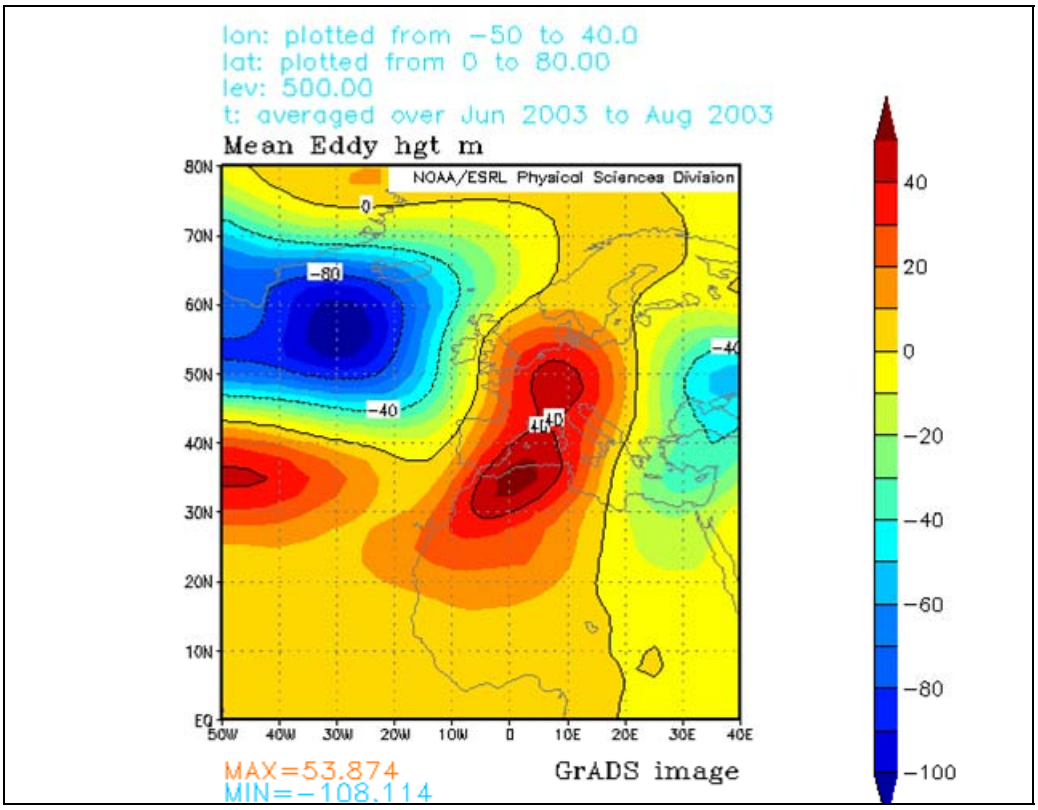

Figure 3.1.2. NCEP-NCAR monthly 500-hPa gridded (2.5^{o} lat. x 2.5^{o} long.) mean geopotential height valid June – August 2003. Solid black lines represent intervals of mean eddy height (m). The zonal mean is subtracted to show the positive 500-hPa height anomaly over Western Europe.

The 500-hPa geopotential height fields corresponding to the strongest blocking signature (06 August – 12 August 2003) showed the geopotential minimum over the Atlantic Ocean registered around 5525 gpm. Over the next two to three days, this feature filled and migrated both north and east towards the European continent. During the same period, the trough appears highly symmetric within the Atlantic basin, nearly mimicking the height ridge over Western Europe, except appearing as an upside-down omega as seen in Figure 3.1.3.

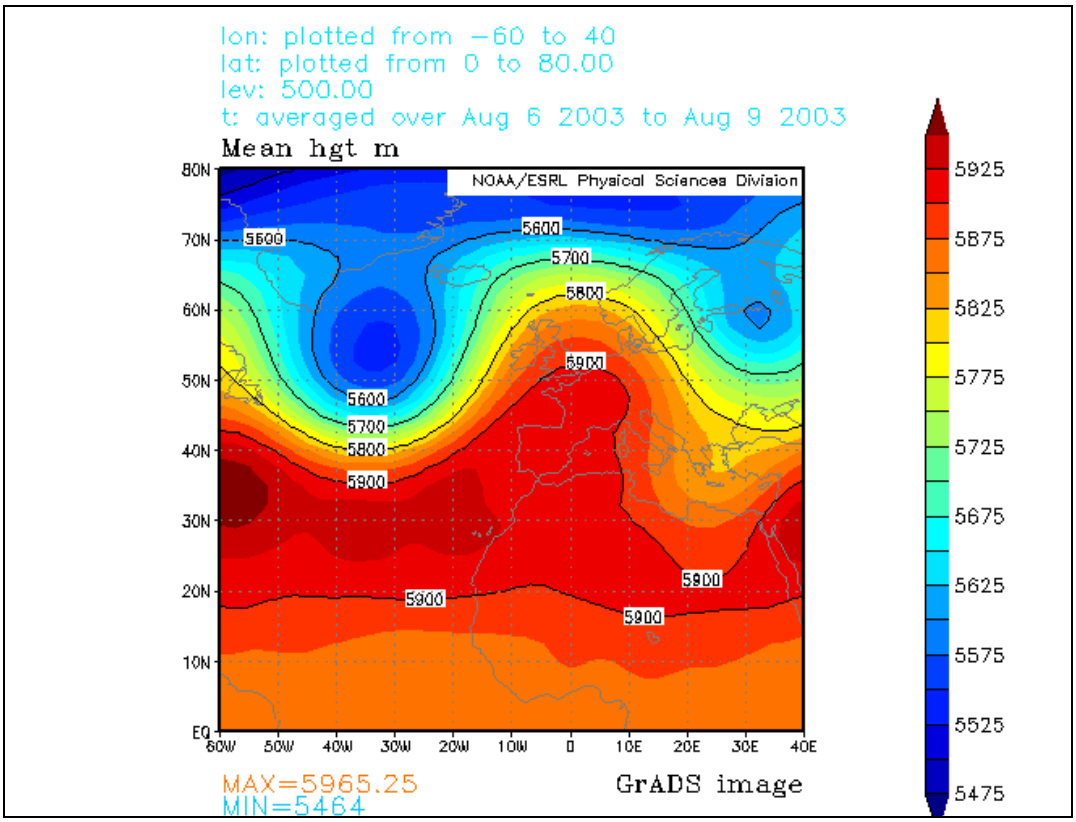

Figure 3.1.3. NCEP-NCAR monthly 500-hPa gridded (2.5° lat. x 2.5° long.) mean geopotential height valid 06 August – 09 August 2003. Solid black lines represent geopotential height contours (m).

The symmetric appearance of both positive and negative height features diminished as the flow became more "sheared" over the next three-day period of 09 - 12 August 2003. In this case, "sheared" is used to convey the appearance of the trough and ridge modifying from neutral to positive. The shearing also acted to amplify the blocking region, allowing the anomalously hot air beneath the blocking ridge to migrate further north and east over Western Europe (Fig 3.1.4). A secondary negative height feature

also appeared to deepen along with the upstream block. Accordingly, this period marked the hottest period of the entire blocking episode.

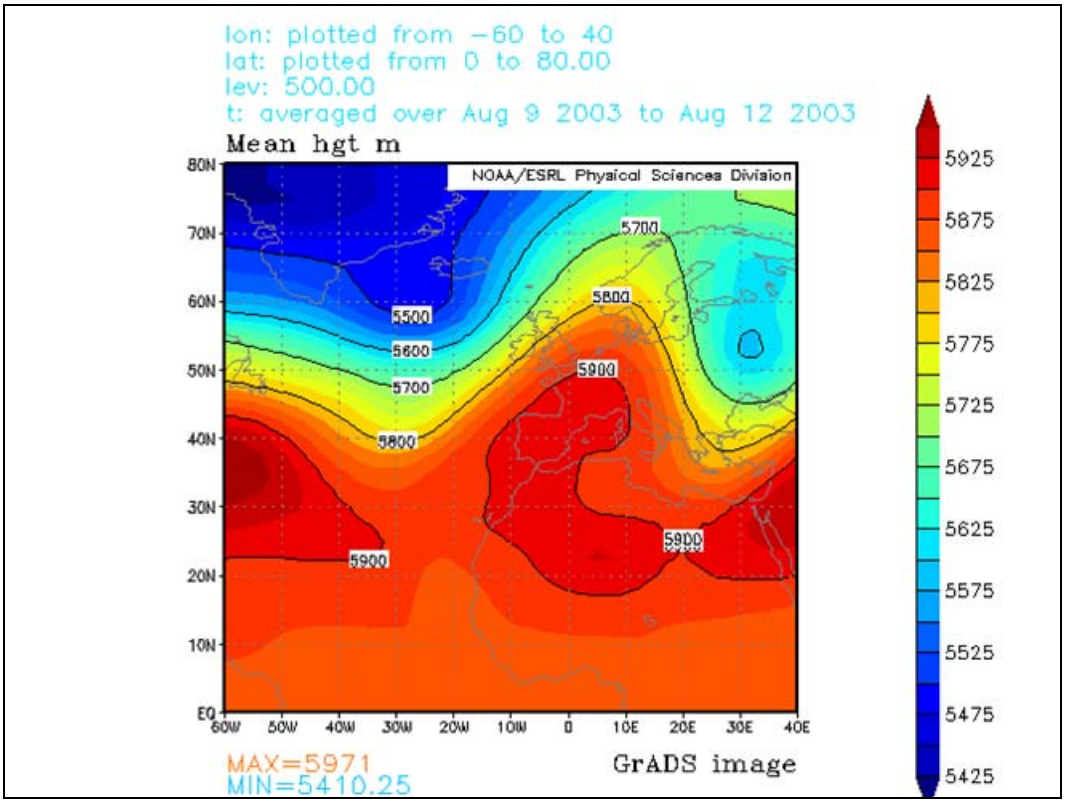

Figure 3.1.4. NCEP-NCAR monthly 500-hPa gridded (2.5^{o} lat. x 2.5^{o} long.) mean geopotential height valid 09 August – 12 August 2003. Solid black lines represent geopotential height contours (m).

The dissipation of the European block, and in turn, the severe heat wave is represented by the de-amplification of the highly meridional flow into a quasi-zonal flow, beginning around 12 August and reaching full fruition on 15 August 2003 (Figure 3.1.5). Along with de-amplification, the height ridge continued to propagate further east.

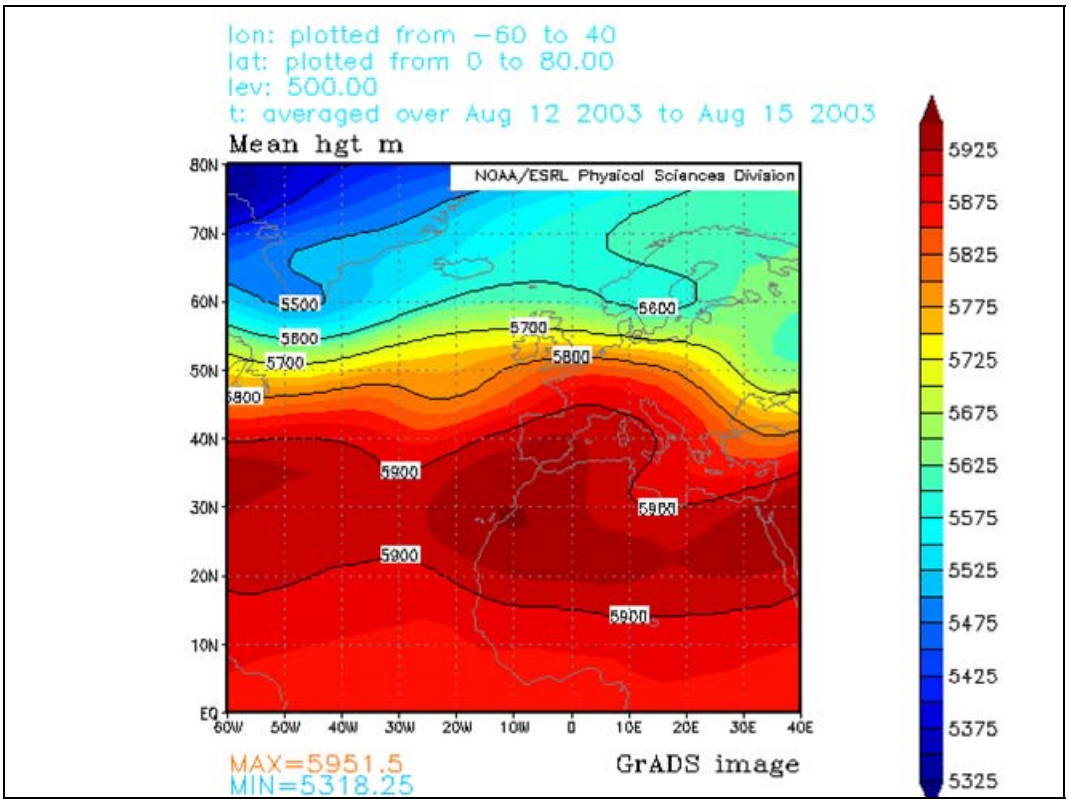

Figure 3.1.5. NCEP-NCAR monthly 500-hPa gridded (2.5^{o} lat. x 2.5^{o} long.) mean geopotential height valid 12 August – 15 August 2003. Solid black lines represent geopotential height contours (m).

b. 850-hPa Mean Temperature Analysis

Upon inspection of the 850-hPa mean temperatures over the same period, a high degree of correspondence existed between the lower level temperature regime and the 500-hPa mean geopotential height patterns. Over the most severe fifteen days of the European heat wave, the abnormally warm air (22^{o}C–27^{o}C) seemed to be related to two source regions located along a belt between the 20^{o}N to 30^{o}N. The first and warmest source region visible in the 850-hPa mean temperature fields is located over central Saudi Arabia, reaching into western Iran. The second visible region of anomalous warmth hugs the northwestern coast of Africa,

with the temperature maximum centered on western Algeria (25°N, 5°W). Taken together, the two warm regions created a dumbbell (figure 3.1.6) feature that expanded and contracted over time. Interestingly enough, as one source region warmed up the other source region cooled down. Spatially, the African source region appears to be less consistent (i.e. expansion and contraction rate more erratic) than that of the Saudi Arabian source region.

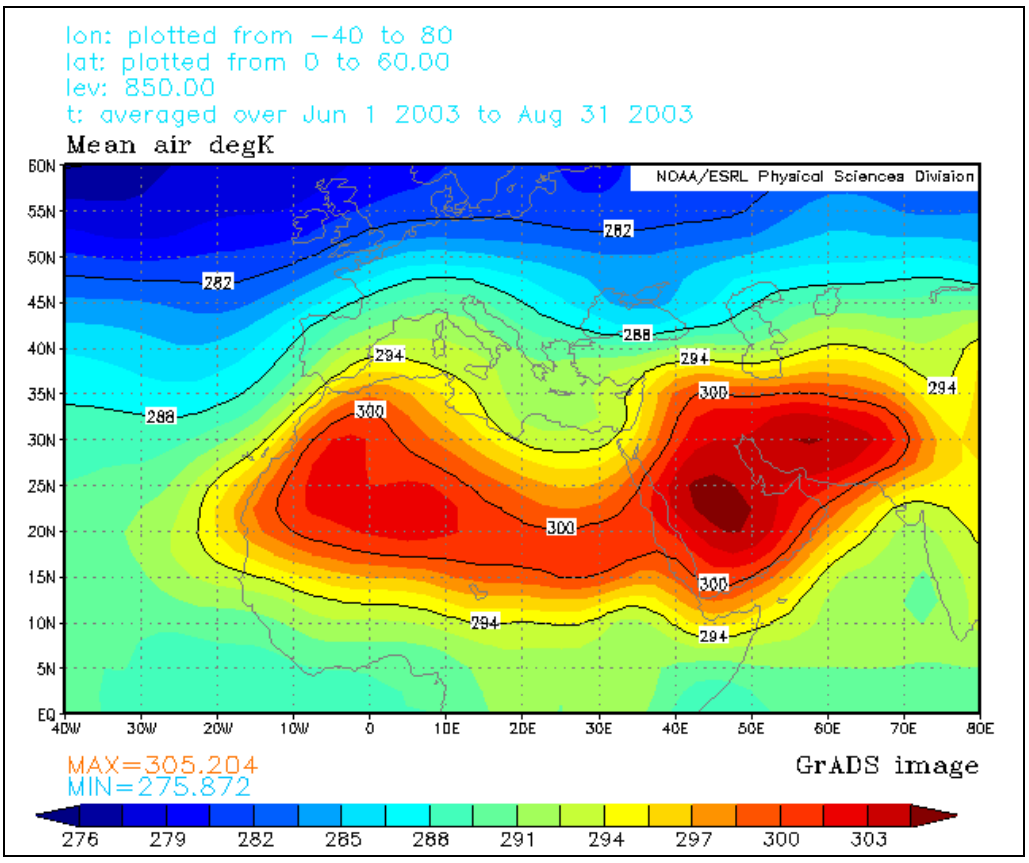

Figure 3.1.6. NCEP-NCAR monthly 850-hPa gridded (2.5° lat. x 2.5° long.) mean temperatures valid 01 June – 31 August 2003. Solid black lines represent isotherms (K).

The NCEP-NCAR 850-hPa mean temperature reanalysis from 01 - 03 August 2003 (Figure 3.1.7) showed a ridge of anomalously warm temperatures gripping much of the Iberian Peninsula. Of particular interest is the 22^{o}C (295 K) mean isotherm, which was nearing the southern boundary of France. Further east, a temperature trough of comparable magnitude and spatial extent existed over the Mediterranean Sea. This particular set-up gives the impression that the hot air from the African source region is being funneled northward in a clockwise fashion underneath the temperature ridge located over Western Europe. Support for this is given by the 500-hPa mean height field for the same period. The strong blocking pattern that is present at 500-hPa is in perfect position to allow for the build up of heat in the lower levels of the atmosphere.

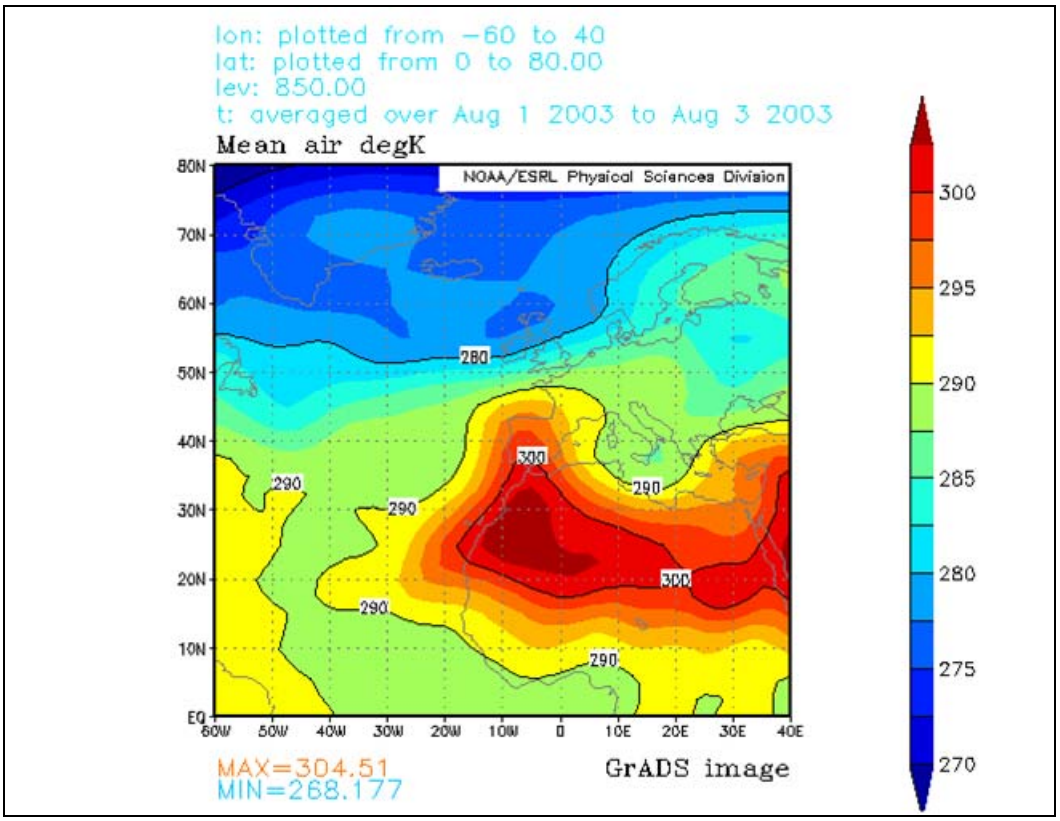

Figure 3.1.7. NCEP-NCAR monthly 850-hPa gridded (2.5^{o} lat. x 2.5^{o} long.) mean temperatures valid 01 - 03 August 2003. Solid black lines represent isotherms (K).

As the positive height anomaly continued to amplify over the next three days, so too did the 850-hPa ridge. In fact, with the 22^{o}C (295 K) mean isotherm covering most of western France, the 27^{o}C (300 K) mean isotherm was nearly touching the southern tip of Spain (Figure 3.1.8).

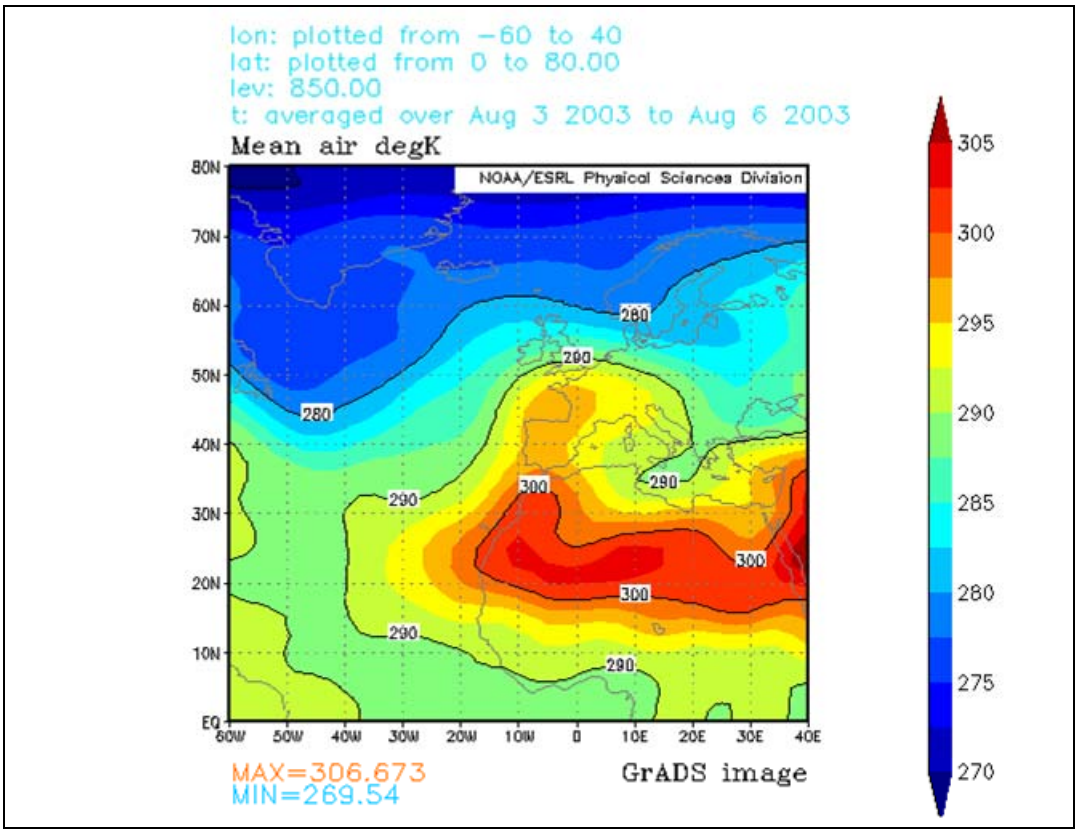

Figure 3.1.8. NCEP-NCAR monthly 850-hPa gridded (2.5^{o} lat. x 2.5^{o} long.) mean temperatures valid 03 – 06 August 2003. Solid black lines represent isotherms (K).

The most active period of the entire month of August occurred for around six days, starting on 06 August. The amplitude of the 850-hPa mean temperature ridge increased in such a way (over the past three days) that a poleward perturbation was evident in the 7^{o}C (280 K) mean isotherm, located around 73^{o}N. For comparison, the 01 August location of this isotherm was 53^{o}N.

Of particular note is the location of the warmest part of the air mass in relation to Europe. As of 09 August, the 24.5^{o}C (297.5 K) mean isotherm was covering much of eastern Spain, France and the southern tip of the

British Isles. Ridging in the temperature field slowly began tilting more positive, as the feature propagated eastward over the European continent. With this eastward propagation, the 24.5°C (297.5 K) mean isotherm continued its northwestward advancement (Figure 3.1.9), eventually covering the whole of Western Europe (as far north and east as 50°N, 10°E).

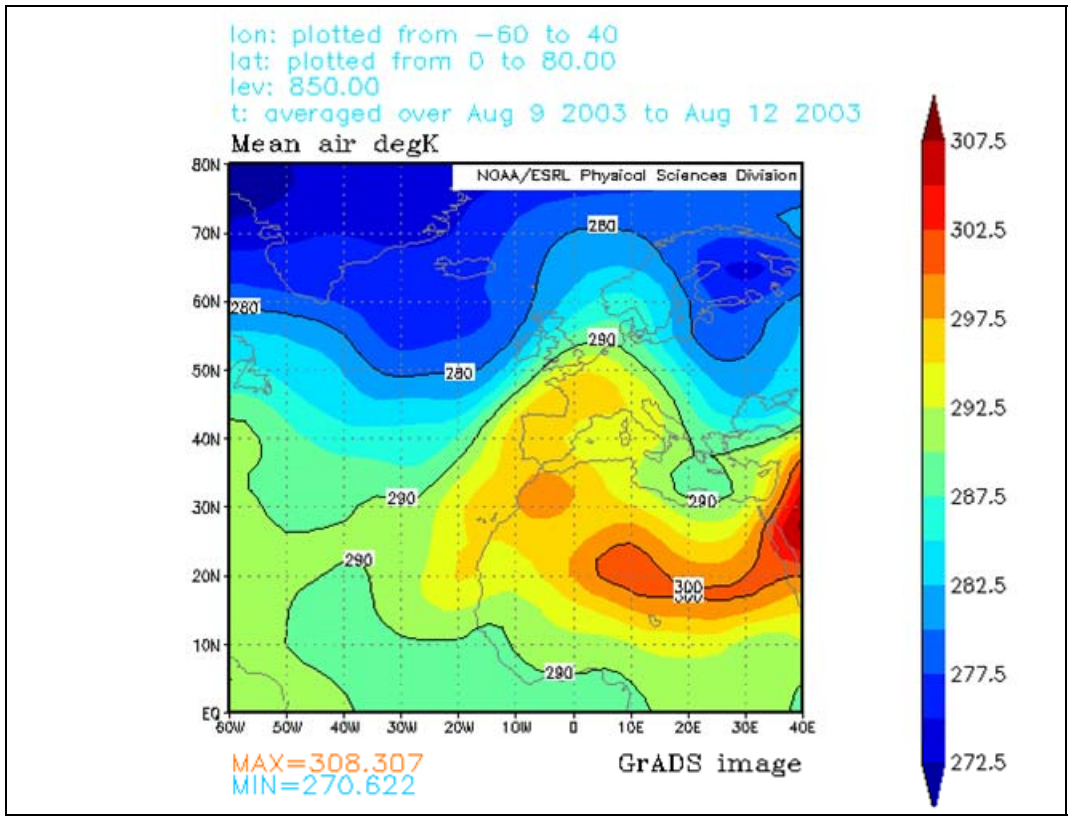

Figure 3.1.9. NCEP-NCAR monthly 850-hPa gridded (2.5° lat. x 2.5° long.) mean temperatures valid 09 -12 August 2003. Solid black lines represent isotherms (K).

While the unbearable heat continued to infiltrate Western Europe, a curious flow feature became evident with time. The hot air seemed to be advecting into the amplifying temperature ridge (which owes its existence to the block) via a clockwise circulation from the African source region. Moreover, it is highly possible that the warm air was being heated even further by air mass modification over the Sahara desert in northern Africa. This cyclonic advection into the amplifying ridge diminished and moved eastward as the trough over the Atlantic moved into the region (Figure 3.1.10)

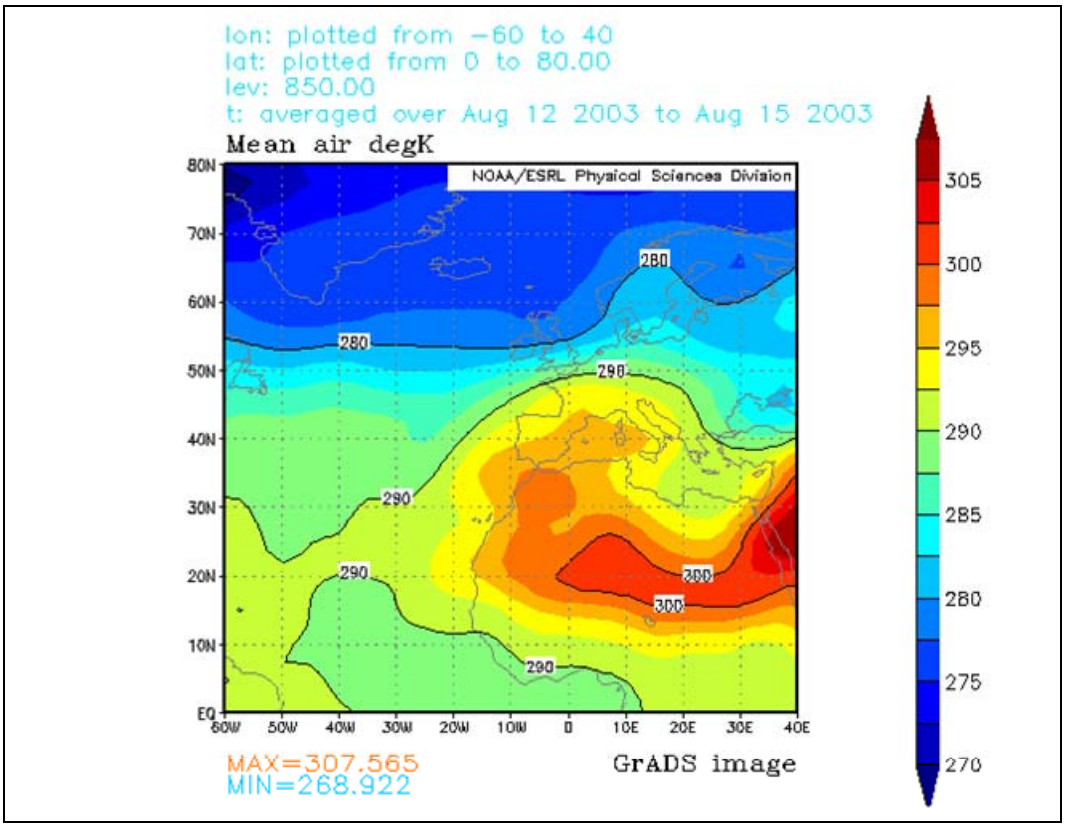

Figure 3.1.10. NCEP-NCAR monthly 850-hPa gridded (2.5^{o} lat. x 2.5^{o} long.) mean temperatures valid 12 - 15 August 2003. Solid black lines represent isotherms (K).

The anomalous heating of the western reaches of Europe finally began to diminish as the 850-hPa temperature ridge bounded by the 22°C (295 K) mean isotherm retreated south and east, towards the southern coast of France and western coast of Italy as seen in the previous figure. After 15 August, the 17°C (290 K) mean isotherm moved into the southern parts of Spain and France, as the ridge continued to de-amplify and move over the Mediterranean. Concurrently, the 500-hPa positive height anomaly had almost completely disappeared. The uncharacteristically hot air retreated back to the source regions, as shown by the mean temperature increases in Figure 3.1.12.

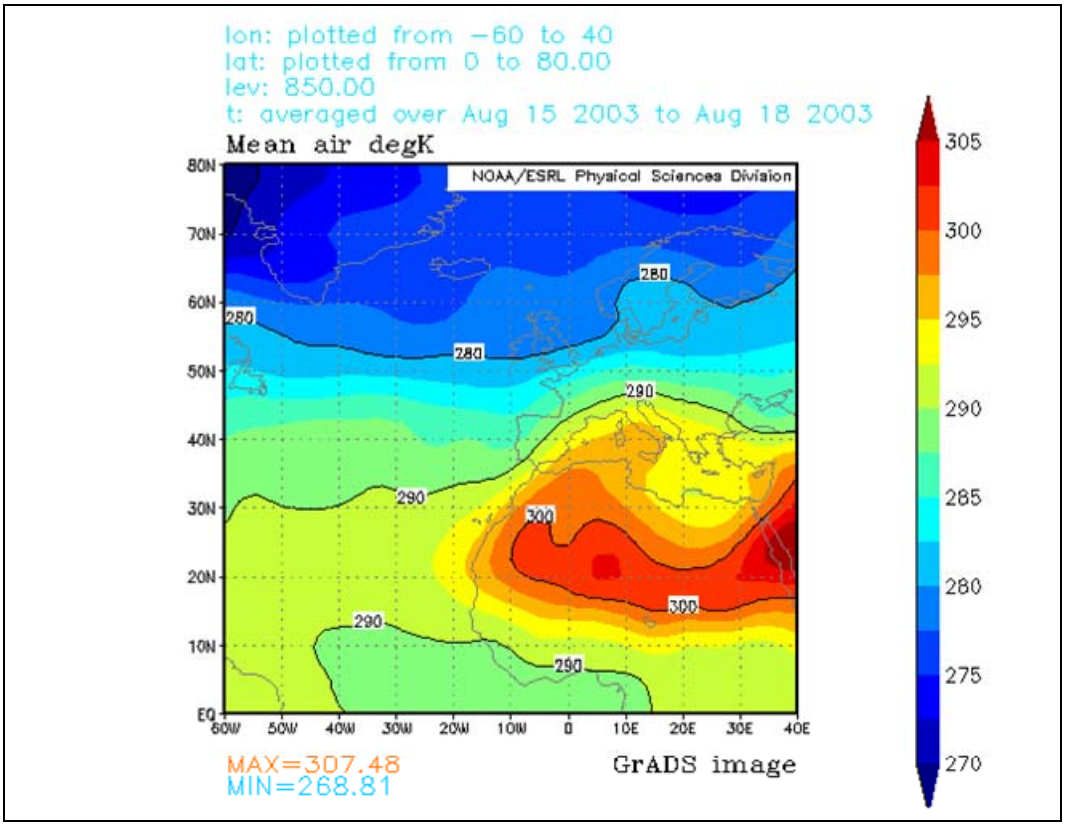

Figure 3.1.11. NCEP-NCAR monthly 850-hPa gridded (2.5° lat. x 2.5° long.) mean temperatures valid 15 - 18 August 2003. Solid black lines represent isotherms (K).

c. 300-hPa Mean Scalar Wind Analysis

A 30-year NCEP-NCAR mean scalar wind analysis at the jet stream level (300-hPa) showed a well-defined quasi-zonal jet situated over the Northern Atlantic basin (Figure 3.1.12). The jet core (winds in excess of 28 ms^{-1}) was found 10^{o} south of the tip of Greenland. The zonal character of the jet stream extended well into the British Isles and as far east as Eastern Europe. Wind speeds in the aforementioned region range from 24 ms^{-1} over Great Britain to 18 ms^{-1} over Western Europe.

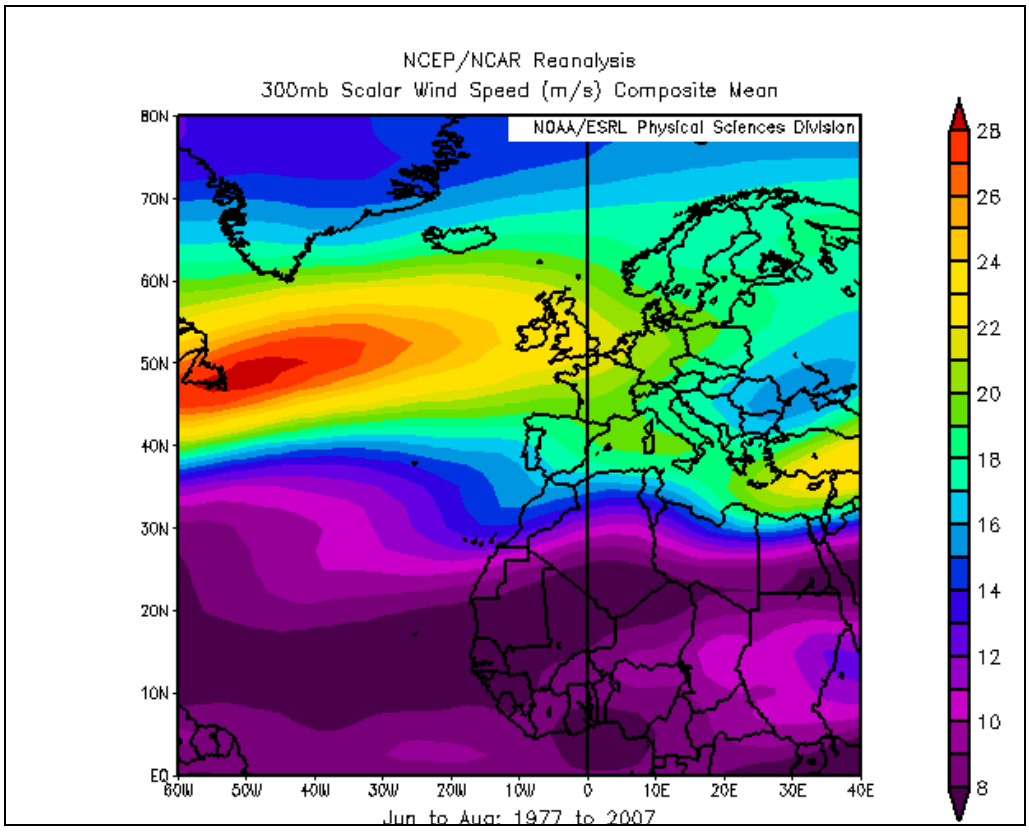

Figure 3.1.12. NCEP-NCAR monthly 300-hPa gridded (2.5^{o} lat. x 2.5^{o} long.) mean scalar winds valid June - August 1977 - 2007. Solid black lines represent isotachs (ms^{-1}). The character of the jet is quasi-zonal.

When the August 2003 mean 300-hPa mean scalar winds were analyzed, a noticeable ridge was found over Great Britain, stretching into Eastern Europe. The ridge axis was centered on the Prime Meridian and at 55^{o}N, two distinct jet cores of similar magnitude (27 ms^{-1}) were located at 20^{o}W and 20^{o}E (Figure 3.1.13). The anticyclonic jet ridge corresponded almost exactly with the 500-hPa blocking ridge.

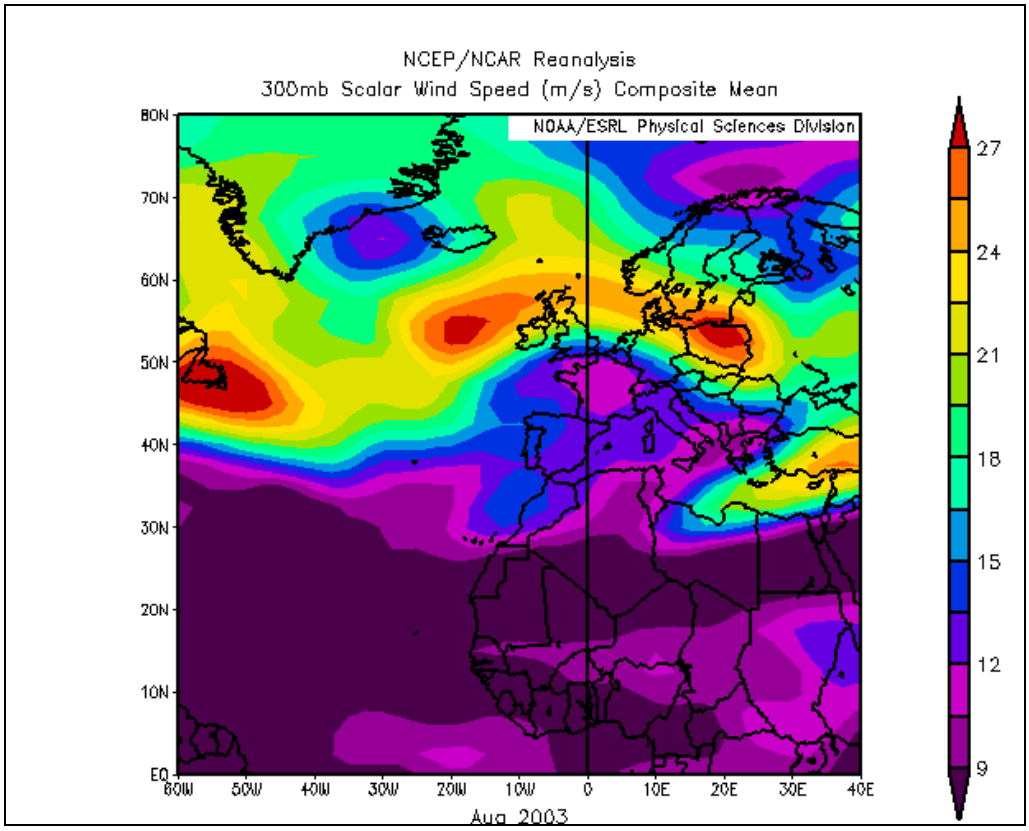

Figure 3.1.13. NCEP-NCAR monthly 300-hPa gridded (2.5^{o} lat. x 2.5^{o} long.) mean scalar winds valid August 2003. Solid black lines represent isotachs (ms^{-1}).

3.2 Gulf of Alaska: 24 June – 05 July 2004

From the NCEP-NCAR mean 500-hPa height reanalyses, a pronounced ridging in the height fields was clearly visible for the period of June - August, 2004. The ridge axis (65^{o}N, 140^{o}W to 55^{o}N, 120^{o}W) is located over the state of Alaska and into parts of British Columbia and the Yukon Territory. Upstream of the ridge, a smaller amplitude trough was found. When the zonal mean is subtracted from the field, the same dipole anomaly is present. A curious feature appears though in that the positive height anomaly was visible as a dipole entity (+7 dams). Upstream of the ridge is deep trough (-4 dam). Both the ridge and trough covered a good portion of the upper Pacific Ocean basin (25^{o}N – 80^{o}N; 140^{o}E – 100^{o}W).

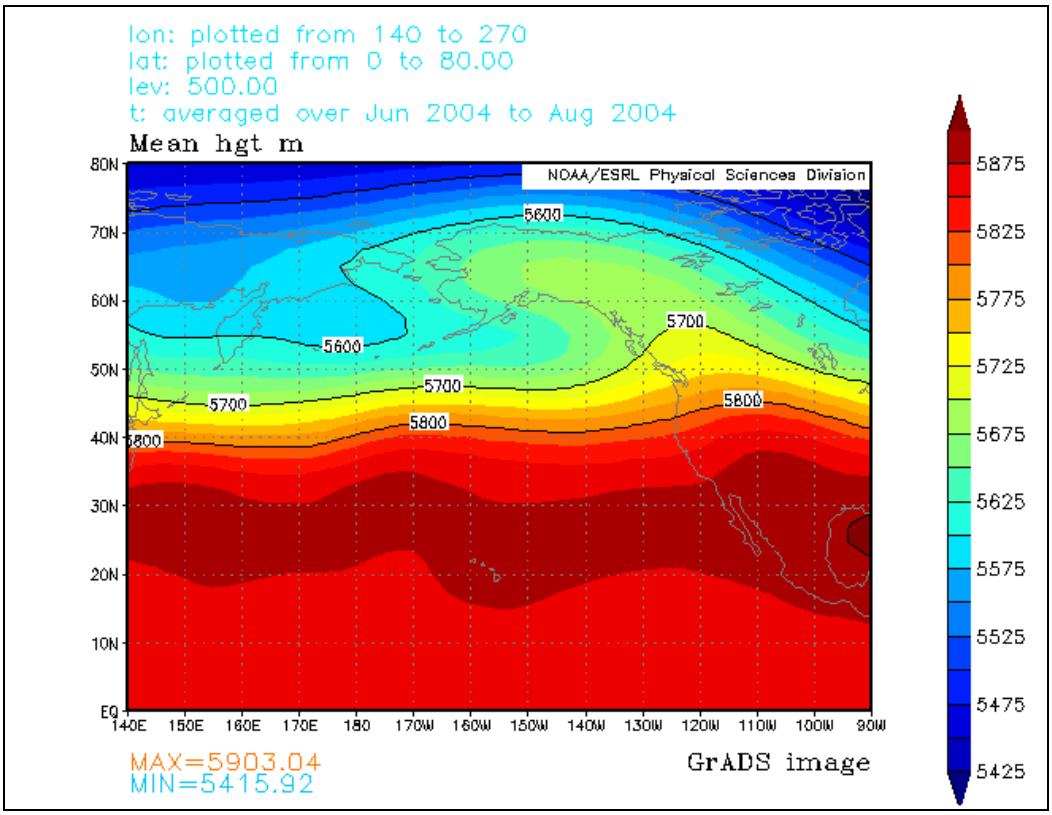

Figure 3.2.1. NCEP-NCAR monthly 500-hPa gridded (2.5^{o} lat. x 2.5^{o} long.) mean geopotential height valid June – August 2004. Solid black lines represent geopotential height contours (m).

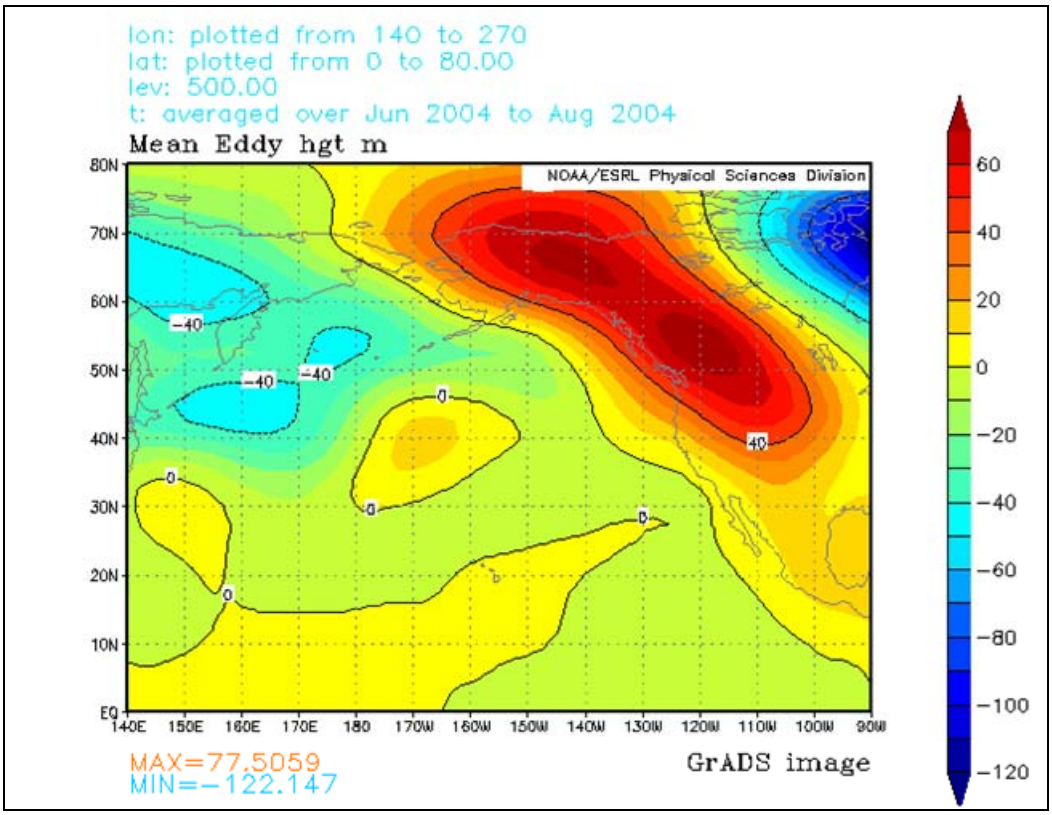

Figure 3.2.2. NCEP-NCAR monthly 500-hPa gridded (2.5^{o} lat. x 2.5^{o} long.) mean geopotential height valid June – August 2004. Solid black lines represent intervals of mean eddy height (m). The zonal mean is subtracted to show the positive 500-hPa height anomaly over Alaska and Western Canada.

Analysis of the “Baked Alaska” blocking event shows that the event was not confined to just one event, but two distinct events. The first event occurred from 24 June through 5 July 2004. The second event occurred much later in the season (5 – 28 August 2004) and lasted nearly twice as long (Figure 3.2.3a&b)

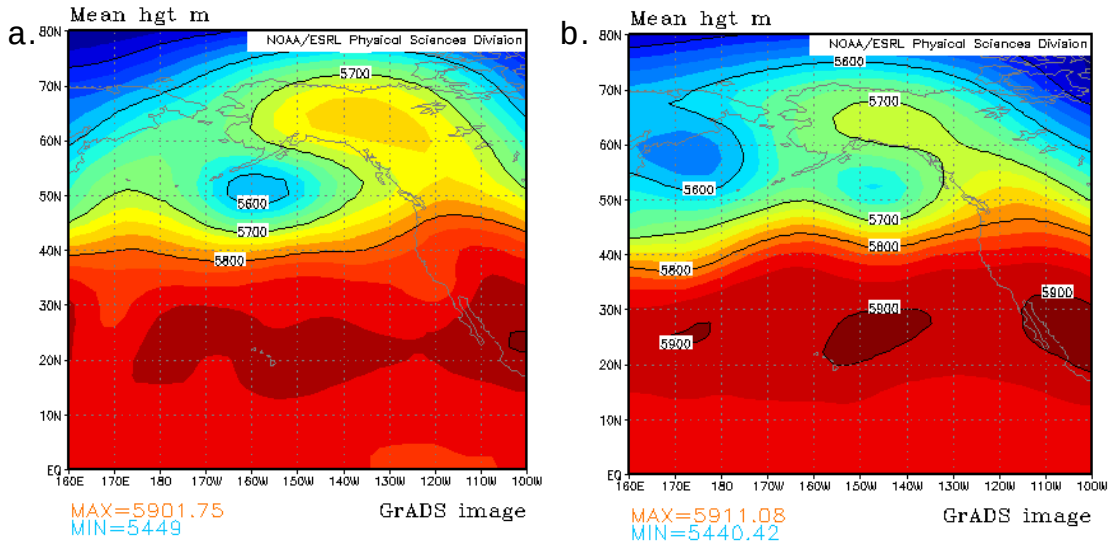

Figure 3.2.3. NCEP-NCAR monthly 500-hPa gridded (2.5^{o} lat. x 2.5^{o} long.) mean geopotential height valid (a) 24 June – 05 July, 2004 & (b) 05 – 28 August, 2004. Solid black lines represent geopotential height contours (m).

Initiation of the block occurred around 24 June 2004. Data from the MU Global Climate Change Group, using the Wiedenmann et al. (2002) Blocking Index shows the event registered as a moderate blocking episode, centering on 130^{o}W and lasting for 11 consecutive days.

a. 500-hPa Mean Geopotential Height Analysis

Analysis of the mean 500-hPa geopotential height fields show the blocking ridge was located on the extreme southern and western coast of the Gulf of Alaska (Figure 3.2.4). Two to three days before the block was in place, the amplification of the ridge itself is very evident, with the 5700 gpm isoheight extending to 70^{o}N and 160^{o}W.

As the positive height anomaly continued to amplify, it appears that higher heights were being advected in a counterclockwise fashion poleward, along the coast of Canada through the Yukon Territory and into the eastern portions of Alaska. Figure 3.2.5 shows the larger height values (5750-5800 gpm) infiltrated much of western Canada and Alaska. The 5800 gpm isoheight remained cutoff from the main area of higher heights, further equatorward.

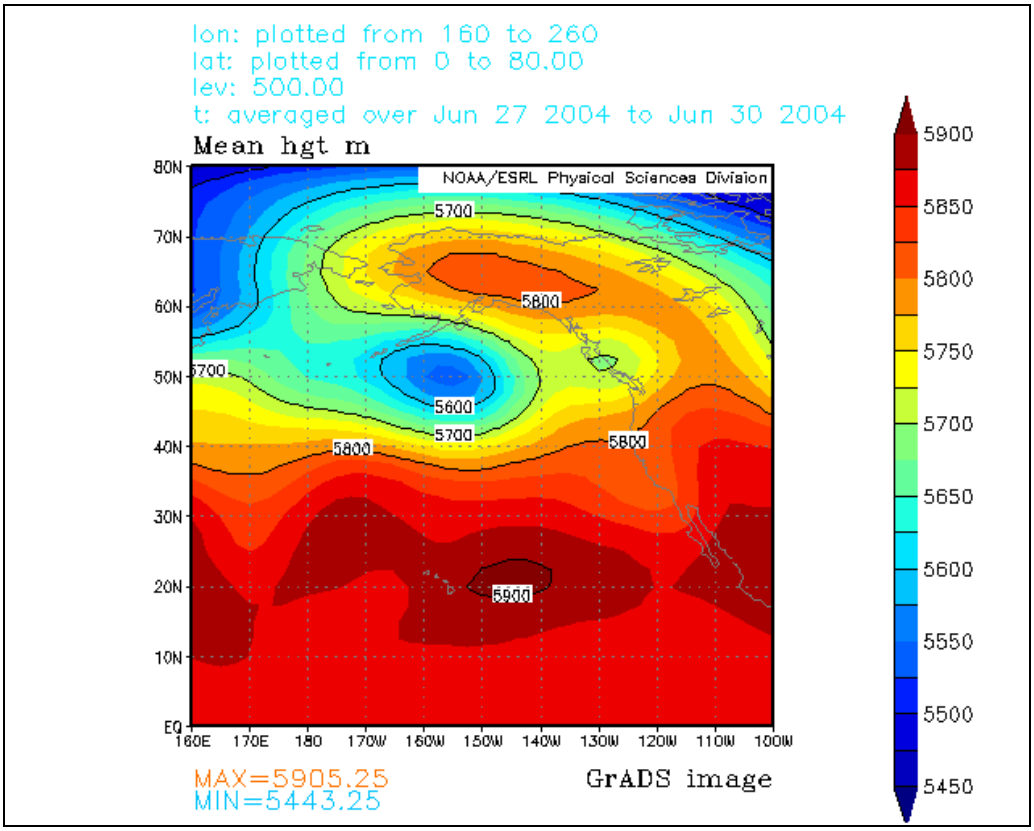

Figure 3.2.4. NCEP-NCAR monthly 500-hPa gridded (2.5° lat. x 2.5° long.) mean geopotential height valid 27 – 30 June 2004. Solid black lines represent geopotential height contours (m).

It is safe to say that the six day period following 24 June saw the most intense blocking, as the counterclockwise advection of higher heights acted to amplify the blocking ridge already in place. However, just as fast as the block strengthened, it quickly de-amplified as the anomalously higher height fields retreated back into the continental United States.

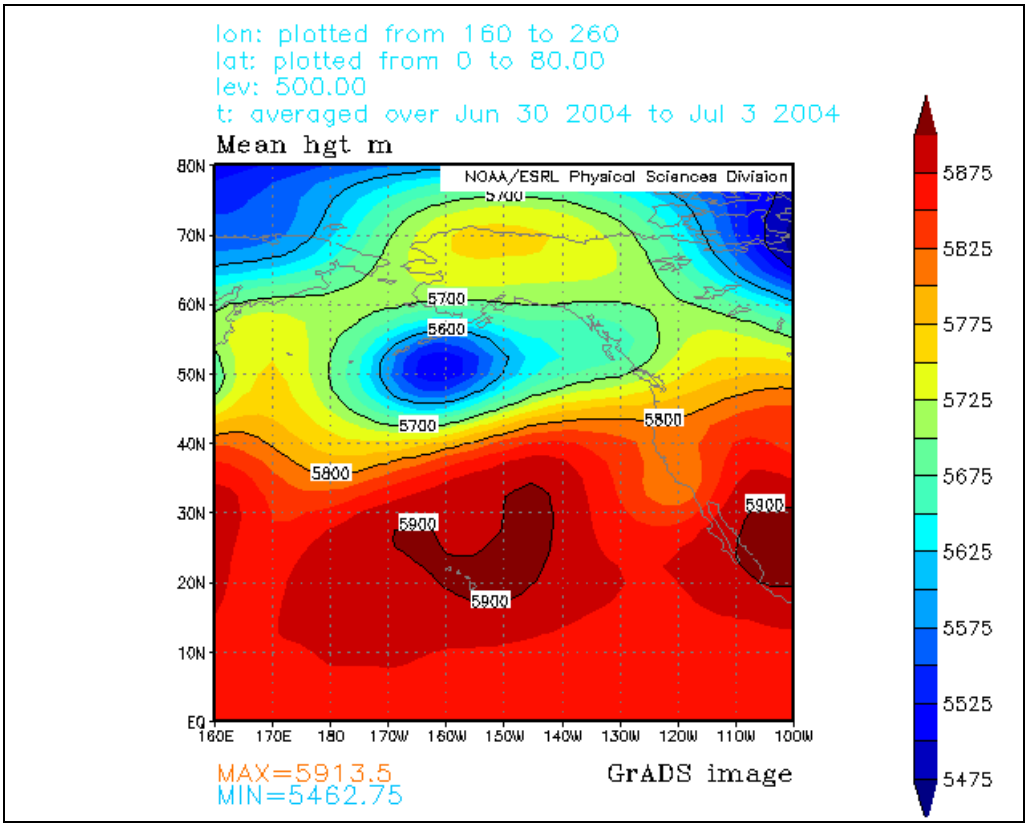

Figure 3.2.5. NCEP-NCAR monthly 500-hPa gridded (2.5^{o} lat. x 2.5^{o} long.) mean geopotential height valid 30 June 2003 – 03 July 2003. Solid black lines represent geopotential height contours (m).

From 30 June to 05 July, amplification of the blocking ridge began to stifle, as the location of lower heights deepened and migrated further east, into the Gulf of Alaska. As of 03 July, the 5700 gpm isoheight was located

over the mid–section of Canada as the block dissipated completely over the following two days.

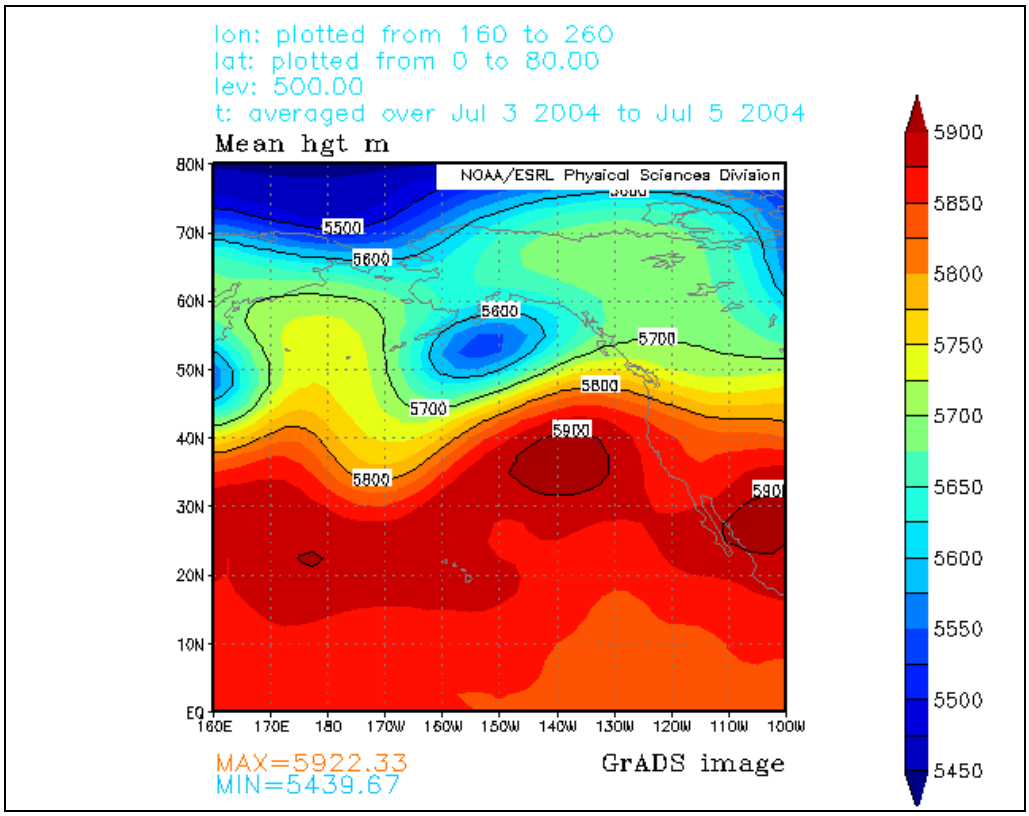

Figure 3.2.6. NCEP-NCAR monthly 500-hPa gridded (2.5^{o} lat. x 2.5^{o} long.) mean geopotential height valid 03 - 05 July 2004. Solid black lines represent geopotential height contours (m).

b. 850-hPa Mean Temperature Analysis

Analysis of the 850-hPa mean temperature fields shows the progression of the anomalously warm air poleward from the source regions in the desert southwest of the United States. Within the blocking region, or rather in the absence of blocking in this region, the normal June - July temperatures at this level range from -1^{o}C (272 k) (southern boundary of

Alaska/Gulf of Alaska) to -9^{o}C (264 K) (northern extent of the peninsula). At the height of the “Baked Alaska” event, mean temperatures in this region were on the order of 16-20^{o}C (289 – 293 K) warmer than normal.

Two days before the block was completely in place, hot air was already streaming into western Alaska. In fact, the mean 15^{o}C (288 K) isotherm was just on the doorstep of Alaska’s eastern border with Canada’s Yukon Territory. Figure 3.2.7 shows that over the next four days, the hottest of the anomalously warm air returned to the west coast of the United States. What remained over Alaska and western Canada was enclosed by the 15^{o}C (288 K) isotherm, with a smaller region (10^{o} lat. X 10^{o} long.) of temperatures reaching 18^{o}C (291 K).

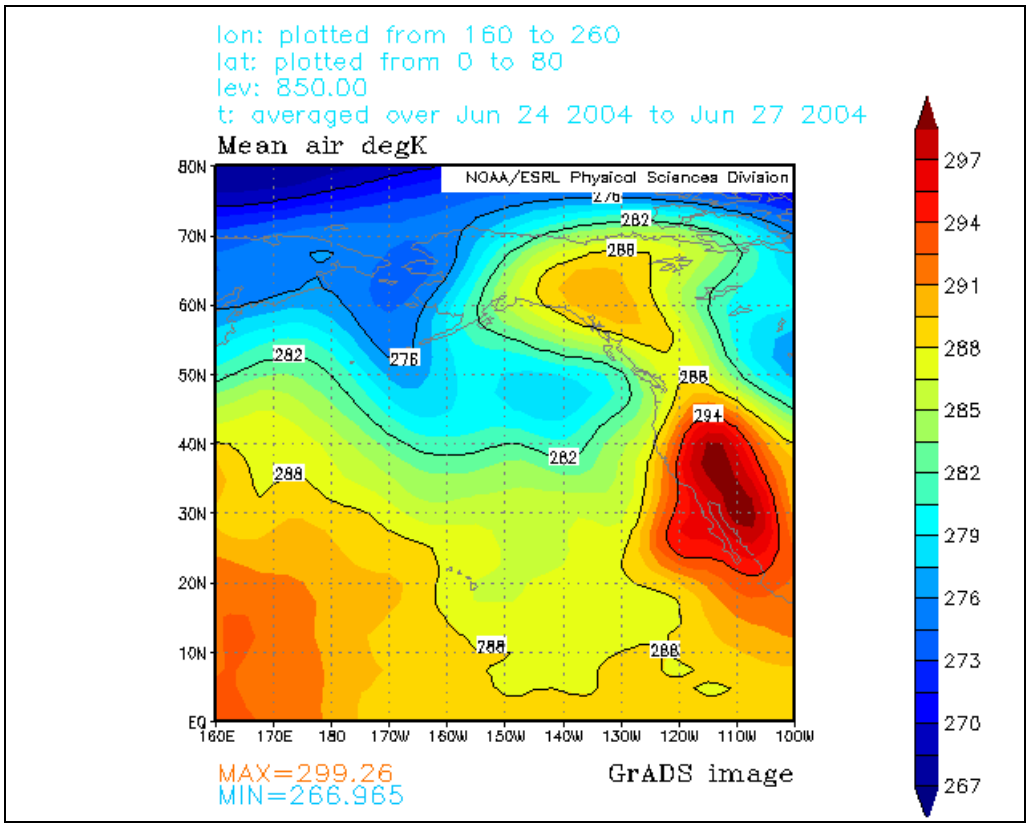

Figure 3.2.7. NCEP-NCAR monthly 850-hPa gridded (2.5° lat. x 2.5° long.) mean temperatures valid 24 – 27 2004. Solid black lines represent isotherms (K).

Since the blocking ridge was still in place, temperature advection north and westward under the ridge was still occurring. Moreover, while the warmest air still remained to the south of the blocking region, above-average warmth was still spreading over the whole of Alaska and into the Bering Strait by 30 June, as the block began to dissipate (Figure 3.2.8).

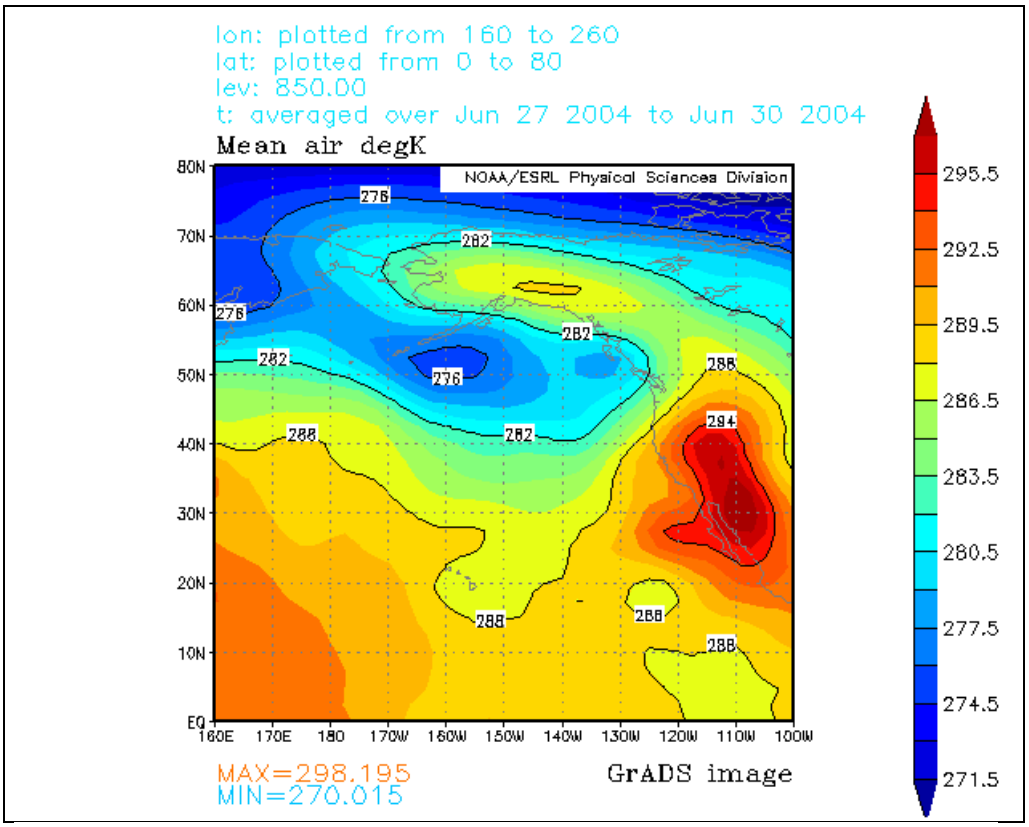

Figure 3.2.8. NCEP-NCAR monthly 850-hPa gridded (2.5 ^{o} lat. x 2.5^{o} long.) mean temperatures valid 27 - 30 June 2004. Solid black lines represent isotherms (K).

The period from 30 June – 05 July saw the eventual return of near-normal temperatures; yet over this period 10^{o}C (283 K) above normal mean temperatures still held strong, even as the block dissipated completely. With no block present, the hot-air regions moved further north and east, as near normal means began to build back into the region.

c. 300-hPa Mean Scalar Wind Analysis

A June – August 30–year climatology for the 300-hPa mean scalar winds details a zonal pattern over the northern Pacific basin (Figure 3.2.9).

The strongest core of winds (26 ms^{-1}) was located just south of the Aleutian Islands, near 57°N. Also of note was a trough in the wind field just off the coast of North America, stretching southwest to Hawaii. A secondary minimum was located over the Alaskan/Canadian border. Wind speeds within this region slow to around 13 ms^{-1}.

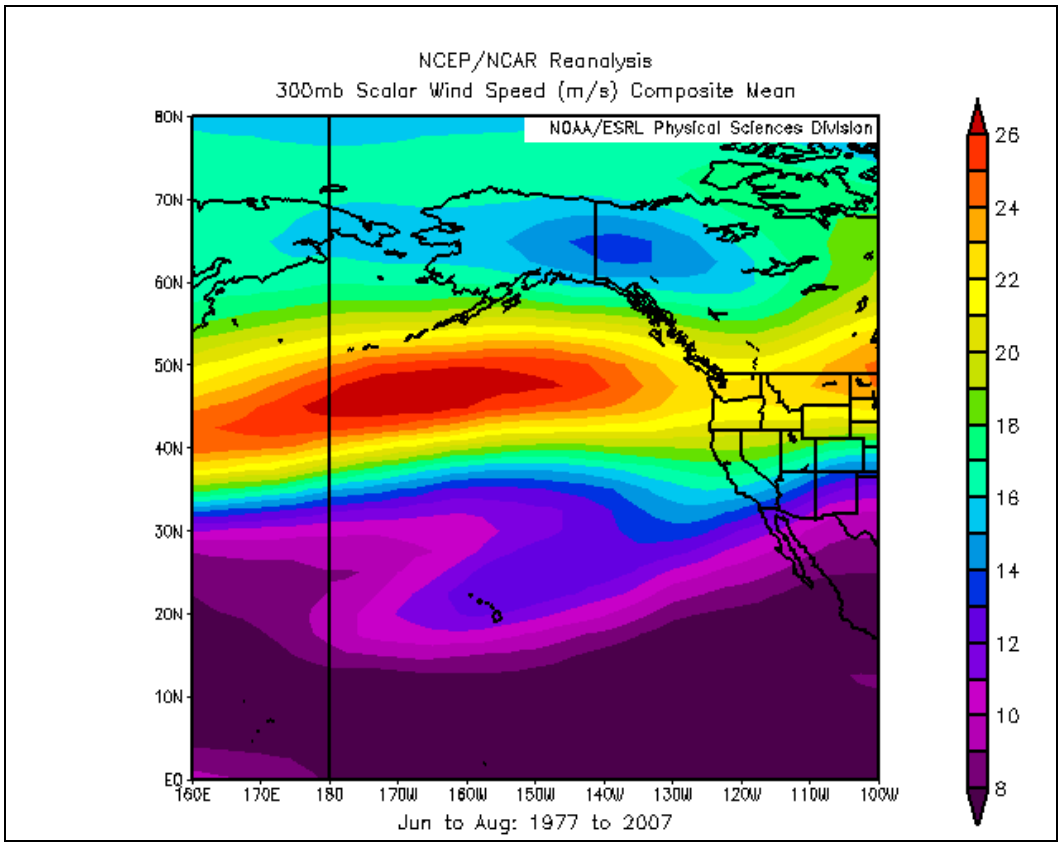

Figure 3.2.9. NCEP-NCAR monthly 300-hPa gridded (2.5° lat. x 2.5° long.) mean scalar winds valid June - August 1977 - 2007. Solid black lines represent isotachs (ms^{-1}).

When analyzing the mean 300-hPa scalar wind data for the first Alaskan blocking event, nothing of note is apparent in the wind field to suggest anything anomalous. As seen in Figure 3.2.10, every feature seen in

the 30-year climatology is in the same relative position. The only difference is the strength of the jet core. For the time period covering June – July 2004, the mean speed within the jet core was 33 ms^{-1}, compared to that of 26 ms^{-1} in the 30–year mean climatology.

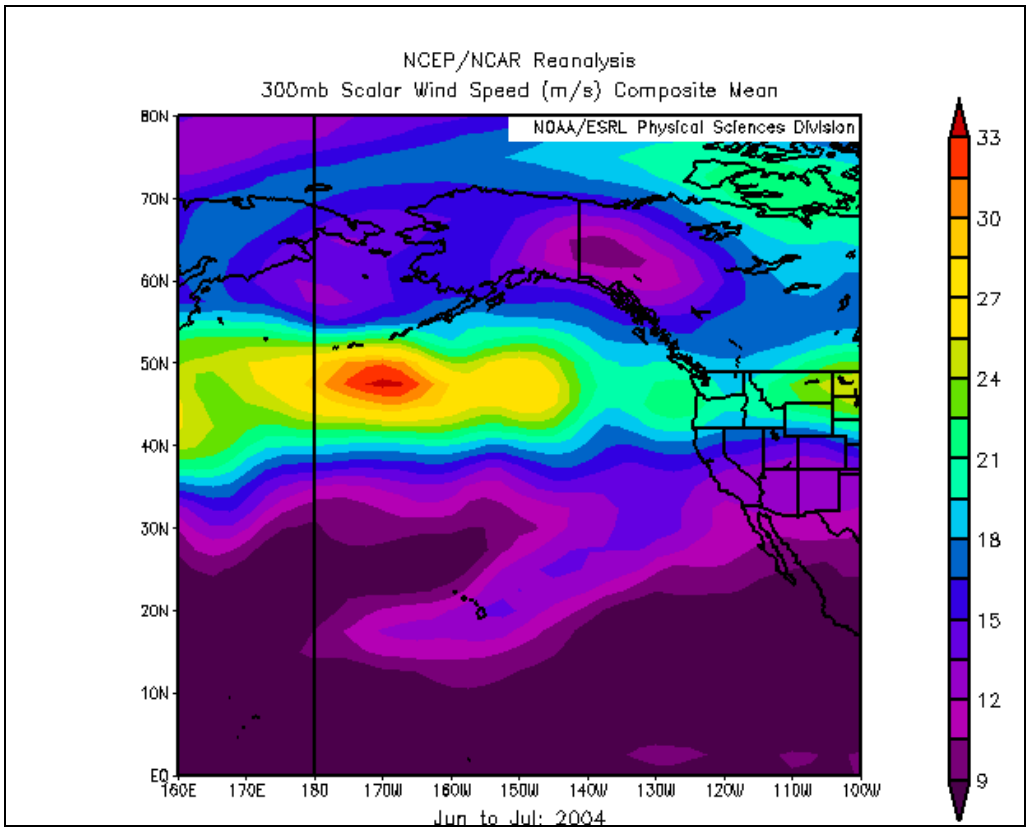

Figure 3.2.10. NCEP-NCAR monthly 300-hPa gridded (2.5° lat. x 2.5° long.) mean scalar winds valid June – July 2004. Solid black lines represent isotachs (ms^{-1}).

3.3 Gulf of Alaska: 05 – 28 August 2004

The second high-amplitude blocking event encompassed almost the entire month of August 2004. While similar to the 24 June – 05 July event, this blocking ridge lasted a consecutive 23.5 days and had a BI value of

2.44. Thus, it was weaker than the first Alaska event. The block was centered on 150°W and made its way to the interior regions of Alaska and western Yukon Territory (Figure 3.2.3 b).

As a matter of analysis, the event was divided into two phases, the first of which covered the period of 05 – 20 August 2004 (Figure 3.3.1). Over this segment of time, the blocking characteristics exhibited a more modified behavior to that of the mid-summer event described above.

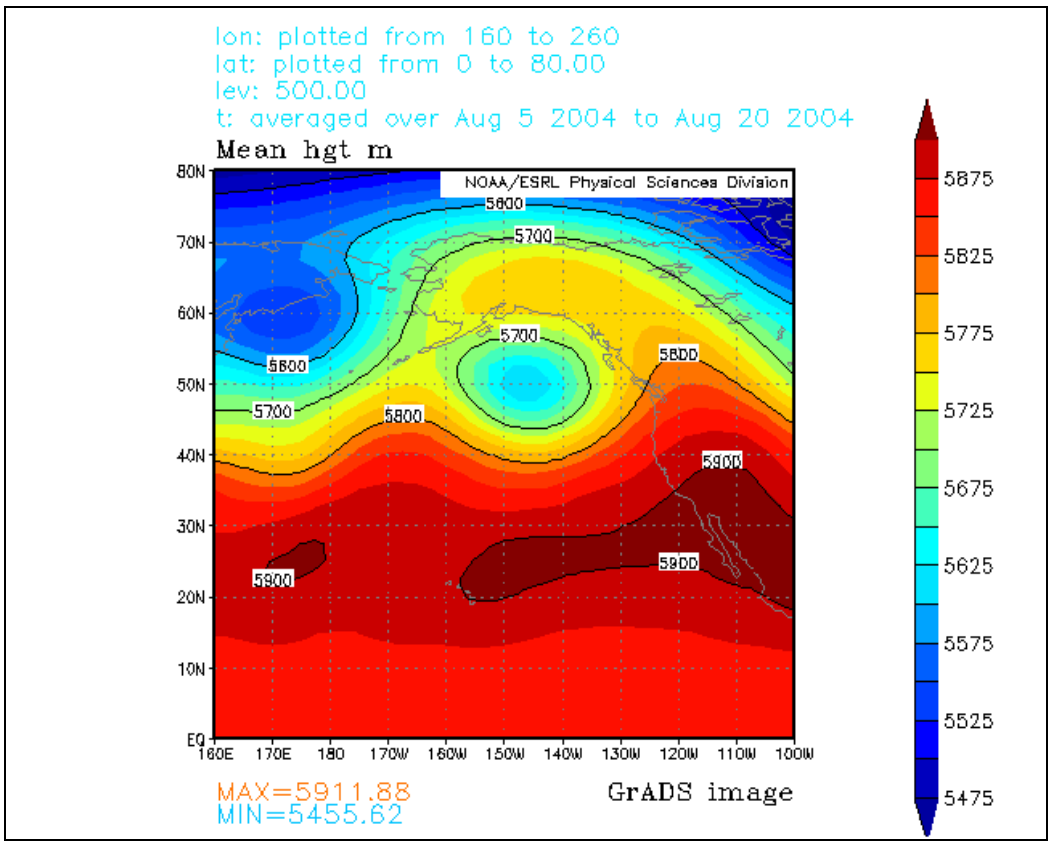

Figure 3.3.1. NCEP-NCAR monthly 500-hPa gridded (2.5° lat. x 2.5° long.) mean geopotential height valid 05 - 20 August 2004. Solid black lines represent geopotential height contours (m).

a. 500-hPa Mean Geopotential Height Analysis

Figure 3.3.2 shows that over the course of the four days following block initiation, a split-flow pattern became prevalent in the 500-hPa mean height field. In the Gulf of Alaska, a negative height anomaly on the order of 5625 gpm was located directly south of the main positive height anomaly. Of particular interest, however, is how this trough remained quasi-stationary over the Gulf of Alaska while the ridge amplified, and over the course of the period, dissipated around the trough. This feature appeared to be the central focus for action in the blocking region.

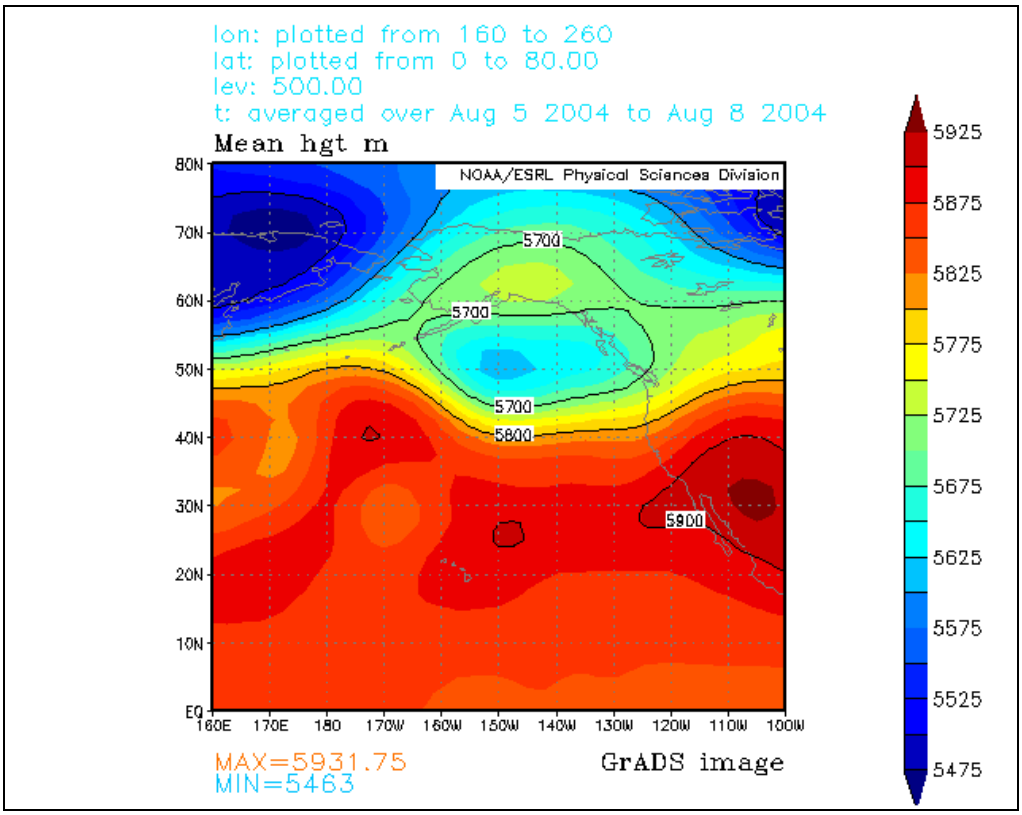

Figure 3.3.2. NCEP-NCAR monthly 500-hPa gridded (2.5° lat. x 2.5° long.) mean geopotential height valid 05 - 08 August 2004. Solid black lines represent geopotential height contours (m). Note the split-flow character of the block.

The four days beginning on 08 August 2004 shows the negative height anomaly responsible for the split-flow block deepened as the block intensified around it. In fact, from 11 August – 14 August, the blocking ridge appeared to break into two sections, producing what appeared to be a two-wave mode across the entire domain of analysis (Figure 3.3.3).

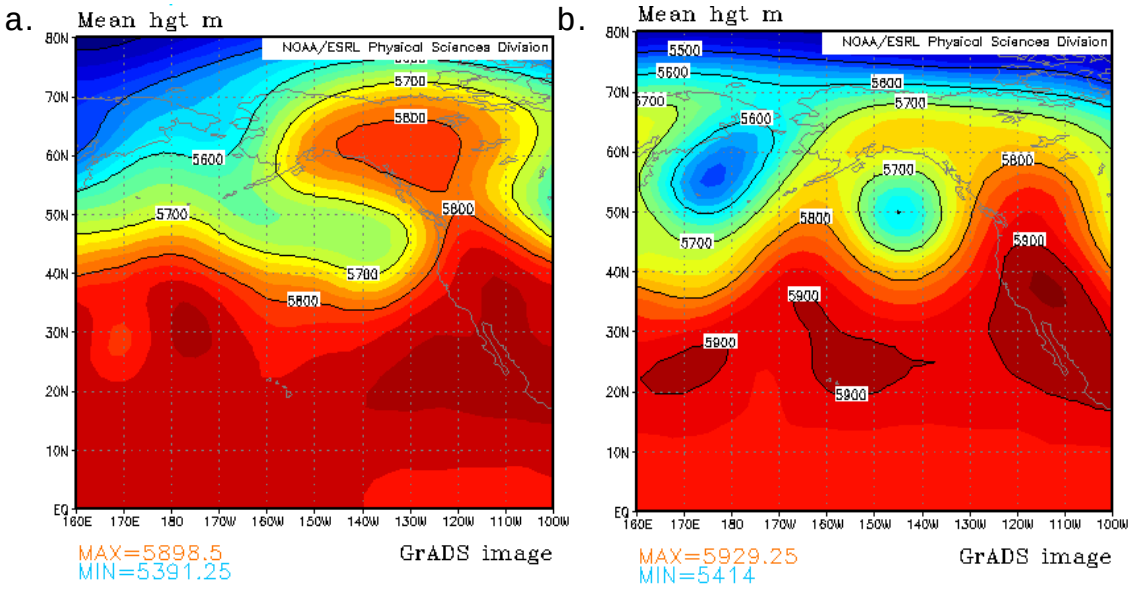

Figure 3.3.3. NCEP-NCAR monthly 500-hPa gridded (2.5 ^{o} lat. x 2.5^{o} long.) mean geopotential height valid (a) 08 - 11 August 2004 & (b) 11 – 14 August, 2004. Solid black lines represent geopotential height contours (m).

Over the same temporal period, the block began to amplify at a very fast rate, with the 5800 gpm isoheight extending poleward from 58^{o}N to 68^{o}N by the 15th. After 15 August, the two-wave mode broke as the block re-enveloped the isolated negative anomaly, producing a donut-shaped configuration. As the southern branch of the split jet began to take a more zonal orientation, the upper branch of the jet became more amplified. Due

to this modification of the flow, the split-flow block began to transform into an omega-type block (Figure 3.3.4).

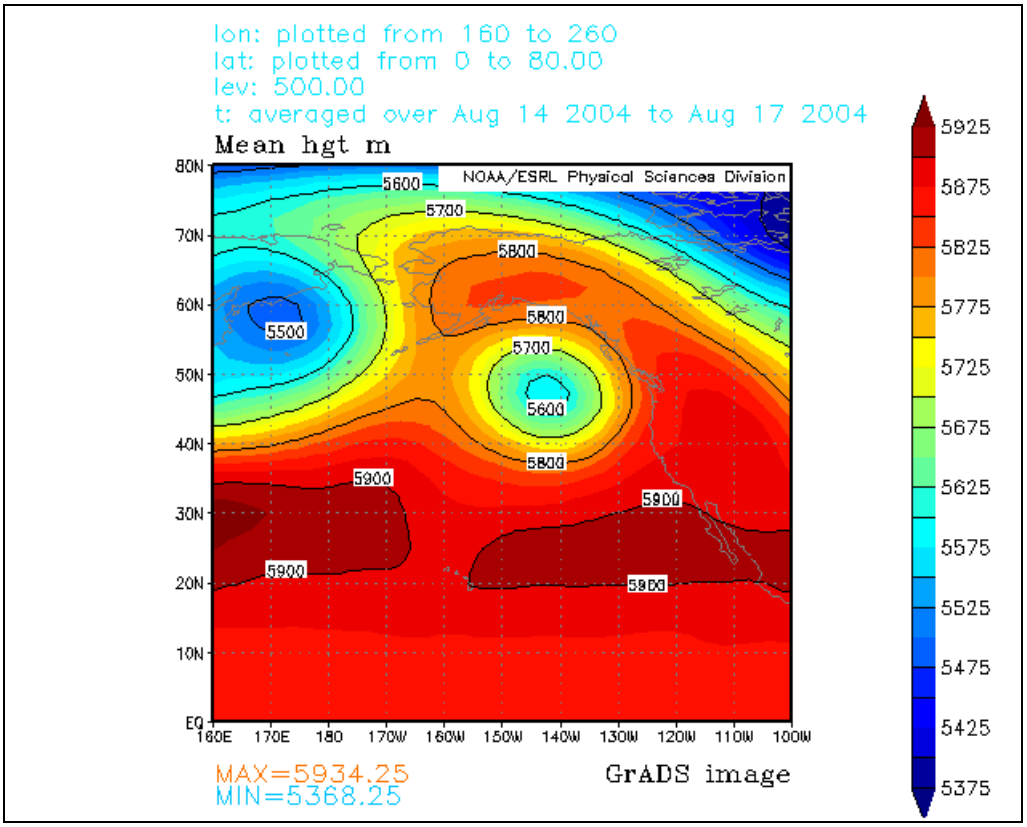

Figure 3.3.4. NCEP-NCAR monthly 500-hPa gridded (2.5° lat. x 2.5° long.) mean geopotential height valid 14 - 17 August 2004. Solid black lines represent geopotential height contours (m).

The second phase of this block began on or around 20 August 2004 when the blocking ridge began to dissipate. During de-amplification, the ridge migrated as far north as 80°N with the 5700 gpm isoheight cut-off from 65°N to 75°N. The days immediately following de-amplification showed the most pronounced omega signature. However, as Figure 3.3.5 shows, the blocking ridge had already began to dissipate as a strong westward

advection of lower heights from the extreme northern reaches of the Northwest Territory.

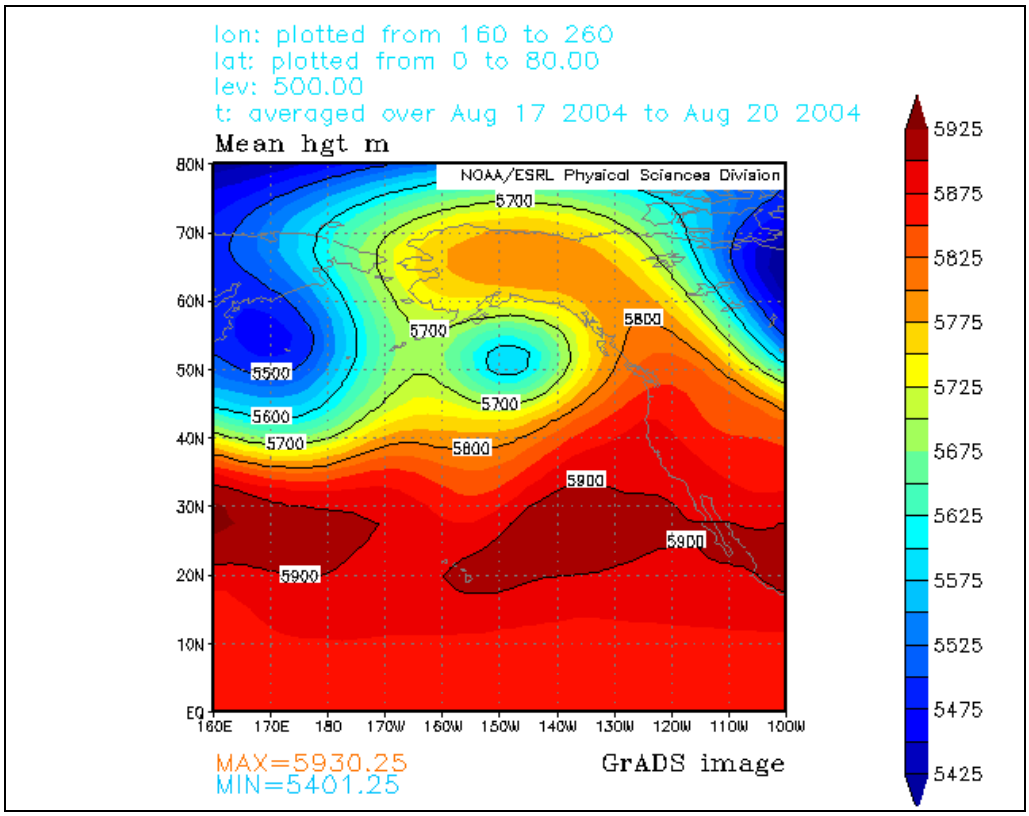

Figure 3.3.5. NCEP-NCAR monthly 500-hPa gridded (2.5^{o} lat. x 2.5^{o} long.) mean geopotential height valid 17 - 20 August 2004. Solid black lines represent geopotential height contours (m).

It is interesting to note a smaller amplitude ridge developed over the Bering Sea and extreme eastern reaches of Russia. Peculiarly, the negative height anomaly over the Gulf of Alaska appeared to be the focusing agent. As the Alaska block dissipated over 20 – 26 August 2004, its negative counterpart over the Gulf of Alaska retrogressed and then merged with another trough in the Bering Sea (Figure 3.3.6).

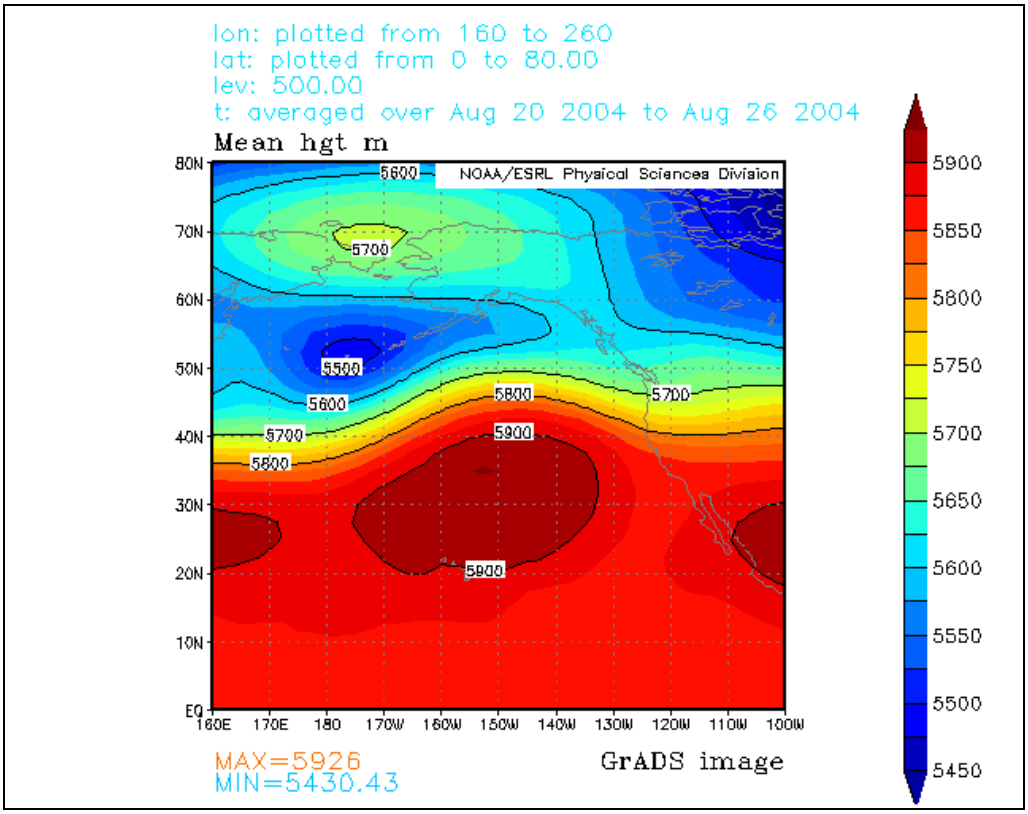

Figure 3.3.6. NCEP-NCAR monthly 500-hPa gridded (2.5^{o} lat. x 2.5^{o} long.) mean geopotential height valid 20 - 26 August 2004. Solid black lines represent geopotential height contours (m).

The last three days of the period showed this feature propagating over the Alaskan Peninsula as the new ridge amplified over the Bering Sea. The block became fully suppressed by 28 August as the mean 500-hPa height field became nearly zonal in character (Figure 3.3.7).

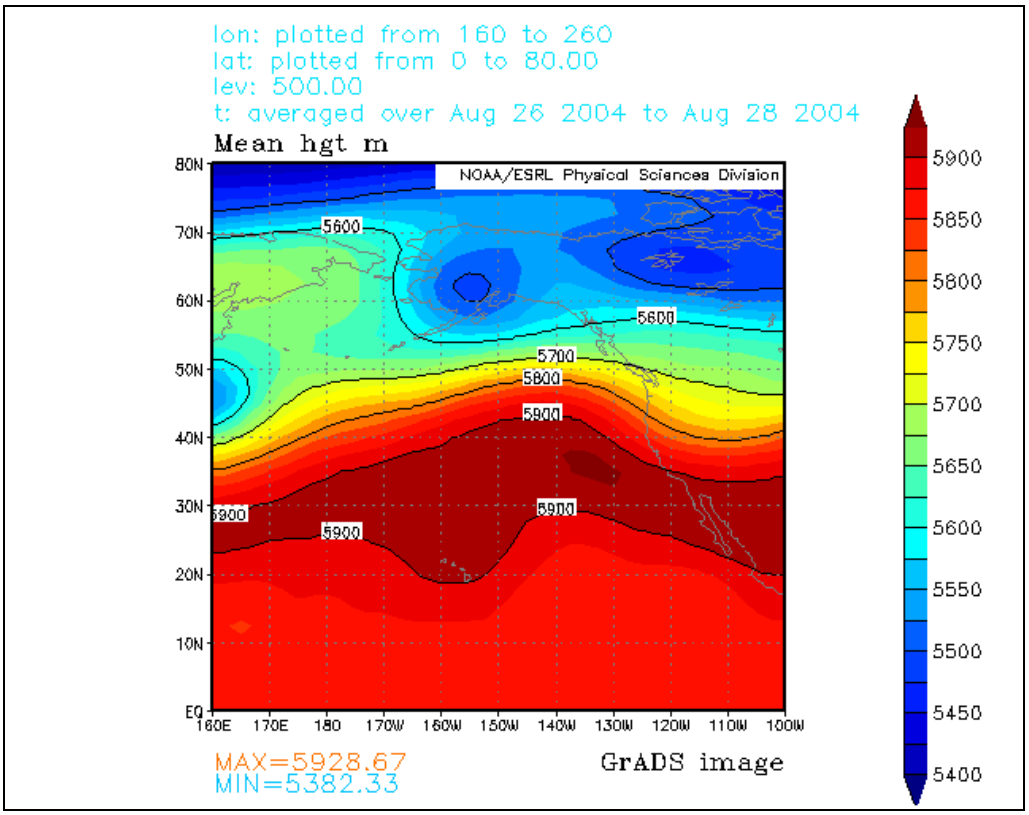

Figure 3.3.7. NCEP-NCAR monthly 500-hPa gridded (2.5^{o} lat. x 2.5^{o} long.) mean geopotential height valid 26 - 28 August 2004. Solid black lines represent geopotential height contours (m).

b. 850-hPa Mean Temperature Analysis

Looking at the 30-year mean 850-hPa temperature climatology for the Alaskan blocking region, it is noticeable that the 1^{o}C (274 K) mean isotherm is curved poleward around the northern boundary of Alaska. As for the southern boundary, the 9^{o}C (282 K) isotherm was located adjacent to the southern coast of Alaska and the western coast of Canada.

The 850-hPa mean temperature analysis for the period of 05 – 28 August 2004 shows a stark contrast to what is normally expected. At block onset and through amplification, temperature values ranged from 12-15^{o}C

higher than normal. However, as Figure 3.3.8 shows for 05 – 08 August, in the region where the negative 500-hPa anomaly was found over the Gulf of Alaska, temperatures approached climatological values. A noticeably isolated region of 850-hPa anomalously warm air was found north (over Alaska) of the 500-hPa height trough, which was located underneath the blocking ridge.

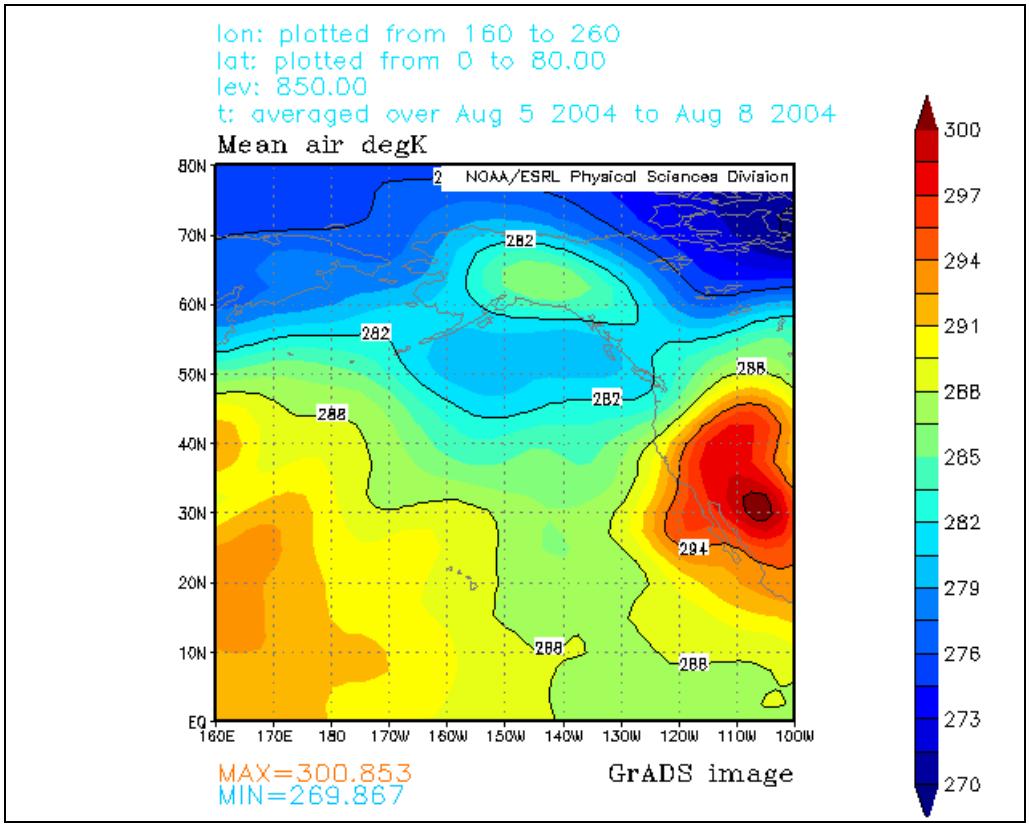

Figure 3.3.8. NCEP-NCAR monthly 850-hPa gridded (2.5 ^{o} lat. x 2.5^{o} long.) mean temperatures valid 05 - 08 August 2004. Solid black lines represent isotherms (K).

Over the next four days, extremely warm air (located under the 500-hPa ridge) began to propagate eastward as the block further amplified. Also

of note is a tongue of anomalously warm air (15°C) moving north over western British Columbia and into the Yukon Territory (Figure 3.3.9).

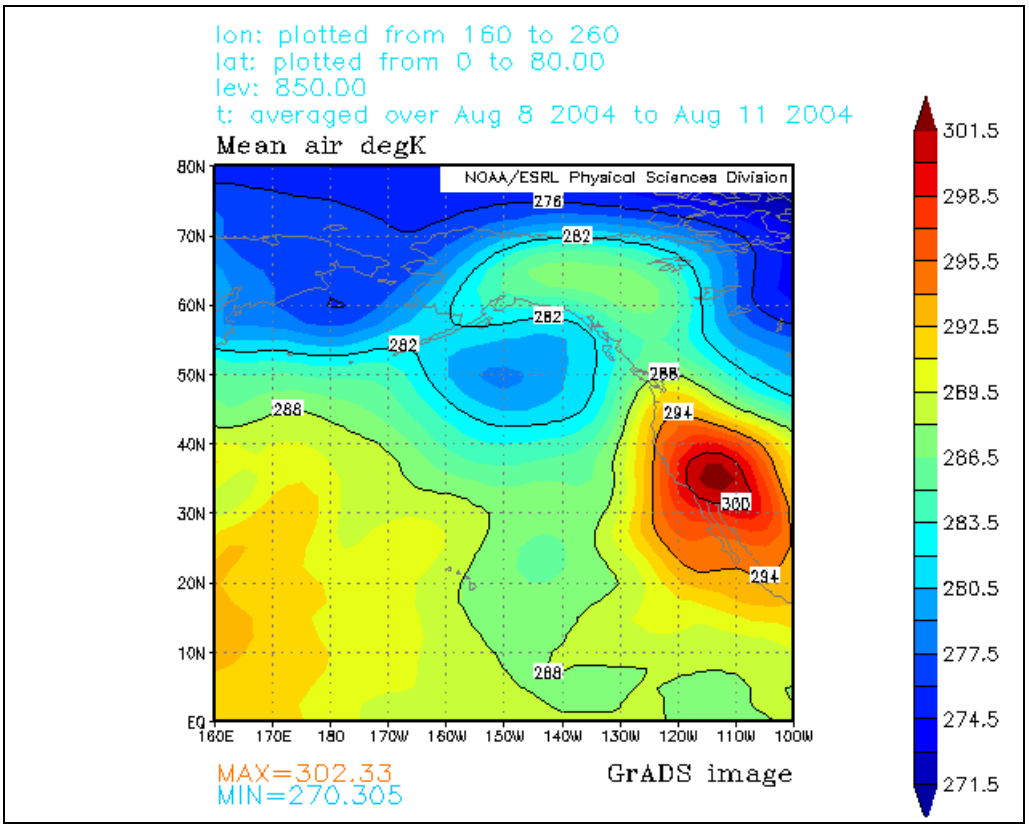

Figure 3.3.9. NCEP-NCAR monthly 850-hPa gridded (2.5° lat. x 2.5° long.) mean temperatures valid 08 – 11 August 2003. Solid black lines represent isotherms (K).

During the height of amplification (as the split-flow blocking ridge broke into two distinct ridges) much of eastern and central Alaska were engulfed in the 12°C (285 K) air. In fact, the donut-shaped pattern visible at 500 hPa height field was also becoming apparent in the 850-hPa mean temperature fields. (Figure 3.3.10).

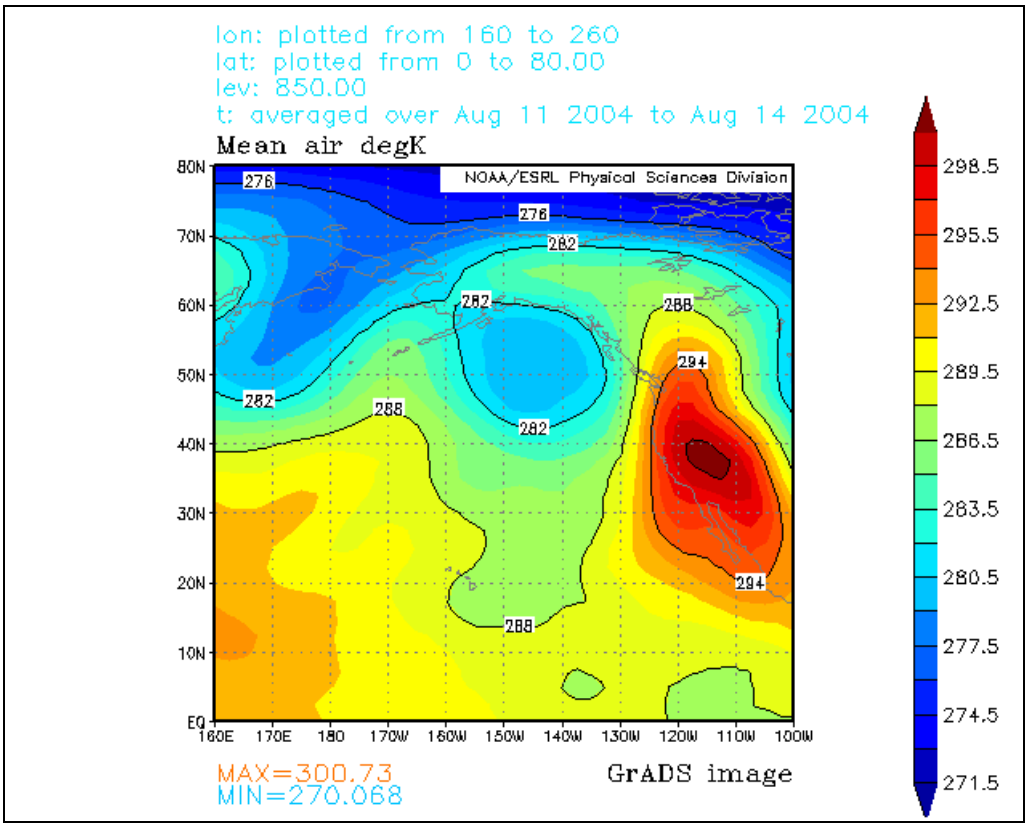

Figure 3.3.10. NCEP-NCAR monthly 850-hPa gridded (2.5^{o} lat. x 2.5^{o} long.) mean temperatures valid 11 – 14 August 2004. Solid black lines represent isotherms (K).

After a quick phase of intense amplification, which in turn modified the original block into a more-pronounced omega signature, the ridge of anomalous warmth shifted into the central reaches of Alaska and Canada. Further west in the blocking domain, cooler isotherms began building in, pushing the temperature ridge further east, as the thermal ridge covered most of western Canada and the Alaska peninsula with the 9^{o}C (282 K) isotherm (Figure 3.3.11).

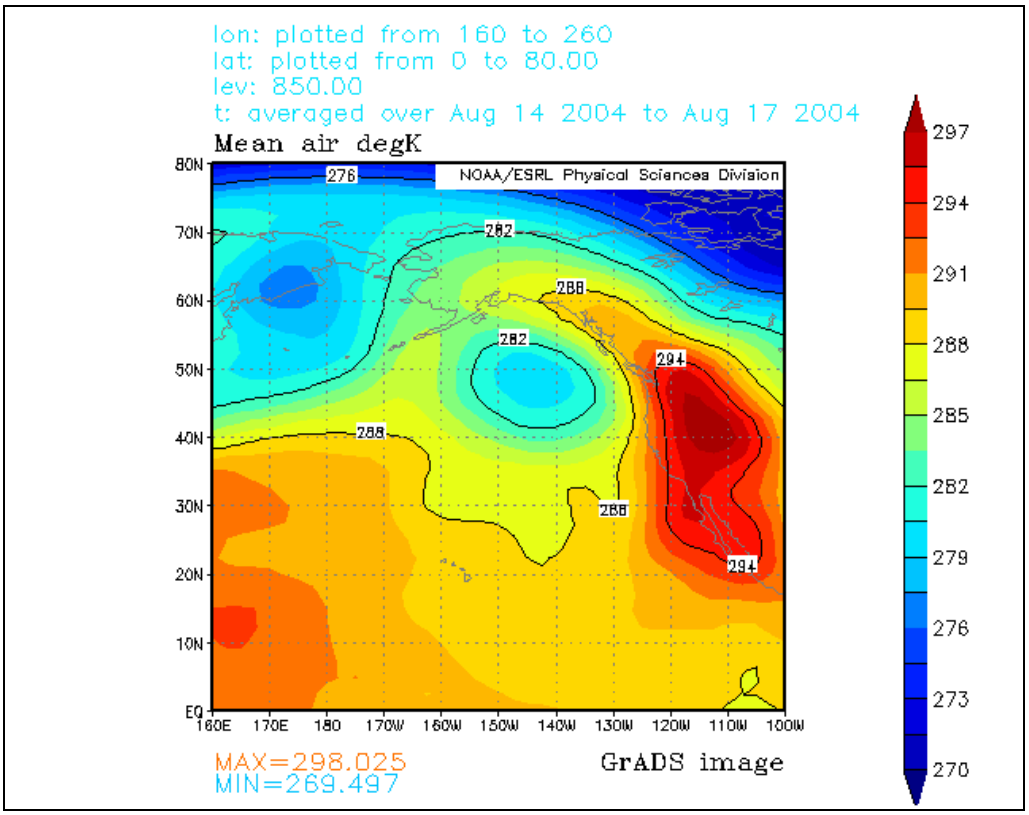

Figure 3.3.11. NCEP-NCAR monthly 850-hPa gridded (2.5 ^{o} lat. x 2.5^{o} long.) mean temperatures valid 14 – 17 August 2004. Solid black lines represent isotherms (K).

Concurrent with the 500-hPa height ridge dissipation, the 850-hPa temperature ridge de-amplified as the 500-hPa trough migrated into British Columbia and filled. Figure 3.3.12 shows this effectively split the thermal ridge along the coast of Canada and isolated the 9^{o}C+ warm air over Alaska. With the de-amplification at 500-hPa, it is likely that the temperature ridge was compressed, forcing the abnormally warm air north and south of the negative height anomaly.

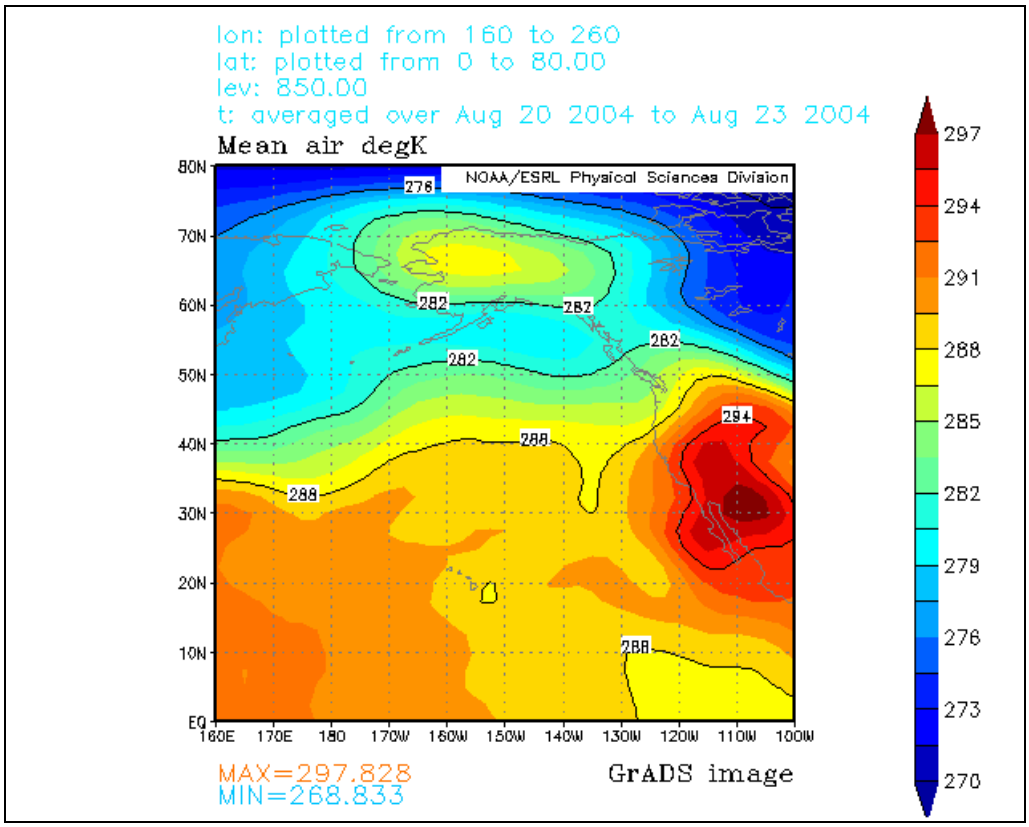

Figure 3.3.12. NCEP-NCAR monthly 850-hPa gridded (2.5 ^{o} lat. x 2.5^{o} long.) mean temperatures valid 20 – 23 August 2004. Solid black lines represent isotherms (K).

The period from 23 – 28 August 2004 showed the return of the 3^{o}C (276 K) isotherm to the northern bounds of Alaska. However, as dissipation at 500-hPa continued, Alaska was still partially covered by the 9^{o}C (282 K) isotherm (Figure 3.3.13). It appears as the new 500-hPa ridge amplified over the Bering Sea, so too did an 850-hPa ridge underneath. Two days later, after the block dissipated completely, temperatures in Alaska returned to near normal. There appeared to be some lag between temperature decreases over the block region and de-amplification of the height ridge itself.

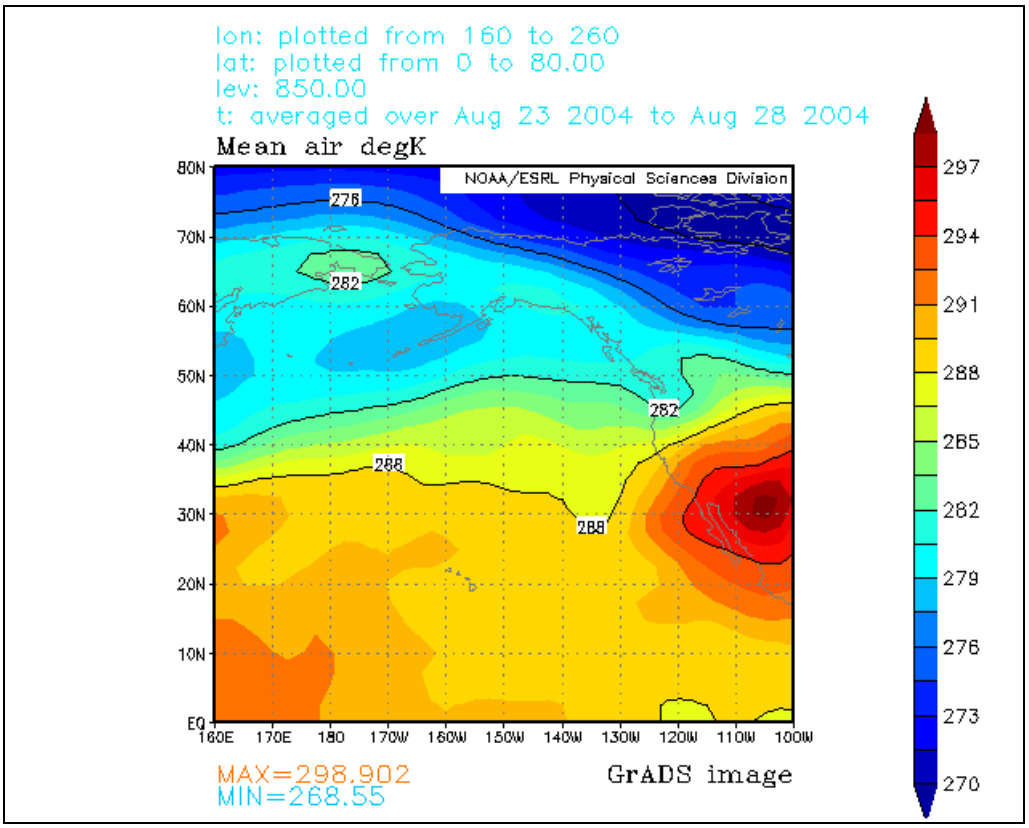

Figure 3.3.13. NCEP-NCAR monthly 850-hPa gridded (2.5^{o} lat. x 2.5^{o} long.) mean temperatures valid 23 – 28 August 2004. Solid black lines represent isotherms (K).

c. 300-hPa Mean Scalar Wind Analysis

The same climatology discussed earlier with respect to the first Alaskan blocking event can be applied to the second event, since the period of the 30-year mean 300-hPa scalar winds covered June through August. While the features prevalent in the climatology corresponded to the second event, there exist some differences. Mainly, there was a large region coinciding with the 500-hPa blocking signature and 850-hPa thermal ridge (Figure 3.3.14).

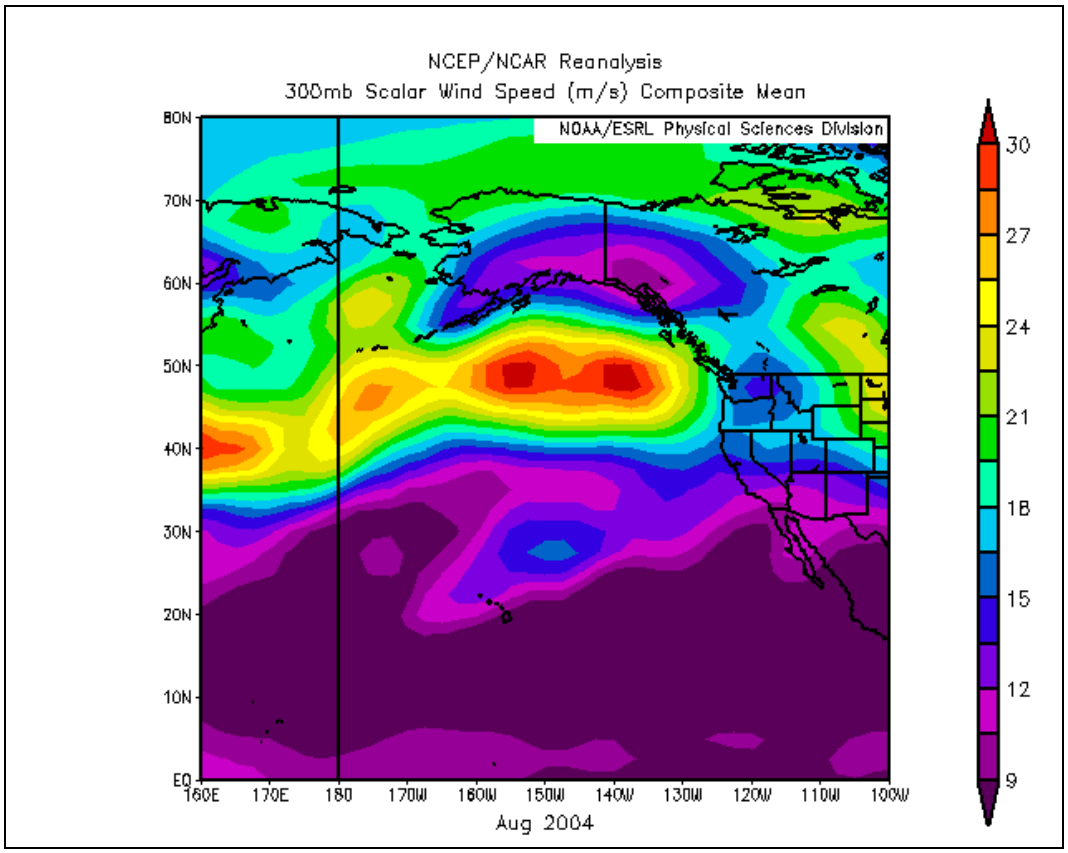

Figure 3.2.14. NCEP-NCAR monthly 300-hPa gridded (2.5° lat. x 2.5° long.) mean scalar winds valid August 2004. Solid black lines represent isotachs (ms^{-1}).

When the 500-hPa field was considered, a split-flow pattern emerged in the isoheights. Specific analysis of the 300-hPa winds suggest that indeed the jet split into two branches, the southern-most branch remaining zonal as the poleward branch became highly amplified. Wedged within the split flow was a wind speed minimum of 9 - 12 ms^{-1}.

Over the Gulf of Alaska, the wind maximum broke into two discrete cores of the same magnitude (30 ms^{-1}) separated by 10° of latitude. This region is consistent with the negative height anomaly found in the 500-hPa

mean geopotential height field (e.g. Figure 3.3.4). It is plausible that the height-field-troughing throughout the vertical extent of the atmosphere (over the Gulf of Alaska) produced a region favorable for wind acceleration, effectively forcing the jet stream to speed up considerably. Via this acceleration, the jet core formed over the underlying features in the mass and thermal fields.

Chapter 4

Dynamic Analysis

In this chapter the blocking events described in previous chapters will be further analyzed with specific emphasis placed on the dynamic characteristics of the flow. When discussing the flow, it will become apparent that both synoptic and planetary scale considerations come into play when determining scale-contributions to the blocking region.

In the first section of this chapter, pressure on the tropopause is analyzed in two distinct ways. The first type of evaluation involves the entire tropopause-pressure field. This type of examination delves into the planetary-scale contributions to the flow. As discussed in Burkhardt and Lupo (2005), a positive contribution from the planetary scale plays an important role in the development and decay of blocking anticyclones. In fact, the planetary scale provides the background onto which smaller-scale eddies grow and decay, in turn affecting the life-cycle/span of prospective blocking flows.

When evaluating pressure on the tropopause, it is crucial to note that increasing (decreasing) pressure on the tropopause is associated with troughs (ridges), and thus lower (higher) geometric heights (Morgan & Nielsen-Gammon 1998; Lupo et al. 2001). Moreover, pressure on the

tropopause was chosen since it is conserved in an adiabatic and geostrophic atmosphere as well as with time;

$$\frac{dp}{dt} = 0 \tag{4.1}$$

thus, we can infer that local changes in pressure (at the tropopause) with time are due to quasihorizontal pressure advection;

$$\frac{\partial p}{\partial t} = -\vec{v} \cdot \nabla p \tag{4.2}$$

Since ridging is analogous to low pressure at the tropopause, then a negative Eulerian tendency is beneficial towards block development and infers “low-pressure advection.” This may seem counter-intuitive, since low-pressure advection (near the surface) acts to weaken ridges of high pressure. However, the level used for this analysis is the dynamic tropopause, thus low-pressure advection is actually the advection of higher geometric heights. The mean eddy pressure anomalies (Figure 4.1) show contribution of low-pressure advection (at the tropopause) into the development of the August 2003 European blocking event. Note the strong low pressure anomaly (high geometric heights) in the region of the 500-hPa blocking ridge.

In an effort to examine the synoptic-scale contributions to the blocking events, the zonal mean is subtracted from the pressure on the tropopause fields. The zonal mean can be looked upon as the neutral component of the

synoptic to planetary scale flow regime. When the zonal mean is neglected, a better view of synoptic scale eddies is attained. In fact, the location of cyclones and anticyclones with respect to the blocking ridge proves to be important in the block initiation and decay.

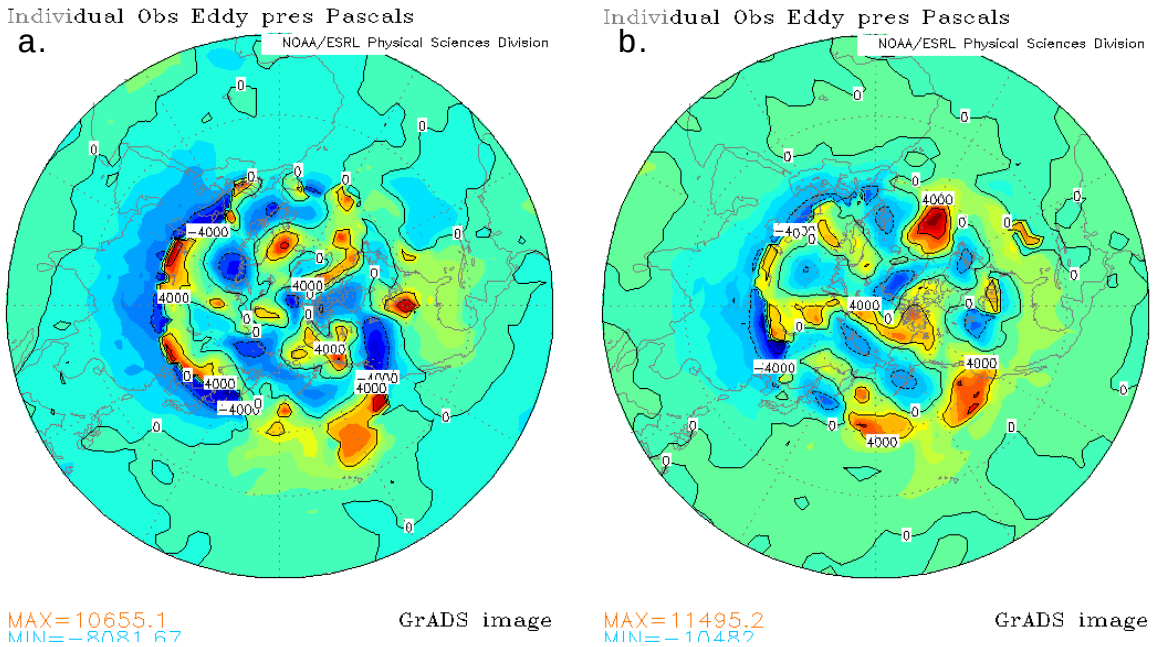

Figure 4.1. NCEP-NCAR daily gridded (2.5 ^{o} lat. x 2.5^{o} long.) pressure on the tropopause valid (a) 1200Z 03 August 2003 & (b) 1200Z 07 August 2003 (Western European event). Solid black lines represent pressure (Pascals). The zonal mean has been extracted for the purpose of showing negative and positive eddy anomalies at the tropopause.

While great effort is placed in the analysis of the pressure on the tropopause fields, the first sections are a cursory examination, and not the main focus of this chapter. These results are important for a few reasons, however. They confirm earlier works by (Lupo et al. (2001) & Burkhardt and Lupo (2005)). Moreover, in building upon these works, this study also seeks

to connect the dynamical study of blocking events to that of the Lyapunov exponent, which is the focus of section two and this chapter.

4.1 Pressure on the Tropopause

a. Western Europe: 06 – 13 August 2003

The 0000 and 1200 UTC NCEP-NCAR daily mean sea-level pressure reanalyses were first evaluated for the three time periods involved in the August 2003 Western European blocking event. These periods correspond to block onset (03 – 06 August), block maturity (06 – 13 August) and block decay (12 – 14 August).

Sea-level pressure (SLP) plots were used to diagnose and evaluate the characteristics of the migratory high and low pressure systems (both upstream and downstream) of the 500-hPa blocking pattern and how they interact with the blocking region itself. These synoptic-scale features also will be important factors when determining the synoptic and planetary contributions throughout the lifespan of the this event

Troughing in the SLP field is evident in Figure 4.1.1, as two areas of low pressure (1009-hPa) developed upstream of the initiating block. The trough was situated poleward of 50^{o}N and centered at 40^{o}W. Over the North Sea, a strong ridge of high pressure (1026-hPa) was found, with the 1020-hPa isobar covering most of west-central Europe.

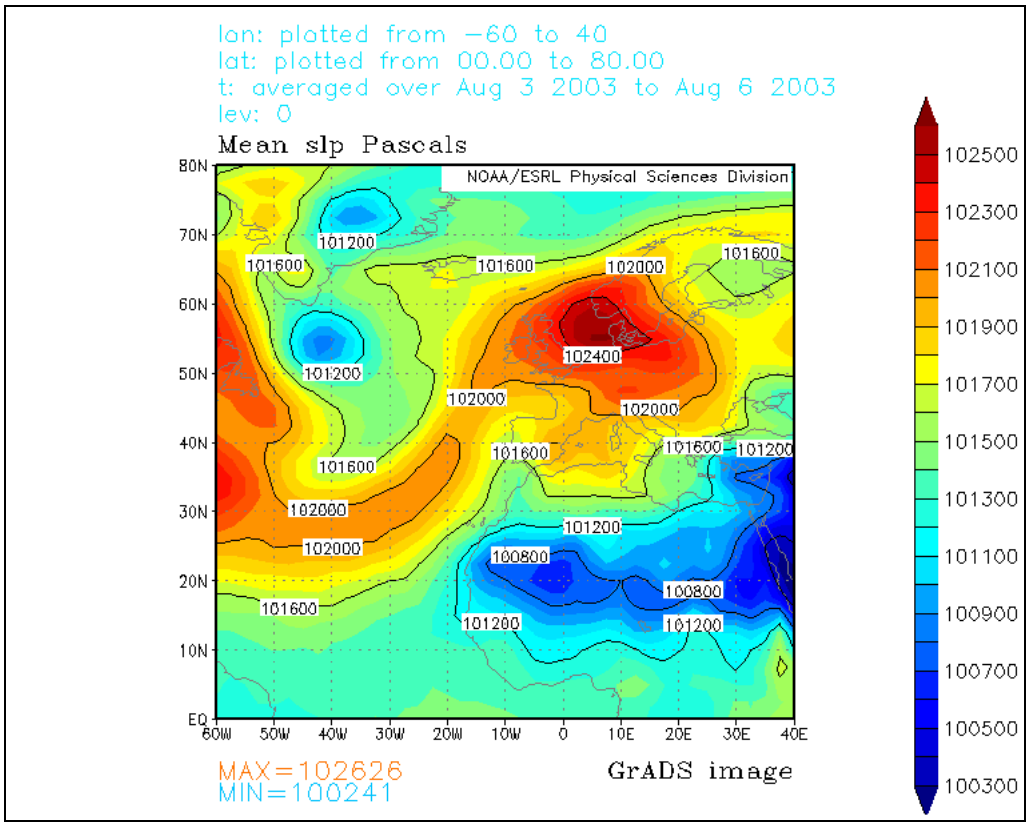

Figure 4.1.1. NCEP-NCAR monthly gridded (2.5° lat. x 2.5° long.) mean sea-level pressure valid 03 – 06 August 2003. Solid black lines represent pressure (Pascals).

The period from 06 – 13 August (Figure 4.1.2) saw the trough deepen over the western Atlantic basin while the high-pressure ridge over Western Europe weakened. At block decay, the 1000-hPa trough continued to deepen as it retrogressed peculiarly further west, over Greenland. The older area of high pressure intensified over the western Atlantic basin as the block at 500-hPa de-amplified (Figure 4.1.3). In lieu of this behavior, it is then likely that the synoptic-scale has not commenced reinforcement of the block, similar to results found in Lupo & Bosart (1999).

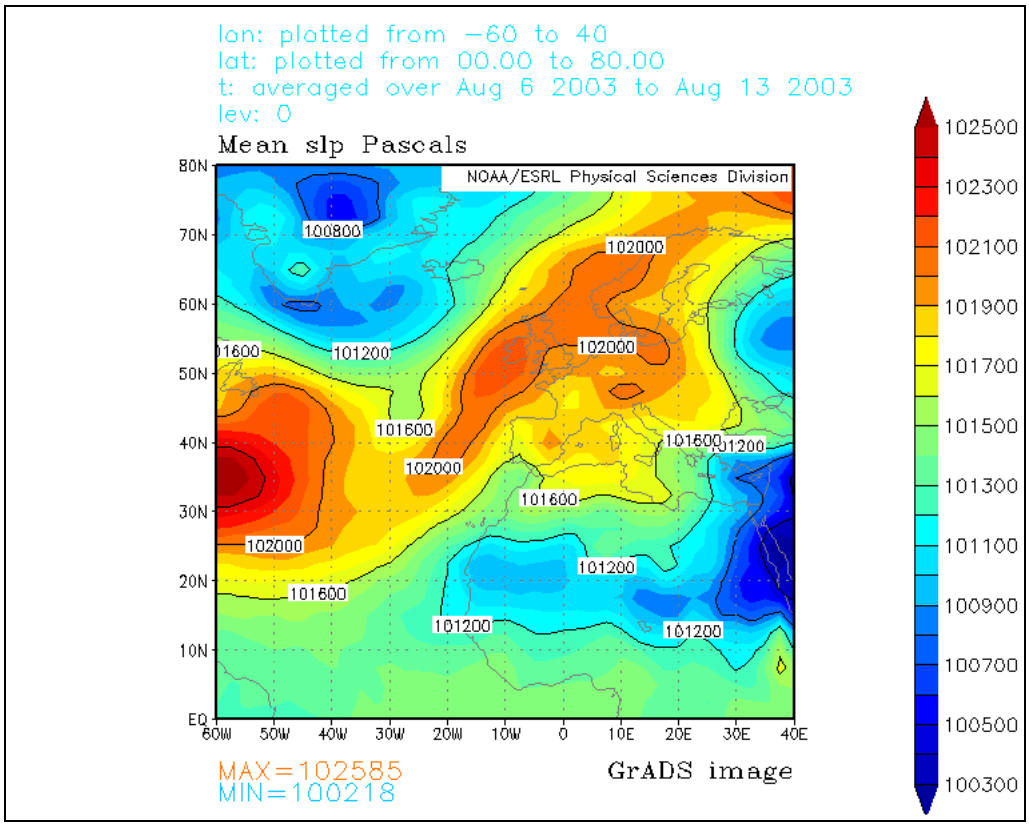

Figure 4.1.2. NCEP-NCAR monthly gridded (2.5^{o} lat. x 2.5^{o} long.) mean sea-level pressure valid 06 – 13 August 2003. Solid black lines represent pressure (Pascals).

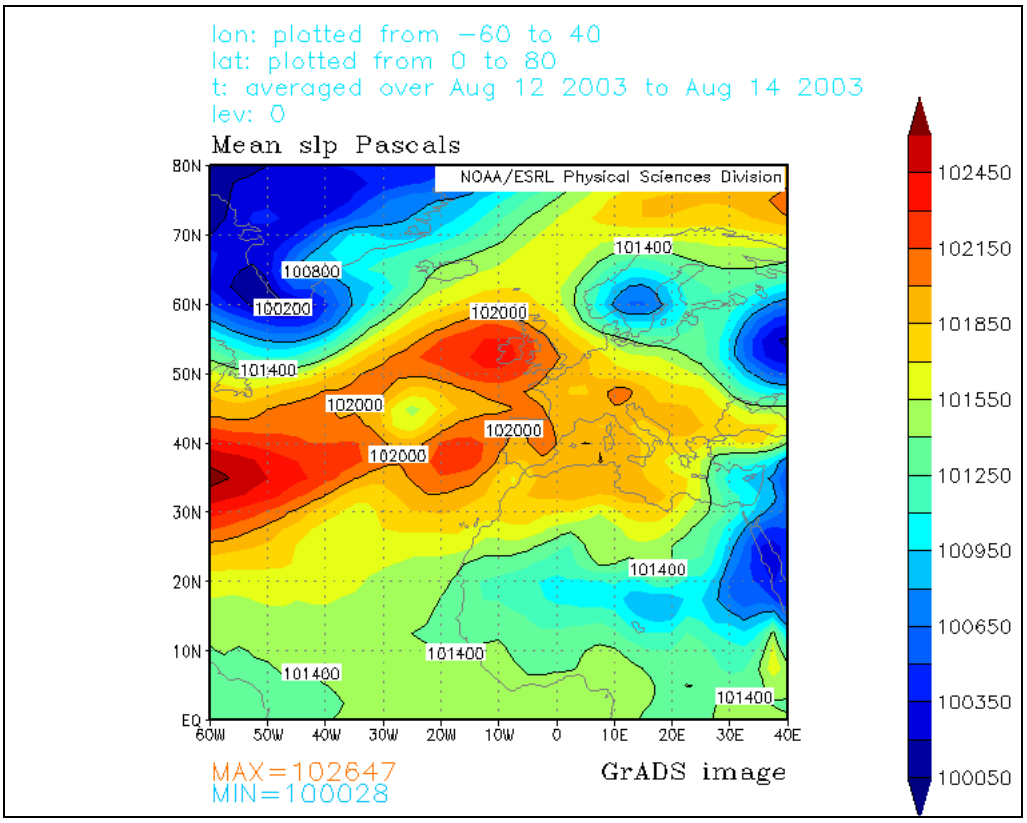

Figure 4.1.3. NCEP-NCAR monthly gridded (2.5° lat. x 2.5° long.) mean sea-level pressure valid 12 – 14 August 2003. Solid black lines represent pressure (Pascals).

Corresponding to these surface pressure features, a large region of higher tropopause extending to 60°N was located in the mean tropopause-pressure plot. The amplitude of the ridge was nearly 20° and produced an omega-like structure in the field (Figure 4.1.4a). Also of note was an anomalously lower tropopause over the surface low-pressure trough found in the mean SLP plots. As the block continued to develop, the tropopause began to lift. This is particularly evident in Figure 4.1.5a. A region of tropopause falls were found on either side of the tropopause ridge, extending poleward from 40°N. Pressure gradients within the tropopause

troughing were much tighter than those found in the apex of the tropopause ridge. This ridge was also found to have migrated further west over Central Europe.

As the positive height anomaly at 500-hPa de-amplified (12 – 14 August), so too did the positive pressure anomaly at the tropopause. The dissipation of the pressure ridge allowed the tropopause to lower to a more climatologically expected level.

Considering the anomalous ridging of the tropopause over the block period, and the corresponding pressure ridging throughout the layer, it is apparent the planetary scale contribution (to the blocking event) is positive. With a contribution as such, the block was strengthened continually for a majority of the mature phase and only started to decay as the ridging halted.

Removing the zonal mean from the pressure on the tropopause plots was the next step in analyzing the interactions between the flow and the blocking ridge. In removing the zonal mean, the synoptic scale contributions become more evident and easier to analyze.

At the onset of this blocking event, the strongest mean positive eddy pressure anomaly (80-hPa) was found 40^{o} upstream from where the 500-hPa blocking ridge is expected (4.1.4b). This distance represents about half a wavelength from the center of the blocking ridge. Studies suggest (e.g. Konrad and Colucci 1988; Lupo and Bosart 1999) along with the results

found in this section, that cyclonic development (found in the mean SLP charts) within a distance of one-half wavelength from the center of the downstream block contributes to the intensification of the block.

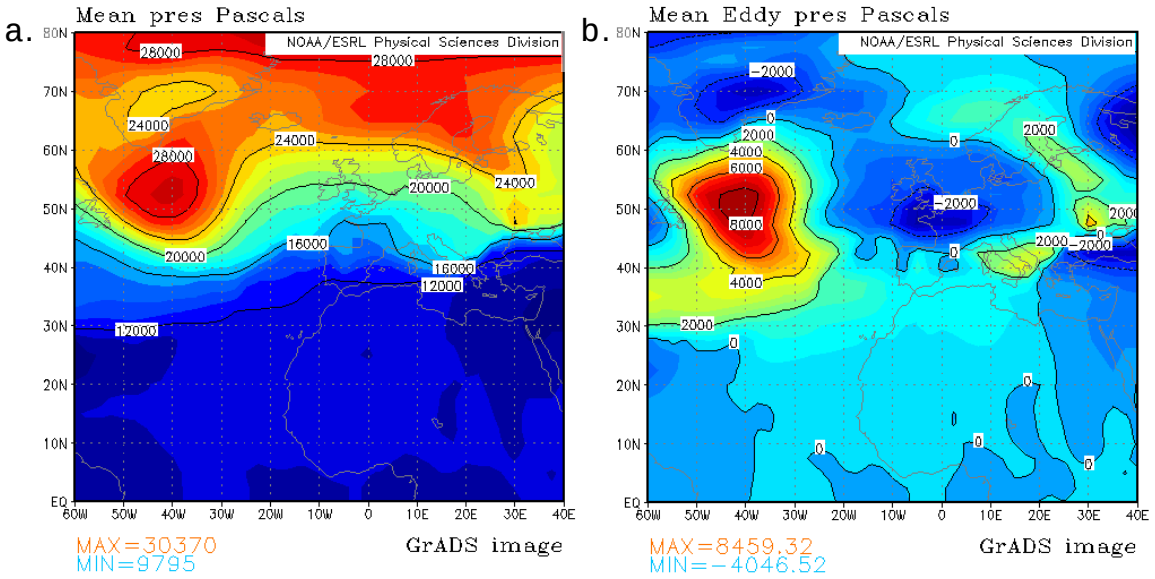

Figure 4.1.4. NCEP-NCAR gridded monthly mean (2.5^{o} lat. x 2.5^{o} long.) (a) pressure on the tropopause & (b) eddy pressure on the tropopause. Both figures valid 03 – 06 August 2003. Solid black lines pressure represent (Pascals).

In fact, during the 06 - 13 August 2003 period, the upstream anomaly weakens to 40-hPa as its negative downstream counterpart (co-located with the block) intensifies to -40-hPa (Figure 4.1.5b). This result suggests a downstream advection of energy from the upstream cyclone into the block, effectively strengthening the block while producing anomalous tropopause ridging. The scale of the positive eddy anomaly and it's apparent contribution to the blocking region suggest a positive synoptic contribution as well, perhaps even more so than the planetary scale.

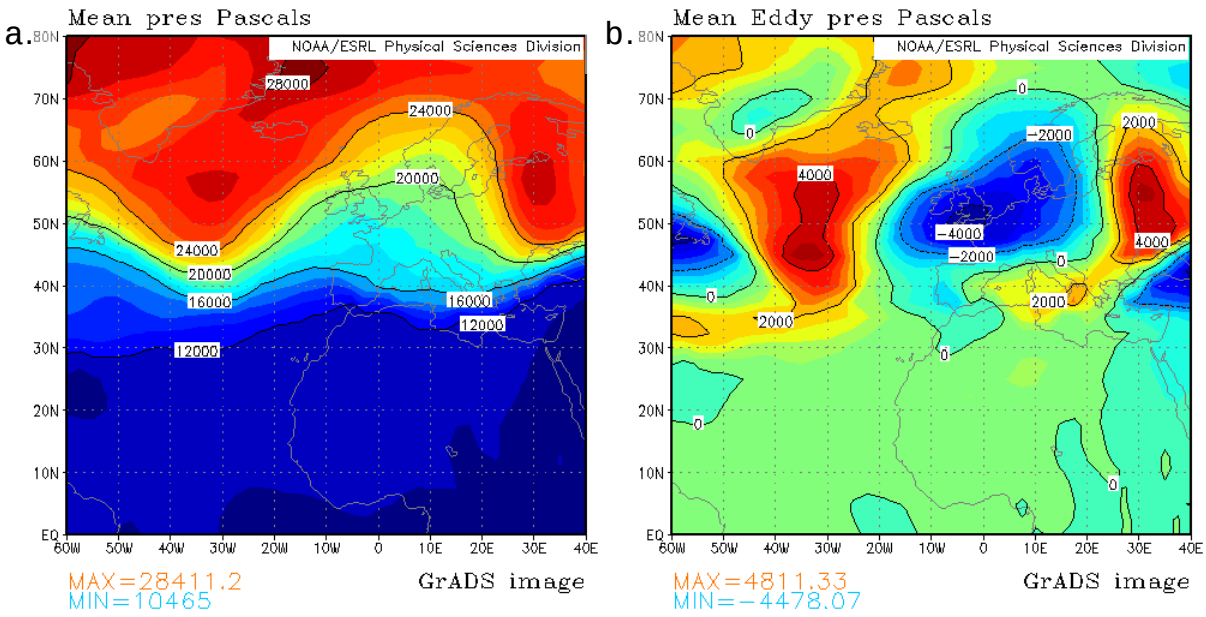

Figure 4.1.5. NCEP-NCAR gridded monthly mean (2.5 ^{o} lat. x 2.5^{o} long.) (a) pressure on the tropopause & (b) eddy pressure on the tropopause. Both figures valid 06 – 13 August 2003. Solid black lines represent pressure (Pascals).

The final figure couplet (Figure 4.1.6) details decay onset for the different scale interactions. It is very interesting to note that during the two-day period beginning on 12 August, the eddy pressure anomalies (both positive and negative) shrank while becoming flatter (with respect to latitude), as the synoptic scale contribution decreased.

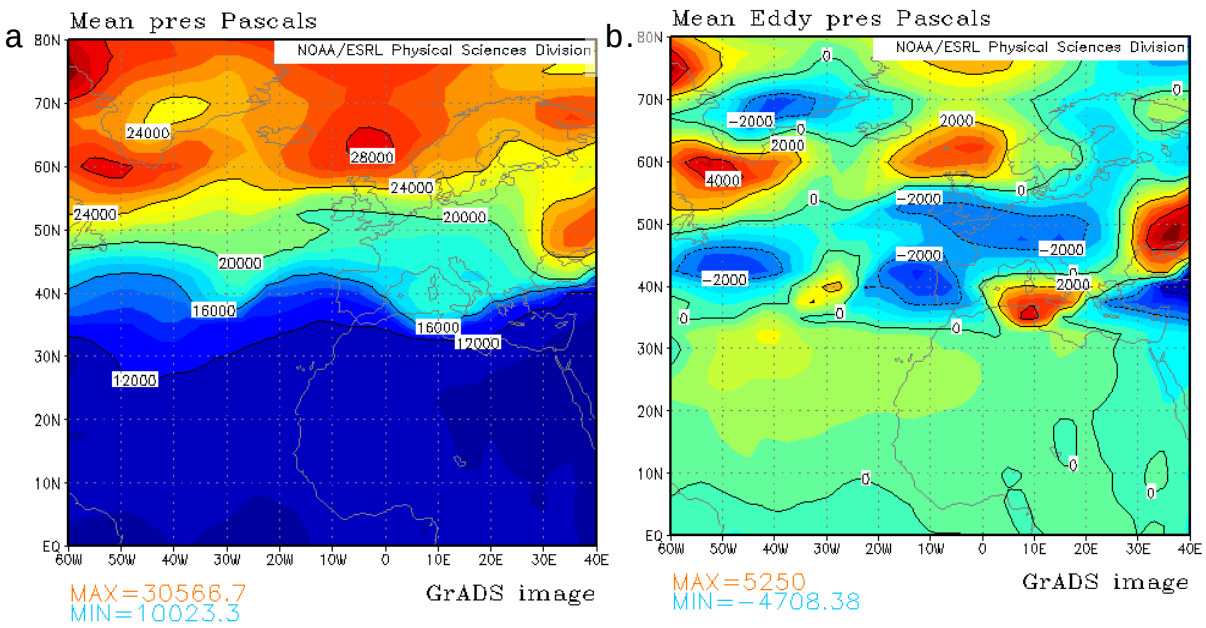

Figure 4.1.6. NCEP-NCAR gridded monthly mean (2.5° lat. x 2.5° long.) (a) pressure on the tropopause & (b) eddy pressure on the tropopause. Both figures valid 12 – 14 August 2003. Solid black lines represent pressure (Pascals).

Table 4.1a shows the contributions at each scale of the Eulerian pressure advection at the tropopause. Positive (negative) values represent a negative (positive) contribution. It is important to remember that these values are averages over the entire period. Thus, while the contribution may not completely agree with the tropopause pressure plots, Appendix A will show the complete breakdown of these results.

Table 4.1a. Eulerian pressure advections and contributions to each scale

Onset (hPa/day)	Maintenance (hPa/day)	Decay (hPa/day)	Scale Contribution
-1.6	9.5	-12.5	Total
3.4	-2.1	-12.5	Synoptic
-5	11.6	0	Planetary

b. Gulf of Alaska: 24 June – 05 July 2004

The shorter of the two “Baked Alaska” events covered only 11 days, as block onset began on 21 June 2004. While this event was shorter, it did behave nearly identical to the second event. Dissipation of the blocking ridge began around 04 July and completed two to three days later.

Analysis of the mean SLP plots for the first Alaskan (Figure 4.1.7) event depicts a sustaining, strong ridge of high pressure (1028-hPa) over the Eastern Pacific for much of the blocking period. A noticeable area of low pressure (1006-hPa) was located over the Bering Strait at block initiation, but filled as the block matured and eventually decayed

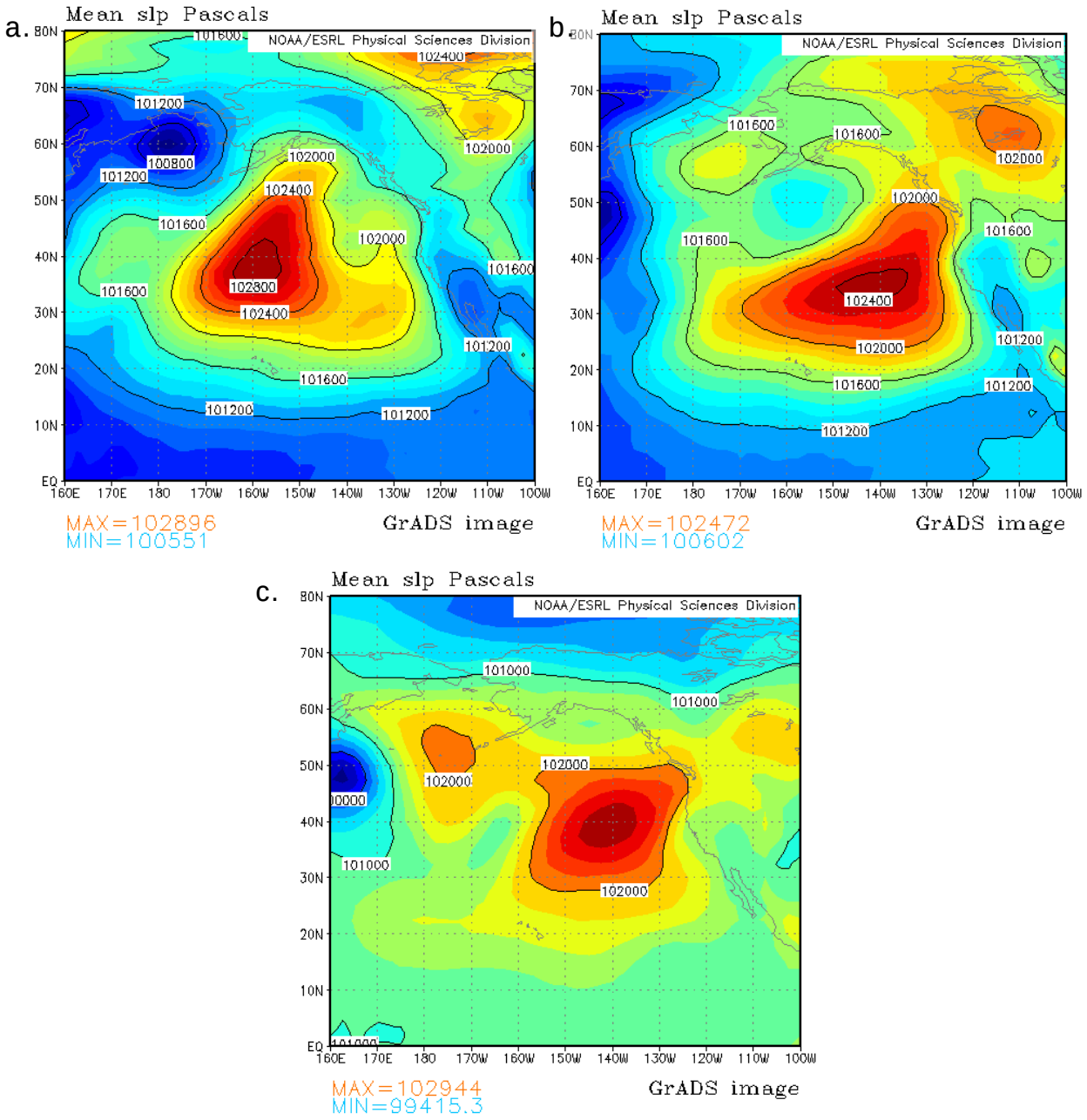

Figure 4.1.7. NCEP-NCAR monthly gridded (2.5^{o} lat. x 2.5^{o} long.) mean sea-level pressure valid (a) 21 – 24 June 2004, (b) 24 June – 05 July 2004 & (c) 04 – 06 July 2004. Solid black lines represent pressure (Pascals).

The high-pressure region found at block onset diminished in strength through the life cycle of the blocking event. The anticyclone also migrated due east as it continued to weaken.

The first noticeable feature in the pressure on the tropopause plots was a well-defined omega structure over Alaska and Western Canada, reaching into the Gulf of Alaska as well (Figure 4.1.8a). This represented a region in which the tropopause was located higher than normal. Just downstream of this, the tropopause was found at a lower atmospheric elevation. The feature that corresponded to this lowering was the surface cyclone found in the mean SLP maps.

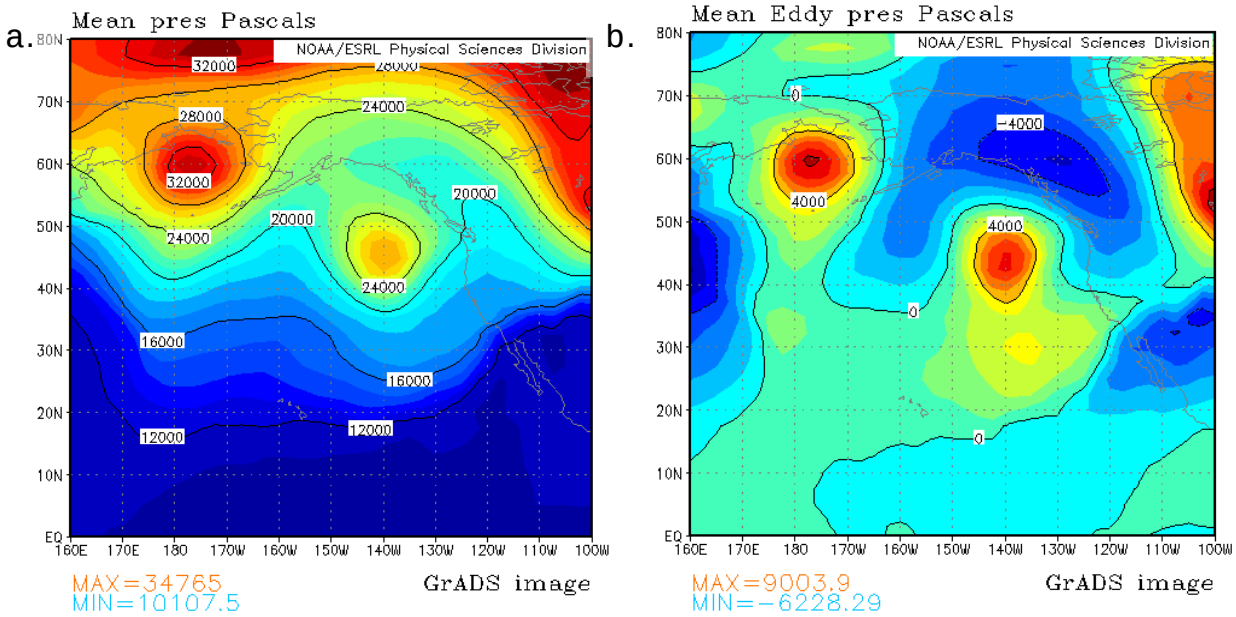

Figure 4.1.8. NCEP-NCAR gridded monthly mean (2.5° lat. x 2.5° long.) (a) pressure on the tropopause & (b) eddy pressure on the tropopause. Both figures valid 21 – 24 June 2004. Solid black lines represent pressure (Pascals).

As the blocking pattern entered maturity, the region of tropopause ridging encountered a migrating tropopause trough which remained constant through decay. This anomaly became embedded in the omega structure, effectively de-amplifying the anomalously high region of tropopause (Figure 4.1.9a). As the block dissipated completely, ridging at the tropopause

continued to occur over the Bering Strait while the region of lower tropopause pressure (centered over the Gulf of Alaska), coincided with the dissipation of the 500-hPa positive height anomaly (Figure 4.1.10a).

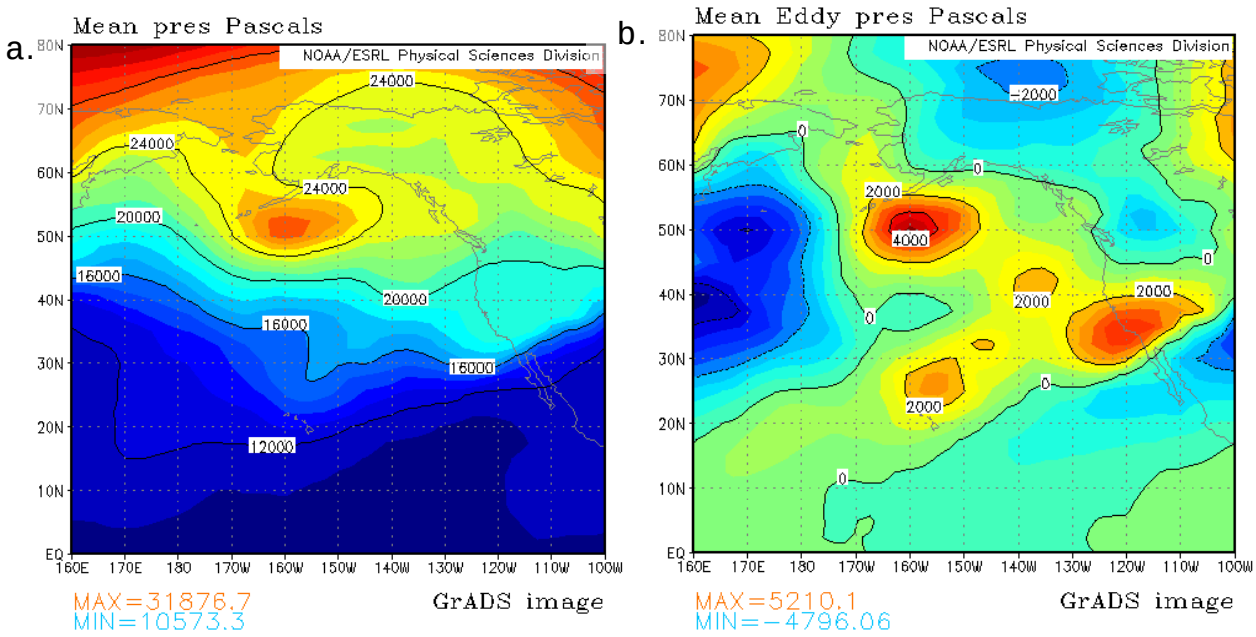

Figure 4.1.9. NCEP-NCAR gridded monthly mean (2.5° lat. x 2.5° long.) (a) pressure on the tropopause & (b) eddy pressure on the tropopause. Both figures valid 24 June 2004 – 05 July 2004. Solid black lines represent pressure (Pascals).

From the mean eddy pressure analysis, the synoptic contribution to the blocking event appears to be greater than that of the planetary scale. The strength and the size of the negative anomalies that covered the Alaskan Peninsula between 21 – 24 June 2004 allude to this (Figure 4.1.8b). The intensity of the positive upstream eddy can be attributed with the cyclone found at the surface; this feature was found to be between one-quarter and one-half of a wavelength from the blocking ridge. This suggests a positive contribution to the growth and upkeep of the block at 500-hPa.

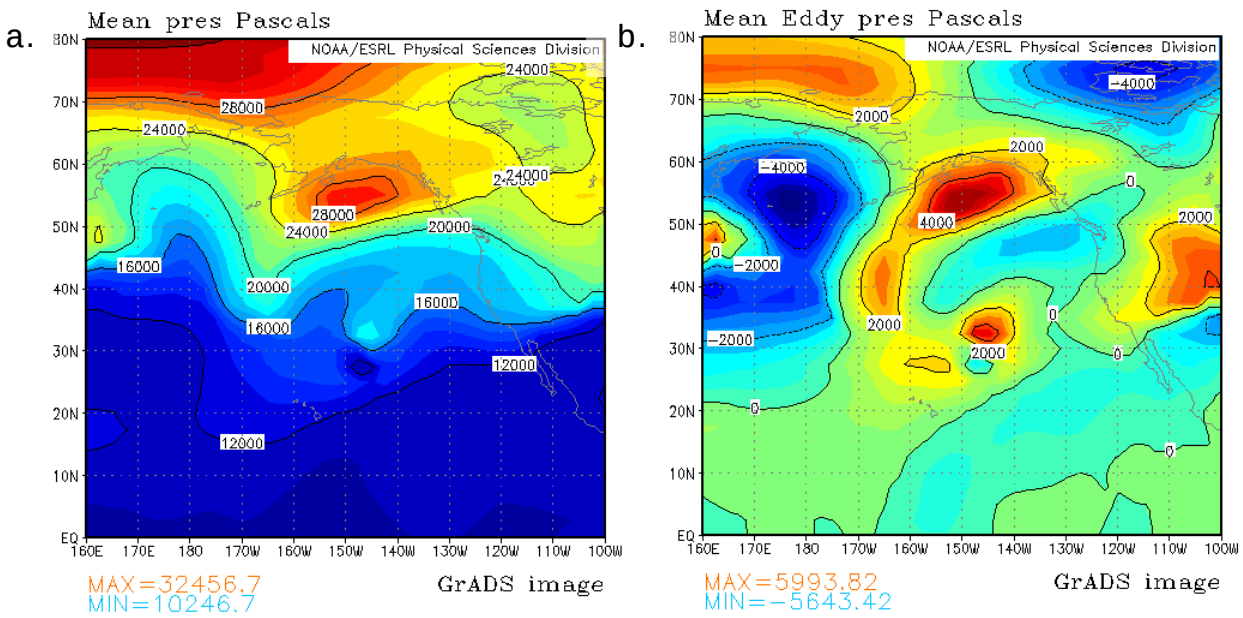

Figure 4.1.10. NCEP-NCAR gridded monthly mean (2.5° lat. x 2.5° long.) (a) Pressure on the tropopause & (b) Eddy pressure on the tropopause. Both figures valid 04 – 06 July 2004. Solid black lines represent pressure (Pascals).

During block maturity and decay, the conspicuous eddy-pressure anomalies at the tropopause maintained their relative size and strength, with the exception of the positive anomalies (4.1.9b). As time lapsed during the event, these features migrated further east into the blocking region, as pressure within the eddies increased. High-pressure advection (lower geometric heights) into the region aided in the de-amplification of the 500-hPa ridge (Figure 4.1.10b).

Just as was found in the August 2004 Western European block, the location of the positive tropopause eddies with respect to the block appears to play an important role in the evolution of the blocking anticyclone. While the planetary scale played a role in the modification of the flow, the migration of these eddies with time seems to coincide with the migration of

the 500-hPa ridge as does the decay of said features. Thus, in this case, the synoptic scale contributions lend greater credence to the maintenance and decay of this event (Table 4.1b).

Table 4.1b. Eulerian pressure advections and contributions to each scale

Onset (hPa/day)	Maintenance (hPa/day)	Decay (hPa/day)	Scale Contribution
-2.5	-4.3	0	Total
-6.7	-4.6	-1	Synoptic
4.2	0.3	1	Planetary

c. Gulf of Alaska: 05 – 28 August 2004

The second blocking event to affect Alaska and Northern Canada lasted 24 days and developed over a four-day period beginning 02 August 2004. The long-lived block mimicked the previous Alaskan block throughout its lifecycle to decay, which began on or around 27 August 2003 and reached completion two days later.

Sea-level pressure plots covering the period from 02 – 05 August are quite similar to those of the previous event. In the east-central Pacific, a large ridge of high pressure (1032-hPa) remained in place as a low-pressure system (1003-hPa) slowly filled (Figure 4.1.11a).

During the lifespan of the blocking event, the geographical extent of the system weakened in strength. The low-pressure system upstream of the Alaskan block remained nearly constant in intensity, however it migrated further south, just off the Aleutian Islands (Figure 4.1.11b). As with the earlier cases, the cyclone remained well within one-half wavelength; thus the

contribution of energy, via the surface cyclone, into the 500-hPa block amplification seems to have occurred.

During the decay stage of the blocking event, the spatial extent and over-all strength of the surface anticyclone continued to increase (4.1.11c). This occurred concurrent to the continued formation of a 1008-hPa cyclone over southern Alaska and the Gulf of Alaska within the blocking region.

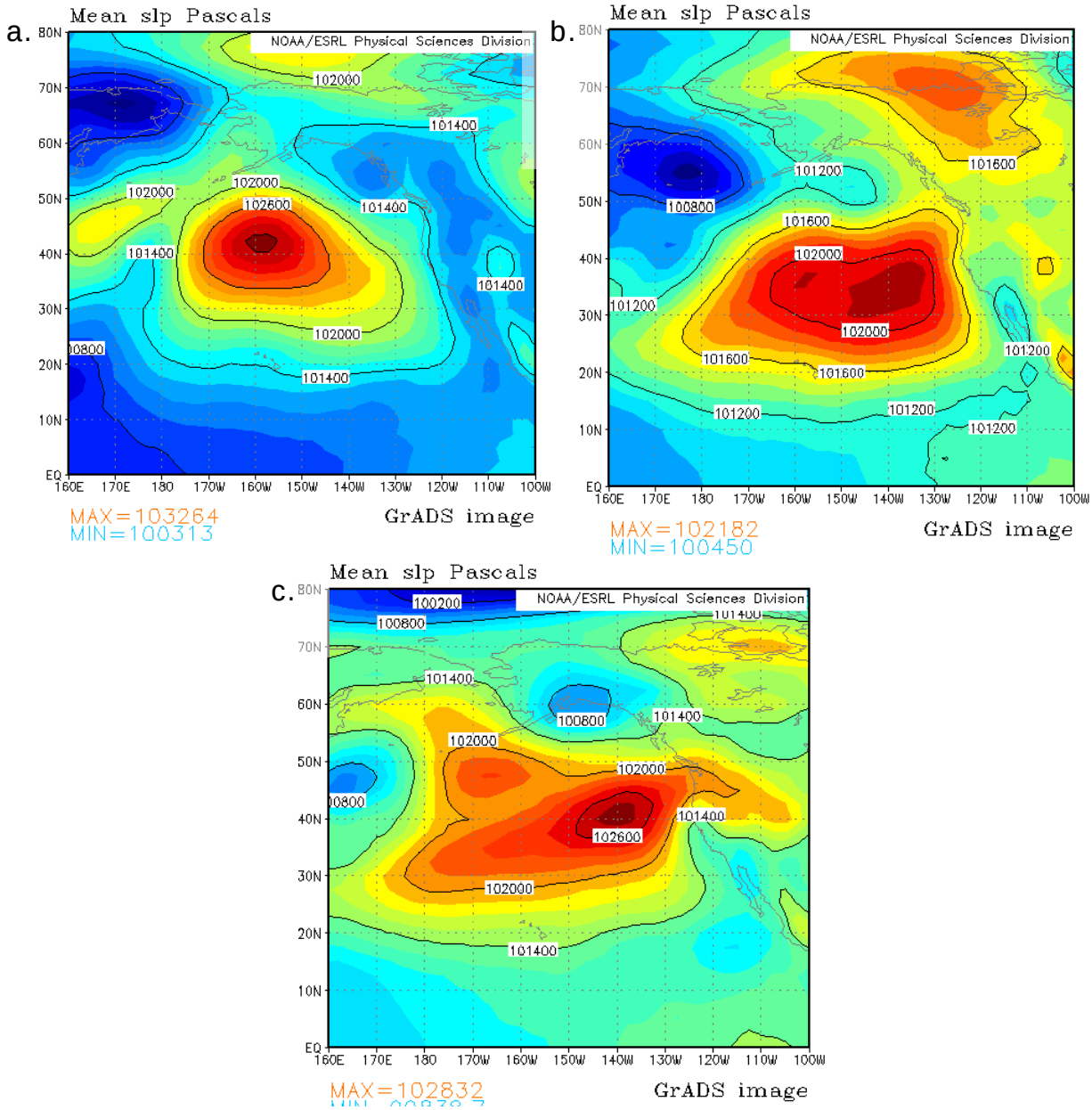

Figure 4.1.11. NCEP-NCAR monthly gridded (2.5° lat. x 2.5° long.) mean sea-level pressure valid (a) 02 – 05 August 2004, (b) 05 – 28 August 2004 & (c) 27 – 29 August 2004. Solid black lines represent pressure (Pascals).

At block onset, a few noticeable features appear in the pressure on the tropopause plots. The first is an extended column of higher tropopause over the Alaskan Peninsula. This ridging in the troposphere produced an omega-

pattern, with two lower tropopause anomalies situated on either side (Figure 4.1.12a). The isobars on the map appeared highly meridional, especially in the region of tropopause ridging.

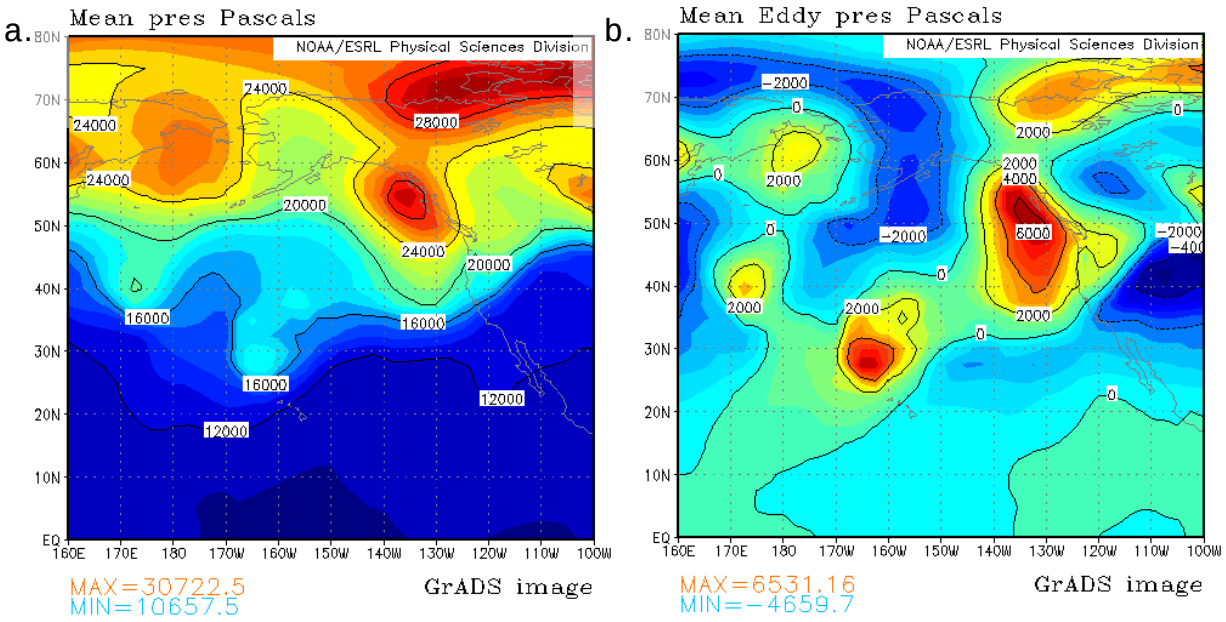

Figure 4.1.12. NCEP-NCAR gridded monthly mean (2.5° lat. x 2.5° long.) (a) Pressure on the tropopause & (b) Eddy pressure on the tropopause. Both figures valid 02 – 05 August 2004. Solid black lines represent pressure (Pascals).

The period of 05 – 27 August saw features not seen at initiation. Around 45°N, the isobars are quite zonal. Poleward, the pronounced ridging of the tropopause is well defined in a high amplitude feature stretching nearly 25° of latitude to 75°N (Figure 4.1.13a). Embedded within this region (as well as upstream) lower tropopause heights are found, which corresponded to surface cyclones and negative pressure anomalies at 500-hPa.

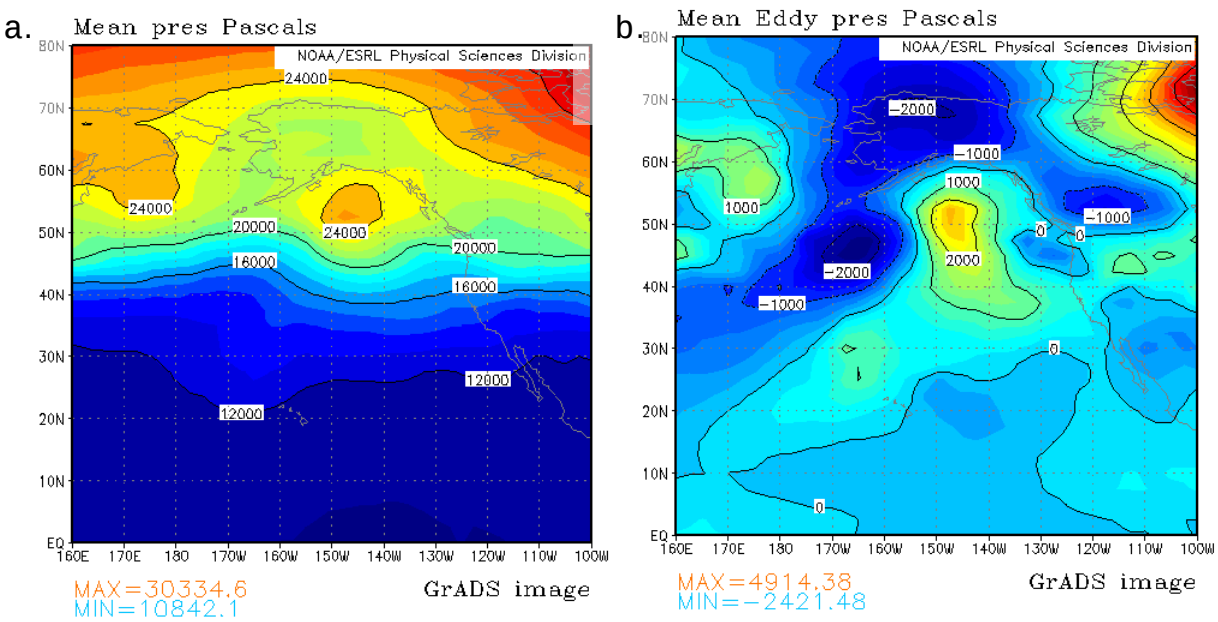

Figure 4.1.13. NCEP-NCAR gridded monthly mean (2.5° lat. x 2.5° long.) (a) pressure on the tropopause & (b) eddy pressure on the tropopause. Both figures valid 05 – 28 August 2004. Solid black lines represent pressure (Pascals).

During decay, prominent regions of tropopause troughing began to replace the tropopause ridging found during the block's mature phase. However, a new pressure ridge in the tropopause was seen forming in the western extents of the blocking region (Figure 4.1.14a).

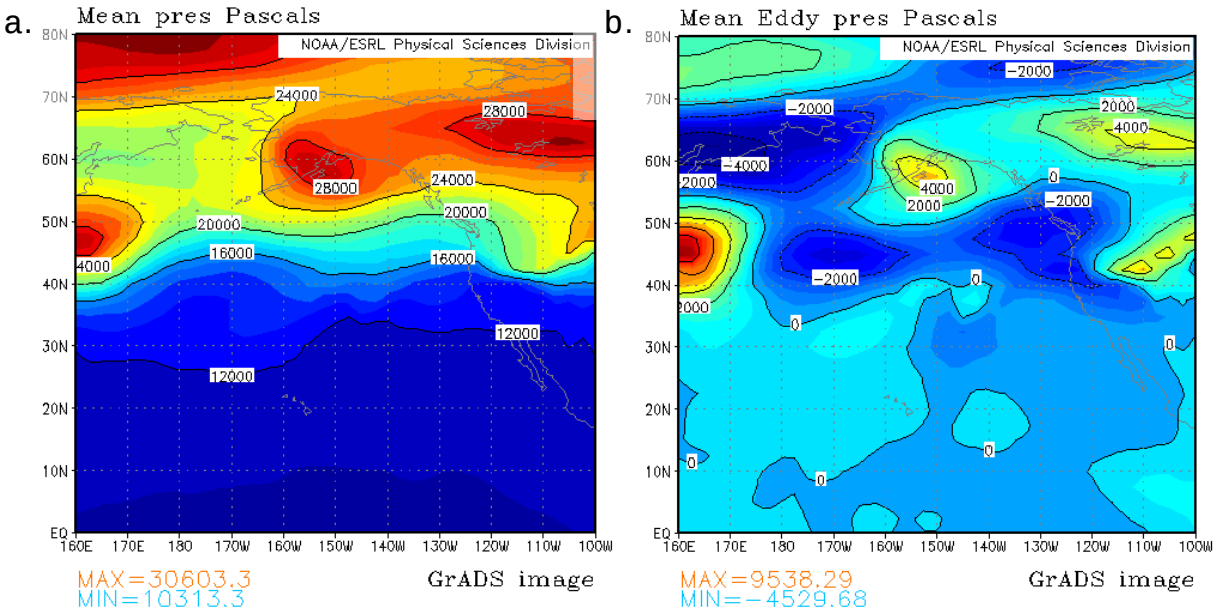

Figure 4.1.14. NCEP-NCAR gridded monthly mean (2.5^{o} lat. x 2.5^{o} long.) (a) pressure on the tropopause & (b) eddy pressure on the tropopause. Both figures valid 27 – 29 August 2004. Solid black lines represent pressure (Pascals).

The synoptic eddies (throughout the lifespan of the block) do not appear as large or strong as seen in the previous event. During 02 – 05 August, the strongest positive-pressure eddy (65-hPa) was located on the downstream leg of the split flow block signature at 500-hPa. Also, a backwards “C” formation is found arcing from the northwest corner of the tropopause pressure plot, equatorward through the Alaskan peninsula and terminating at the trip of the Aleutian Islands (Figure 4.1.12b). This negative pressure structure, along with the positive anomaly, are the features of focus throughout the entire event.

During the main portion of the event, the positive anomaly propagated into the southern reaches of the Gulf of Alaska. Through this time, the pressure in the eddy dropped nearly 40-hPa to around 25-hPa, producing a

hole-like structure in the pressure field. The omega feature that surrounded this region correlated well to the omega-blocking ridge at 500-hPa (Figure 4.1.13b).

The eddy pressure features became more zonal as the block de-amplified and finally dissipated completely, by 28 August. The only structures of note at dissipation are those located north of 40^{o}N latitude on the western parts of the map domain (Figure 4.1.14b). In this region, a negative pressure anomaly was building in as a new blocking event initiated.

Analysis of the mean eddy pressure features suggest that synoptic scale processes may not be as important in contributing to this blocking event. The planetary scale troughing and ridging, in relation with surface pressure features and the blocking ridge at 500-hPa suggest a nearly equal contribution from the large and small scales (Table 4.1c).

In this case, it seems the planetary scale provided a favorable background in which the synoptic scale eddies were able to augment the 500-hPa positive height anomaly. The positive contributions to the blocking flow (via planetary flow considerations) allowed for continued amplification in the first few days of the blocking event.

Table 4.1c. Eulerian pressure advections and contributions to each scale

Onset (hPa/day)	Maintenance (hPa/day)	Decay (hPa/day)	Scale Contribution
3.3	-1.0	30	Total
1.7	-1.0	15	Synoptic
1.7	-1.0	15	Planetary

4.2 Local Lyapunov Exponents

Lyapunov exponents, as discussed in Chapter two, are powerful because they can be utilized as a diagnostic tool when studying the degree of predictability in local flows. Inherently, this examination of predictability lends to the study of the flow stability itself. Consequently, Lyapunov exponents prove to be highly potent in their description of dynamic flows, since the equations governing the flow need not be explicitly solved.

When implementing these exponents in this study, it became apparent that the stability (rather stability changes) of the large-scale planetary background flow are key in all phases of the blocking episode. As will be shown, abrupt changes in the planetary flow greatly correlate with abrupt changes in exponent variability over a given temporal period.

In terms of plotting regional Lyapunov exponents, calculations come directly from Equation 2.3.3. As for the graphical representation of the exponent, the sum of positive Lyapunov exponents is placed along the ordinate with respect to time. The temporal spacing is placed along the abscissa for a stationary box of a given latitude and longitude (representing the spatial domain of the blocking region) as seen in the Lyapunov figures.

When diagnosing atmospheric flow regimes using Lyapunov exponents, regions having relatively smaller positive values (on the vertical axis) are highly correlated to blocking episodes in both hemispheres. As stated earlier, abrupt changes in the “positiveness” of the exponent can be

used to pinpoint the time periods and trends relating to certain stages of the blocking flow (i.e. initiation, maintenance, and decay).

Also of note, the sum of the Lyapunov exponents is analogous to the area-averaged enstrophy of the dynamic system. Enstrophy, as a physical quantity, is merely one-half the square of relative vorticity and conserved in two-dimensional invicid flows (Leith 1968). Enstrophy becomes important in understanding the dissipative effects of large scale eddies on various flow regimes, including blocking.

For all calculations herein, the 500-hPa 0000Z data was used, as well as the latitude box covering 20^{o}-80^{o}N. The longitude box differed only as specified by the blocking region (whether Western Europe or Alaska). Limitation of the longitude box produced higher quality output and thus more specific results.

a. Western Europe: 06 – 13 August 2003

When considering the Western European heat wave of 2003, the period of 01 – 15 August 2003 is highly important, since this span of time was when the blocking anticyclone was at its strongest. Analysis of the Lyapunov exponents (confined to a longitude box covering 60^{o}W to 40^{o}E and a latitude box covering 20^{o} to 80^{o}N) showed a steep decrease in the positive nature of the exponent in the period directly preceding block initiation (Figure 4.2.1). This behavior is expected, in that the flow becomes more predictable when the sum values of the exponent are closer to zero. A

greater degree of variability is evident from around 05 – 08 August as the block matured, with Lyapunov values spiking to around $1.4x10^{-10}$, the second largest peak in the 31 day period. After this brief period of flow instability, the blocking regime stabilizes until the blocking pattern begins to decay on or around 12 August.

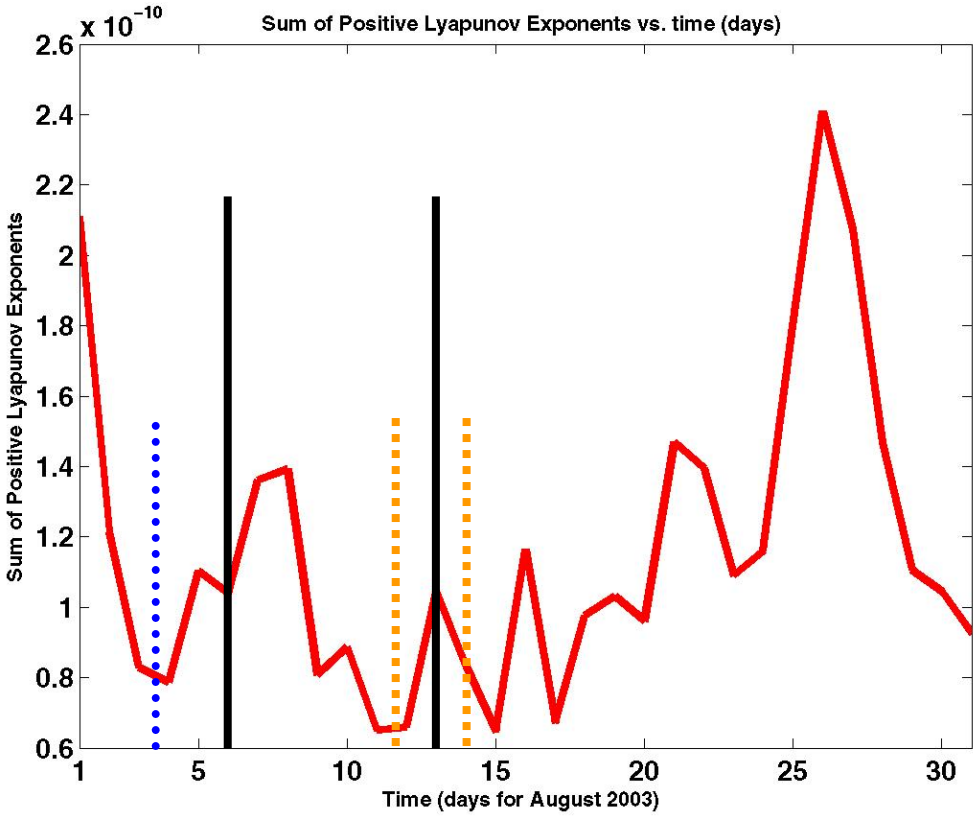

Figure 4.2.1: The area-averaged enstrophy using Eq. 2.3.3. Lyapunov exponents are found on the ordinate with respect to time (days), along abcissa represents the stationary box (60°W to 40°E and 20°N to 80°N) in the mid-latitudes of the Northern Hemisphere. Valid from 01 – 31 August 2003. Solid black vertical lines represent the period of block maintenance; dashed blue line represents block onset; dashed gold lines represent the period of block decay.

This analysis is consistent with the premise that a minimum state of enstrophy (a more stable flow) should represent the blocking flow as seen in the less-positive nature of the Lyapunov exponents. This pattern in the

exponents suggests that during block maintenance, the flow regime is highly stable and only begins to dissipate as the planetary scale vacillates to another phase (i.e. dissipation).

b. Gulf of Alaska: 24 June – 05 July 2004

When considering the Alaskan events as a whole, the domain of the Lyapunov exponents differs from that of the 2003 European event for obvious regions. As discussed previously, the more specific the stationary latitude and longitude boxes, the more accurate the outputted summed positive Lyapunov exponents. Thus, the stationary box for both Alaskan events covers a longitudinal area of 160^{o}E – 100^{o}W, and a latitudinal area from 20^{o} to 80^{o}N.

Figure 4.2.2a shows a steep decrease in enstrophy from around $2.1x10^{-10}$ to $0.9x10^{-10}$ in the days preceding the initiation of the blocking pattern. Analysis of such behavior suggests the planetary flow was stabilizing until the event began. There is a noticeable $0.6x10^{-10}$ rebound two days before the block; this spike is minor, however, when compared to the exponents becoming precipitously less positive days before.

During block initiation, the flow became more stable as the exponents approached the minimum of the temporal period, nearing $0.8x10^{-10}$ by 24 June. For the duration of block maintenance and maturity the sum of positive exponents steadily rose until an abrupt decrease began on 02 July

and lasted until 05 July. When the behavior of the exponents during this period is evaluated, the results suggest the pattern is that of block dissipation. Compared to previous analyses in earlier chapters, the behavior of the exponent corresponds well to each stage of the blocking episode (as show in the pressure on the tropopause and 500-hPa mean geopotential height plots, for example).

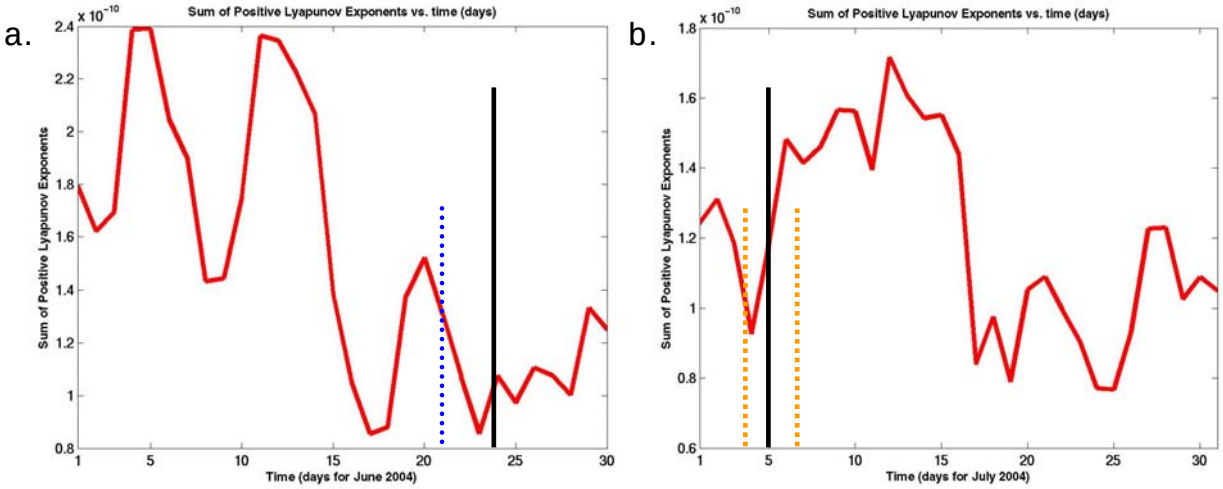

Figure 4.2.2: The area-averaged enstrophy using Eq. 2.3.3. Lyapunov exponents are found on the ordinate with respect to time (days), along abscissa represents the stationary box (160°E to 100°W and 20°N to 80°N) in the mid-latitudes of the Northern Hemisphere. Valid from (a) 01 – 30 June 2004 & (b) 01 – 31 July 2004. Solid black vertical lines represent the period of block maintenance; dashed blue line represents block onset; dashed gold lines represent the period of block decay.

The fact that the flow remained relatively steady (a minimum enstrophy state) through the strongest period of the block verifies previous findings of Lupo et al. (2005) and Hussain et al. (2007) that the blocking flow represented a strongly barotropic state on the planetary scale. Specifically, the large-scale flow is more predictable during minimal periods

of enstrophy and thus the most intense part of the block should represent a period of higher predictability.

c. Gulf of Alaska 05 – 28 August 2004

As seen in the previous events, a sharp decrease in enstrophy preceding the initiation of the block is apparent in Figure 4.2.3. During the period of block initiation, there existed a steady rise in the exponents (from 0.6×10^{-10} to around 1.2×10^{-10}). Again, such a drastic change in the sum of positive exponents represents the transition of the planetary scale flow from a more zonal phase into a highly meridional phase.

Fluctuations of enstrophy during the next period of the block seem irregular, compared to the previously discussed events. However, the length of the maintenance and maturity phase (05 – 28 August) may offer some clues to the variability in enstrophy. Over this 23-day period, smaller scale processes (on the synoptic scale) definitely acted upon the blocking anticyclone as seen in the synoptic analyses contained in Section 3.3.

Another feature of note is an anomalously intense spike of positive values around 22 August. This spike looks to represent the beginning of the decay phase of the block, as well as the amplification a new blocking ridge near the western boundary of the domain (160^{o}E). Perhaps this variability within the domain produced this signature in the Lyapunov exponents due to the sharp gradients being produced over a relatively small region. With two

blocks occurring in the same spatial and temporal extents, it is plausible that a superposition of sorts is occurring in the Lyapunov plots. Only as the main block decayed did the enstrophy curve begin to return to its more expected behavior.

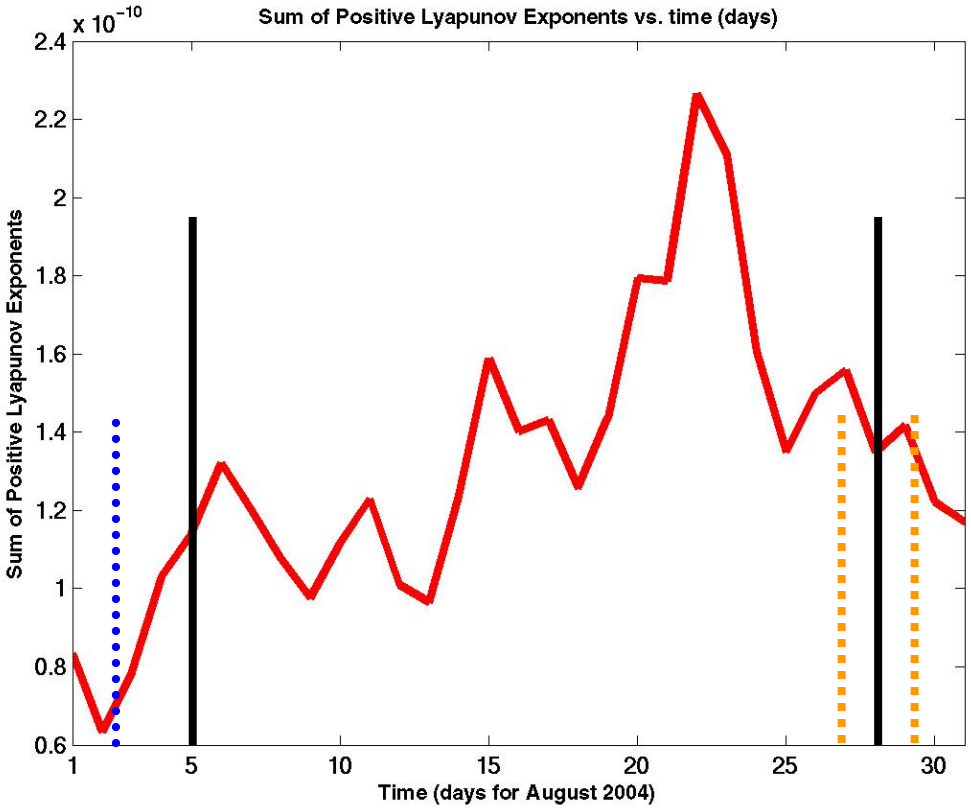

Figure 4.2.3: The area-averaged enstrophy using Eq. 2.3.3. Lyapunov exponents are found on the ordinate with respect to time (days), along abscissa represents the stationary box (160°E to 100°W and 20°N to 80°N) in the mid-latitudes of the Northern Hemisphere. Valid from 01 – 31 August 2004. Solid black vertical lines represent the period of block maintenance; dashed blue line represents block onset; dashed gold lines represent the period of block decay.

Chapter 5

Discussion, Summary, and Conclusions

5.1 Discussion

The objectives of this study were to address several fundamental questions:

- Does the planetary-scale act as a favorable background and reinforce synoptic-scale processes with respect to blocking?
- Can local Lyapunov exponents (enstrophy) be used as a means of diagnosing blocking onset/decay by determining changes in local flow stability characteristics?
- Does Lyapunov exponent analysis reinforce pressure-on-the-tropopause analysis as a diagnostic quantity?

Presented now are the results and outcome of the analyses contained in the previous chapters. When discussing the first fundamental question, the results found in Chapter four show a strong tendency for the planetary scale to produce a favorable background in which the blocking flows can develop.

When evaluating the Western European event of summer 2003, plots of pressure on the tropopause show a positive contribution (i.e. a situation in which block development was more likely to occur) to the onset and maintenance of the blocking anticyclone. Extreme gradients, especially during the mature phase of the block, were also found in the tropopause pressure fields (Figure 3.1.3). These gradients developed on the boundaries

between the planetary scale ridge/trough couplet covering the entire domain of the blocking region.

For the purposes of synoptic examination, the zonal mean was subtracted from the mean tropopause pressure plots. This analysis technique allows for the examination of synoptic scale eddies and their interaction with the blocking ridge itself. During block maintenance, a positive pressure feature was found less than one-half of a wavelength from the central axis of the block (and co-located with a surface cyclone). This suggests Eulerian low-pressure advection and in turn, the advection of higher geometric heights. Higher geometric height advection into the blocking ridge effectively amplified and strengthened the European block.

The resulting interpretation shows that indeed the planetary scale (troughing and ridging) played an important role in blocking onset and maintenance, but a stronger contribution form the synoptic scale eddies (cyclones and anticyclones) allowed the Western European event to strengthen. This intensification only reinforced the heat wave occurring over Europe. It is interesting to note, however, that planetary contributions appeared to produce a more positive role during block decay, as the planetary flow shifted into a new geostrophic phase.

As with the 2003 Western European event, the two 2004 Alaskan events behaved very similarly. During the first event, the strength of the positive and negative pressure eddies pointed towards a greater tendency

for synoptic-scale contributions affecting the block region. In fact, surface cyclogenesis upstream of the blocking anticyclone again allowed for the strengthening of the block. Intense meridional variations in the flow (on the planetary scale) produced large gradients (Figure 3.3.3). With such strong gradients, intensification of the synoptic features imbedded within the flow produced favorable results for blocking.

Slight variations in the planetary and synoptic contributions to the second Alaskan blocking episode are apparent in the mean tropopause pressure plots. During the lifespan of this event, the planetary scale did indeed provide a conducive background for the development of the blocking anticyclone over Alaska. However, the size and strength of supporting synoptic scale pressure eddies (and co-located surface features) tended to show the synoptic scale as more involved in this episode (Figure 4.1.12b). This, nonetheless, does not downplay the role of features on the planetary scale in the development of smaller scale entities. Specifically the maturity and intensification of those smaller eddies reinforced a larger scale environment favorable for block onset and maintenance.

As the above paragraphs have stressed, the breakdown of these three separate events show the synoptic scale eddies fed on energy from the larger scale background. Due to this, positive energy contributions on the planetary scale filtered down into the synoptic scale. In turn, these eddies advected higher geometric heights into the blocking ridge, greatly amplifying

the block until a point in which the planetary scale ceased or slowed its downward energy transport. When this occurred, the planetary scale began to change the character of its flow stability profile, thereby vacillating into a new, more zonal phase. This process effectively pacified the meridional flow regime, which is of the utmost importance for block maintenance.

Changes in the flow stability character of the planetary scale are not inherently obvious in the synoptic or dynamic analyses. Moreover, the predictability of such changes (especially when considering blocking anticyclones) is one of the major shortcomings in the study of atmospheric blocking. The events discussed in this study (i.e. the European heat wave of 2003 and “Baked Alaska” 2004) cannot be prevented, as they are naturally occurring atmospheric phenomena. Nevertheless, if forecasts for blocking onset were possible, the economic, social and societal effects may be mitigated by advance preparation alone. The mathematical entity known as the local Lyapunov exponent appears to be one of the most promising weapons in the arsenal of blocking diagnostics and thusly, a way of producing higher quality forecast as well as greater forecast lead time. These exponents, as discussed in Section 4.2, are very powerful in that they can be utilized when studying the degree of stability of a given atmospheric flow. Understanding stability lends to the understanding of flow predictability. In this study, local Lyapunov exponents were used to evaluate atmospheric flow characteristics directly related to blocking anticyclones. The results of

chapter four reveal a surprising connection between the behavior of the atmospheric flow (directly preceding block onset/decay) and the change in character of the sum of positive Lyapunov exponents.

Exponent analysis was performed on each event after the analyses completed in Chapter 3 and the beginning of Chapter 4. As discussed in these chapters, block onset through decay were detailed for each event. Specific dates can be found in Table 1.1. Of particular importance were the dates of block onset. Previous studies have shown that the forecastibilty of onset is still predominantly difficult. The results shown in this study suggest that the local Lyapunov exponent may help depreciate the previous statement greatly.

The onset of the European block began on 03 August 2003. Following two days of initial development, analysis showed the block reached full intensity until 12 August when the block began to decay. When the sum of positive Lyapunov exponents is plotted versus time, several interesting features arise. The first, and perhaps most significant (as Figure 4.2.1 shows) was a steep drop in the “positiveness” of the exponent (around 1.3×10^{-10} in just over one day). Since a less positive exponent represents a stabilizing atmosphere, it becomes apparent that a major shift in the planetary flow was occurring just prior to block initiation. After the onset of the blocking event, a slight rebound was prevalent and remained until the block began to dissipate. One would expect relatively smaller positive values

since a blocking regime represents a minimum state of enstrophy, and thus a more stable flow. Only immediately before block decay did the exponents begin to decrease towards the monthly minimum enstrophy. This action alone mimics the temporal period prior to blocking onset.

The first Alaskan summer event of 2004 was highly comparable to the European blocking episode of 2003. Directly preceding initiation a precipitous drop in the exponents occurred analogous to that of the European initiation (4.2.2a). However, a more-positive spike developed as initiation began. This pattern suggests the flow was destabilizing until the planetary scale fully modified into the new state of geostrophy (represented as the stable block). Exponents remained relatively stable until another anomalous drop directly before decay ensued (Figure 4.2.2b).

The length of the second Alaskan block provides for a blocking pattern that differed in a few respects from the first two events. In spite of this, closer examination of the Lyapunov exponents shows results corresponding to the previous events. At block onset (02 August 2004) enstrophy was at a minimum, due again to a sharp decrease in the exponents (Figure 4.4.3). A minor spike appeared and remained until the blocking anticyclone reached its main phase. After about 05 August, the Lyapunov exponents remained relatively stable. Due to synoptic interactions during the long lifespan of the block, a large positive spike (2.0×10^{-10}) was found around 18-20 August. Synoptic and dynamic interpretation showed a new block forming on the

western border of the domain, as well as dissipative-like behavior in the Alaskan block. These concurrent events acted to produce further destabilization in the flow and hence, anomalous actions throughout the latter stages of the event. Enstrophy dropped by nearly the same magnitude only days before the ridge decayed, signifying an approaching flow regime change.

The consequences of this section are fascinating in that a highly noticeable pattern emerges in the sum of positive Lyapunov exponents. In all three cases, a steep decrease in enstrophy always preceded the initiation of a blocking anticyclone. Correspondingly, a steady decrease of enstrophy also preceded blocking decay. Taken individually, when the exponents became less-positive, a transition in the stability profile of the planetary scale flow ensued. Only after block onset did the exponents remain stable. This represented a quasi-complete transition form a zonal current to a highly meridional (and thus blocked) current. The decay of the block merely signified the reversion of the high amplitude flow back to a more zonal orientation.

In terms of stability, the basic premise found in the exponent analysis is one of the planetary scale flow becoming highly unstable prior to block initiation and dissipation. Moreover, this oscillation between flow states coupled with the fact that blocking flows are inherently stable suggests the buildup of gradients (see Chapter 3) produces the necessary background

instability for planetary scale flow transitions. This analysis demonstrates the power of local Lyapunov exponents (and the related physical quantity of enstrophy) in the study of blocking regimes and large-scale flow transitions.

Local Lyapunov exponents, with respect to pressure on the tropopause, appears to add strength (and in so doing, extra power) to this diagnostic quantity. While Lyapunov exponents offer an astonishing look into the changes in the flow regimes on the planetary scale, mean tropopause pressure plots aid in the identification of synoptic scale eddies. These smaller scale structures effectively feed on energy from higher scales. Section 4.1 produced a dynamic examination of how the processes on the small (synoptic) and large (planetary) scales interact in the formation, maintenance and decay of blocking events. Since each scale provides a positive contribution, in terms of blocking onset and decay, a correlation should exist between changes in the advection of pressure at the tropopause and changes in the Lyapunov exponents. Changes in these pressure advections correspond to changes in the advection of geometric heights. These height elements coincide with features found throughout the atmosphere (e.g. surface cyclone, 850-hPa thermal ridges, 500-hPa height anomalies, etc.). Any abrupt changes within the planetary scale flow produce ensuing modifications in these structures and hence modification to weather patterns in general. As a result, changes in intensity or the propagation of these tropopause pressure eddy anomalies should lend credence to

concurrent changes in the large scale flow itself. Dynamically, every atmospheric scale is connected. Accordingly, the changes suggested above should be mirrored in the behavior of the local Lyapunov exponents. The results from the dynamic analyses appear to verify this statement.

5.2 Conclusions

This study was devised to answer several fundamental questions:

- Does the planetary-scale act as a favorable background and reinforce synoptic-scale processes with respect to blocking?

  Using dynamic analysis of pressure on the tropopause plots as well as synoptic analyses (performed at 300-hPa, 500-hPa and 850-hPa), it was found the planetary scale provided a background environment conducive to block development and maintenance. During the mature phase of the block, there existed extreme large-scale gradients in the mean tropopause pressure fields. These gradients developed on the boundaries between the planetary scale ridge/tough couplets that were present in each of the studied events. The atmospheric instability produced via these gradients allowed for the transitioning between atmospheric flow regimes, include that of the blocking phase itself. It is important to note that synoptic scale processes also augment the planetary scale contributions.

Since the favorable planetary scale background existed, synoptic scale eddies were allowed to form upstream and downstream of the blocking anticyclone (near the large gradients). Upstream interaction of surface cyclones (within one-half wavelength from the blocking ridge axis) acted to amplify the blocking anticyclone.

In each case, planetary scale energy augmented synoptic scale processes, which induced further amplification of the blocking ridge. Concurrent with the strengthening of the blocking event, gradients on the planetary scale also increased in intensity. This give and take of energy between scales eventually led to the de-amplification of the meridional flow and the dissipation of the blocking anticyclone.

- Can local Lyapunov exponents (enstrophy) be used as a means of diagnosing blocking onset/decay by determining changes in local flow stability characteristics?

The findings of this study are remarkable in that these exponents show great promise in understanding the large scale flow characteristics seen in atmospheric blocking. When each case was examined using plots of the sum of positive Lyapunov exponents versus time, a steep decrease in enstrophy always preceded the initiation of a blocking anticyclone. Correspondingly, a decrease in enstrophy preceded blocking decay in each event. Taken as a whole,

when the exponents became less-positive, a transition in the stability profile of the planetary scale flow ensued. After block initiation (dissipation) the exponents remained stable, representing a quasi-complete transition from (to) a zonal flow to (from) a highly meridional, and thus blocked, flow.

When discussing the character of stability, the most essential feature found in the analysis of area-averaged enstrophy (given by Lyapunov exponents) is one of the large scale flow becoming highly unstable prior to block onset/decay. One of the physical mechanisms responsible for this is the build-up of instability via gradients in the temperature and mass fields. Once enough instability has been accumulated, the flow is forced to find a new geostrophic state.

The vacillation between flow states and the fact that blocking flows are inherently stable support the statement above. Furthermore, the power of local Lyapunov exponents is highly evident from the analyses provided in this study. Not only can these entities determine local fluid stability (or changes in stability), they also aid in the analysis of the predictability of large scale flows, specifically atmospheric blocking.

- Does Lyapunov exponent analysis reinforce pressure on the tropopause analysis as a diagnostic quantity?

    Local Lyapunov exponents do an exceedingly great job determining the onset and decay of blocking flows as previously discussed. This study has shown the interconnectivity between the planetary and synoptic scales when examining blocking events. When probing the character of the planetary scale flow regime, it has been shown that any abrupt changes within this scale produce resulting modifications on synoptic scale structures and in turn, alterations to weather patterns in general. As a result, changes in intensity or the propagation of eddies in the tropopause pressure fields should signal large scale flow restructuring. Since planetary flow vacillations produce changes on the smaller scale, these subsequent synoptic adjustments should be emulated in plots of the sum of positive Lyapunov exponents.

In conclusion, the results found in this thesis study have shown the power of local Lyapunov exponents as a means of determining the onset and decay of extreme cases of atmospheric blocking. While ensuing extreme weather phenomena cannot be prevented, the possible implication of the local Lyapunov exponent analysis points at the possibility of the creation of higher quality block onset forecasts and extended lead time for forecasts in

general. Additionally, it has been shown the degree that planetary scale plays a role in the development and maintenance of blocking anticyclones. While this scale may not directly produce blocking events, it certainly creates the background character conducive for synoptic scale processes via eddies formation and interaction. Due to these interactions, manifestations of the block itself are found throughout the atmosphere, whether as a surface anticyclone, an 850-hPa thermal ridge, a 500-hPa positive height anomaly or as a positive pressure eddy on the tropopause.

Intrinsically though, the dynamic and synoptic description of atmospheric blocking (as detailed in the analyses contained in this study) is matched in power by the Lyapunov exponent examination. By understanding the concept of enstrophy and the basic premise set forth in Lupo et al. (2005) "…that atmospheric blocking should be thought of as a quasi-stationary circulation whose state is best analyzed by its stability characteristics," a profound hope is created in that the promise of an eventual understanding of the stability character of atmospheric blocking will lead to a more complete knowledge with respect to the predictability of large scale atmospheric flows.

Appendix A: Pressure on the Tropopause Data

A. 06 – 13 August 2003

Day	dp(total) [hPa]	dp(synoptic) [hPa]	dp(planetary) [hPa]
3	-10	-20	10
4	-10	10	-20
5	10	0	10
6	0	20	-20
7	10	0	10
8	0	0	0
9	0	0	0
10	-10	0	-10
11	0	5	0
12	0	-25	20
13	-20	-10	-10
14	0	-10	0

B. 24 June – 05 July 2004

Day	dp(total) [hPa]	dp(synoptic) [hPa]	dp(planetary) [hPa]
21	0	0	0
22	0	-10	10
23	0	10	-10
24	-15	-20	5
25	0	-10	10
26	15	0	15
27	0	10	-10
28	0	0	0
29	0	0	0
30	-20	-10	-10
1	-20	0	-20
2	0	-20	20
3	-10	-10	0
4	0	0	0
5	-10	-2	-8
6	20	2	18

C. 05 – 28 August 2004

Day	dp(total) [hPa]	dp(synoptic) [hPa]	dp(planetary) [hPa]
2	20	10	10
3	10	-5	15
4	-10	10	-20
5	0	-10	10
6	10	20	-10
7	30	0	30
8	-10	-10	0
9	-30	-30	0
10	0	10	-10
11	0	0	0
12	20	20	0
13	-10	-20	10
14	0	10	-10
15	0	10	-10
16	-10	-20	10
17	-10	10	-20
18	10	-10	20
19	10	10	0
20	0	10	-10
21	10	-30	40
22	-10	10	-20
23	10	20	-10
24	-20	-40	20
25	-70	-20	-50
26	-10	-10	0
27	40	40	0
28	30	20	10
29	19	-20	39

References

Alaskan Climate Research Center, 2004: Record breaking summer of 2004. http://climate.gi.alaska.edu/News/summer04.html.

Austin, J.F., 1980: The blocking of middle latitude westerly winds by planetary waves. *Quart. J. Roy. Meteor. Soc*., **106**, 327-350.

Burkhardt, J.P., and A.R. Lupo, 2005: The planetary and synoptic scale interactions in a Southeast Pacific episode using PV diagnostics. *J. Atmos. Sci.*, **62**, 1901-1916.

Cohen, R.A., and D.M. Schultz, 2005: Contraction rate and it's relationship to frontogenesis, the Lyapunov exponent, fluid trapping, and air stream boundaries. *Mon. Wea. Rev.*, **133**, 1353 – 1369.

Colucci, S.J., 1985: Explosive cyclogenesis and large-scale circulation changes: Implications for atmospheric blocking. *J. Atmos. Sci.,* **42**, 2701-2717.

Constantin, P., C. Foias, R. Teman, 1985: Attractors representing turbulent flows. *Mem. Amer. Math. Soc.*, **53**.

Danielsen, E.F. and R.S. Hipskind, 1980: Stratospheric-tropospheric exchanges at polar latitudes in summer. *J. Geophys. Res.*, **85**, 393-400

Dymnikov, V.P., Kazantsev, Ye. V., Kharin, V.V., 1992: Information entropy and local Lyapunov exponents of barotropic atmospheric circulation. *Izv. Russ. Acad. Sci. Atmopsher. Ocean. Phys*., **84**, 911-920.

Galarneau, T. J., Jr., L. F. Bosart, and A. R. Aiyyer, 2008: Closed anticyclones of subtropical and middle latitudes: A 54-year climatology (1950–2003) and three case studies. *Frederick Sanders Monograph, Meteor. Monogr.,* Amer. Meteor. Soc., in press.

Hoskins, B., M. McIntyre and A. Roberston, 1985: On the use and significance of isentropic potential vorticity maps. *Quart. J. Roy. Meteor. Soc.*, **111**, 877-946.

Hussain, Athar, A.R. Lupo, C. Strong, and S. Dostoglou, 2007: A diagnostic study of the atmospheric blocking using Lyapunov exponents over a 50 year period. *Pre-prints of the 19th Conference on Climate Variability and Change, 14-18 January, 2007, San Antonio, TX*

Kalnay, E., and Coauthors, 1996: The NCEP-NCAR 40-Year reanalysis project. *Bull. Amer. Meteor. Soc*, **77**, 437 – 471.

Kelsey, Eric and L.F. Bosart, 2006: Supertyphoon Dale (1996): A remarkable storm from birth through extratropical transition to explosive reintensification that impacted the tropics, mid-latitudes and the Arctic. *Pre-prints of the 27th Conference on Hurricanes and Tropical Meteorology, 24 – 28 April, 2006, Monterey, CA*

Konrad, C.E. and S.J. Colucci, 1988: Synoptic climatology of 500 mb circulation changes during explosive cyclogenesis. *Mon. Wea. Rev.,* **116**, 1431-1443.

Kovats, S., T. Wolf and B. Menne, 2004: Heat wave of August 2003 in Europe: Provincial estimates of the impact on mortality. *Euro. Surveill.*, **8**, [http://eurosurveillance.org/ew/2004/040311.asp#7].

Lorenz, E.N., 1963: Deterministic nonperiodic flow. *J. Atmos. Sci.,* **20**, 130-141.

Leith, C. E., 1968: Diffusion approximation for two-dimensional turbulence. *Phys. Fluids*, **11**, 671–673.

Lejenas, H. and H. Okland, 1983: Characteristics of Northern Hemisphere blocking as determined from a long time series of observational data. *Tellus*, **35A**, 350 - 362

Lupo, A.R., I.I. Mokhov, S. Dostoglou, A.R. Kunz, and J.P. Burkhardt, 2005: The impact of the planetary scale on the decay of blocking and the use of phase diagrams and Lyapunov exponents as a diagnostic. *Pre-prints of the 21st Conference on Weather Analysis and Forecasting/17th Conference on Numerical Weather Prediction, 1-4 August, 2005, Washington, DC.*

Lupo, A.R., J.J Nocera, L.F. Bosart, E.G. Hoffman and D.J. Knight, 2001: South American cold surges: Types, composites and case studies. *Mon. Wea. Rev.*, **129**, 1021-1041.

Lupo, A.R and L.F. Bosart, 1999: An analysis of a relatively rare case of continental blocking. *Q. J. R. Meteor. Soc*. **125**, 107 – 138.

Lupo, A.R. and P.J. Smith, 1995a: Climatological features of blocking anticyclones in the Northern Hemisphere. *Tellus*, **47A**, 439-456.

Lupo, A.R. and P.J. Smith, 1995b: Planetary and synoptic-scale interactions during the life cycle of a mid-latitude blocking anticyclone over the North Atlantic. *Tellus*, **47A**, 575-596.

Lupo, A.R., I.I. Mokhov, S. Dostoglou, A.R. Kunz, and J. P. Burkhardt, 2007: The impact of the planetary scale on the decay of blocking and the use of phase diagrams and enstrophy as a diagnostic. *Izvestiya, Atms-Oc.,* **43,** 45 – 51.

Lyapunov, A.M., 1966: *Stability of motion*. Academic Press

Morgan, M.C. and J.W. Nielsen-Gammon, 1998: Using tropospheric maps to diagnose midlatitude weather systems. *Mon. Wea. Rev.,* **126**, 2555-2579.

Nielsen-Gammon, J.W., 2001: A visualization of the global dynamic tropopause. *BAMS,* **82,** 1151-1167.

Nielsen-Gammon, J.W. and R.J. Lefevre, 1996: Piecewise tendency diagnosis of dynamical processes governing the development of an upper-tropospheric mobile trough. *J. Atmos. Sci.,* **53**, 3120-3142.

Pesin, J.B., Characteristic Lyapunov exponents and smooth ergodic theory. *Russian Math. Surveys*. **51**, 314-322.

Pirard, P., S. Vandentorren, M. Pascal, K. Laaidi, A. Le Tertre, S. Cassadou and M. Ledrans, 2005: Summary of the mortality impact assessment of the 2003 heat wave in France. *Euro. Surveill.*, **10**, [http://eurosurveillance.org/em/v10n07/1007-224.asp].

Skiba, Y.N., 2002: On the spectral problems in the linear stability study of flows on a sphere. *J. Math. Anal. Appl*., **270:1**, 165-180.

Triedl, R.A., E.C. Birch, and P. Sajecki, 1981: Blocking action in the Northern Hemisphere: A climatological study. *Atmos-Ocean*, **19**, 1-23.

Rex, D.F., 1950a: Blocking action in the middle troposphere and its effects upon regional climate. I: An aerological study of blocking action. *Tellus*, **2**, 196-211.

Rex, D.F., 1950b: Blocking action in the middle tropospheric westerlies and its effects on regional climate. II: A climatology of blocking action. *Tellus*, **2**, 1577-1589.

Walters P., 1982: *An introduction to ergotic theory*. New York, Springer-Verlag.

Wiedenmann, J.M., A.R. Lupo, I.I. Mokhov, and E. Tikhonova, 2002: The climatology of blocking anti cyclones for the Northern Hemisphere: Block intensity as a diagnostic. *J. Climate*, **15**, 3459-3474.

World Meteorological Organization, 1992: *International Meteorological Vocabulary.* 2nd ed. WMO, 784 pp.